DEVELOPMENT OF COCONUT BASED CHOCOLATE BY 3D PRINTING TECHNOLOGY

by

SARATH KUMAR S

(2019-18-024)

DEPARTMENT OF PROCESSING AND FOOD ENGINEERING

KELAPPAJI COLLEGE OF AGRICULTURAL ENGINEERING

AND TECHNOLOGY, TAVANUR - 679573, MALAPPURAM

KERALA, INDIA

2022

DEVELOPMENT OF COCONUT BASED CHOCOLATE BY 3D PRINTING TECHNOLOGY

by

SARATH KUMAR S

(2019-18-024)

THESIS

Submitted in partial fulfilment of the requirement for the degree

MASTER OF TECHNOLOGY

IN

AGRICULTURAL ENGINEERING

(Processing and Food Engineering)

Faculty of Agricultural Engineering and Technology

Kerala Agricultural University

DEPARTMENT OF PROCESSING AND FOOD ENGINEERING

KELAPPAJI COLLEGE OF AGRICULTURAL ENGINEERING

AND TECHNOLOGY, TAVANUR - 679573, MALAPPURAM

KERALA, INDIA

2022

DECLARATION

I hereby declare that this thesis entitled "**DEVELOPMENT OF COCONUT BASED CHOCOLATE BY 3D PRINTING TECHNOLOGY**" is a bonafide record of research work done by me during the course of research and the thesis has not previously formed the basis for the award of any degree, diploma, associateship, fellowship or other similar title of another University or Society.

Place: Tavanur

Date: 3|01|23
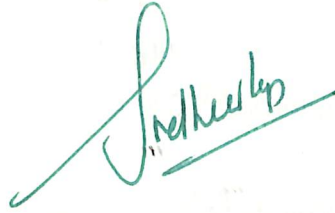
SARATH KUMAR S

(2019-18-024)

CERTIFICATE

Certified that the thesis entitled **"DEVELOPMENT OF COCONUT BASED CHOCOLATE BY 3D PRINTING TECHNOLOGY"** is a *bonafide* record of research work done independently by **Mr. SARATH KUMAR S (2019-18-024)** under my guidance and supervision and that it has not previously formed the basis for the award of any degree, diploma, fellowship or associateship to him.

Place: Tavanur

Date: 8|1|23

Dr. SUDHEER K. P.

(Major Advisor, Advisory Committee)

Professor & Head

Dept. of Agricultural Engineering
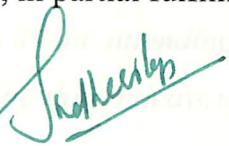
College of Agriculture, Vellanikkara

CERTIFICATE

We, the undersigned members of the advisory committee of **Mr. SARATH KUMAR S (2019-18-024)** a candidate for the degree of Master of Technology in Agricultural Engineering with major in Processing and Food Engineering, agree that the thesis entitled **"DEVELOPMENT OF COCONUT BASED CHOCOLATE BY 3D PRINTING TECHNOLOGY"** may be submitted by **Mr. SARATH KUMAR S (2019-18-024)**, in partial fulfilment of the requirement for the degree.

Dr. Sudheer K. P. (Major Advisor)
Professor & Head
Dept. of Agricultural Engineering,
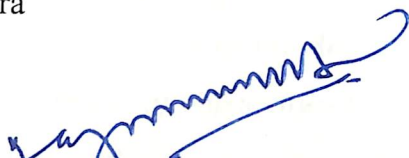College of Agriculture,
Vellanikkara

Dr. Prince M.V. (Member)
Professor & Head
Dept. of Processing and Food
Engineering
KCAET, Tavanur

Dr. Rajesh G. K. (Member)
Assistant Professor
Dept. of Processing and Food
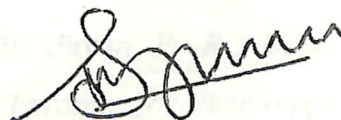Engineering
KCAET, Tavanur

Dr. Suresh Kumar P. K. (Member)
Professor,
Dept. of Agricultural Engineering,
College of Agriculture,
Vellanikkara

EXTERNAL EXAMINER
Dr. Sajeev M. S.
Principal Scientist
Division of Crop Utilisation
CTCRI, Sreekaryam, Thiruvananthapuram

ACKNOWLEDGEMENT

Kumar and *Sarala K*. Their blessing and love are the source of my spirit every moment. I have been highly fortunate and lucky to express my heartfelt thanks to my dearest sister *Saranya S. Kumar* and my friends for their kind blessings and well wishes showed on me.

One last word; since it is practically impossible to list all the names who have contributed to my work, it seems proper to issue a blanket of thanks for those who helped me directly or indirectly during the course of study.

... ... any omission in this small manuscript does not mean lack of gratitude.

Sarath Kumar S

*Dedicated to my Parents,
Teachers and dear friends*

Table of contents

LIST OF TABLES

LIST OF FIGURES

LIST OF PLATES

LIST OF APPENDICES

SYMBOLS AND ABBREVIATIONS

Symbols	Abbreviations
%	Percentage
/	Per
>	Greater than
<	Less than
±	Plus or Minus sign
a^*	Greenness or redness
AC	Alternating Current
AOAC	Association of Official Agricultural Chemists
ANOVA	Analysis of variance
b*	Blueness or yellowness
B	Chroma value
°C	Degree Celsius
cc	Cubic centimeters
CCD	Central Composite Design
CTCRI	Central Tuber Crops Research Institute
Dept.	Department
et al.	And others
E322	Lecithin
ΔE	Delta E
Fig.	Figure
G	Gram
g/min	Gram per Minute
Hz	Hertz

Hp	Horse power
ie.,	That is
KCAET	Kelappaji College of Agricultural Engineering and Technology
k Cal	Kilocalorie
L*	Lightness or darkness
Min	Minute
Mm	Millimetre
mm/s	Millimetre per second
mm^3/s	Millimetre cube per second
N	Newton
No.	Number
Nm	Nanometre
Pa	Pascal
Pa s	Pascal second
Rpm	Revolutions per Minute
RSM	Response Surface Methodology
S	Second
STL	Stereolithography
TPA	Texture profile analysis
V	Volt
a_w	Water activity
Dn	Nozzle Diameter
Vd	Extrusion rate
Vn	Printing Speed

CHAPTER 1
INTRODUCTION

Three-dimensional (3D) printing is a novel food preparation concept based on additive manufacturing (AM) technique that has been widely used in almost all industries such as automobiles, architecture, textiles, medicine and in the field of military. The concept of 3D printing in food processing industries is an upcoming technology with a wide range of applications. In food applications, this technique is known as food-layered manufacture (FLM) and the technology offering features like personalized nutrition, taking into consideration of the age, health and diet of the consumer and also customized designing of foods based on individual preferences. The function of additive manufacturing in the field of food processing is not just to produce foods in a single step, but also to develop foods with new texture and nutritional enrichment.

In the recent years, the consumer approach towards a healthy diet is progressively increasing, which demands the food industry to deliver suitable as well as nutritious food (Manstan and McSweeney, 2020). As a topic of the hour, 3D printing receives the attention of food technologists in unwinding its potential advantages in the food sector. 3D food printing is forecasted to be a promising technology than robotics-based food manufacturing because it paves an approach for the personalization and customization of foods, modification of traditional recipes, simplifying customized food supply chain (Kumar *et al.*, 2020). According to the recent market research estimates, the global market for 3D printing was estimated to be worth roughly 12.6 billion US dollars in 2020 and is expected to increase at a compound annual growth rate of 17% between 2020 and 2023, (Statista, 2021).

In contrast to the traditional food processing, material selection is quite an important factor that determines the printability of foods and are broadly categorized as natively printable (chocolates, cheese, starch), non-printable (rice, flesh foods, fruits and vegetables) and alternative ingredients (algae, fungi, insects, lupin seeds) (Sun *et al.*, 2015). Many

studies were reported on the addition of hydrocolloids and starch-based food items for making the non-printable and alternative ingredients into printable form. Hot melt extrusion printing can convert raw food ingredients such as chocolates to ready-to-serve end products. Chocolates are commonly used for the demonstration of 3D food printing because it can be patterned by hot-melt extrusion and it becomes solid at room temperature (Mantihal *et al.,* 2017). In this focus, the present study aimed at the development of coconut based chocolate by 3D food printing technology.

Coconut (*Cocos nucifera*) is a very versatile and indispensable food item which is considered as a complete food source, rich in calories, vitamins and minerals. Coconut kernel contains 7% dietary fiber and 5% proteins, in addition to 34-60% oil content. Coconut kernel protein possesses cardio-protective and anti-diabetic properties and dietary fibre constitutes significant hypo cholesterolemic effect. In 2020, global coconut production amounted to about 61.52 million metric tons (Statista, 2020).

Chocolate contains high concentrations of refined sugar and saturated fat content derived from the cacao bean itself. Although chocolate contains high amount of saturated fats, the two major fatty acids are palmitic and stearic acids. In addition, it also contains energy providing macronutrients. Chocolate and cocoa (*Theobroma cacao*) have beneficial health effects related to cardiovascular disease, metabolic syndrome, neurodegenerative diseases and other chronic health conditions. Global cocoa production is expected to reach about five million tons in the 2021/2022 crop year (Statista, 2022).

Deficiency of complex carbohydrates like dietary fiber is a matter of concern which poses major health issues causing chronic diseases such as cardiovascular diseases, obesity, colon cancer, hypertension and diabetes mellitus. The recommended acceptable intake of dietary fibre is 28.8 g/day for adults, but actual intake was found to be lower than this limit (Krishnaraj *et al.*, 2019). Consumer awareness about nutrition and dietary consumption patterns has raised the demands for inclusion of increased dietary fibre intake in a regular diet. Considering all these factors, the development of chocolate enriched with coconut

dietary fibre is a need of the hour. Chocolate, being a frequently consumed food item preferred by most of the people, incorporation of dietary fibre into it is an easy way to provide fibre enrichment without a drastic change in eating habits. With this aim, the study focused on the applicability of 3D printing for fibre enrichment of chocolate.

As chocolate is a common printing ink, there is great scope for 3D printing of chocolate. Till now no studies have been reported on the printing of chocolate enriched with coconut dietary fiber. The optimal 3D printing process can aid in the restructuring of traditional chocolate products and improving the global competitiveness and profitability in chocolate marketing. Based on the methodology of the study for preparation of coconut fortified chocolate, the following objectives are frame;

Objectives of Study

1. To formulate printing material (ink) for coconut based chocolate

2. To optimize the process variables for 3D printing of coconut based chocolate

3. To analyse the quality of 3D printed coconut based chocolate

CHAPTER II

REVIEW OF LITERATURE

2.1 COMPOSITION OF CHOCOLATE

Theobroma cacao tree seeds or cocoa beans are used to make chocolate products. The fact that chocolates are particularly rich sources of several important nutrients and phytochemicals that can support a balanced diet (Lecumberri *et al.,* 2007; Ieggli *et al.,* 2011) highlights resurgence in interest in such goods. A combination of cocoa mass, cocoa butter and sugar is used to make edible chocolate; this mixture is then refined, conched, tempered and lastly moulded (Wieland, 1972; Lees and Jackson, 1973). For dark chocolate, the amounts of cocoa liquor, cocoa mass, and sugar are chosen based on the organoleptic quality and desired flavour.

Chocolate is a high-nutrient food with a quick metabolism and good digestion. Its composition includes sugar, milk and cocoa which aids in the proper absorption of lipids, proteins, carbohydrates, vitamins and minerals (Campos and Benedet, 1994). Although little is known about its bioavailability, cocoa beans are a significant source of minerals like copper, iron and magnesium. The fresh cocoa bean's approximate chemical composition is 50-56% water, 30-32% fat, 10-15% proteins, 5-6% polyphenols, 4-6% starch, 4-6% pentosans, 2-3% cellulose, 2-3% sucrose, 1-2% theobromine, 1% acids, and 1% caffeine (Bertazzo *et al.,* 2011).

In addition, the nutritional makeup, polyphenol content, fermentative quality and volatile flavours of the cocoa bean contribute to its quality (Schwan and Wheals, 2004). In terms of its overall nutritional value, the cocoa bean is regarded as a whole food (Minifie, 1989).

2.1.1 Primary metabolites in cocoa

Chocolate and cocoa is one of the most popular food items which also provides important nutrients like fat, protein, carbohydrates, fiber, polyphenols and minerals.

According to USDA (2016), 100 g of cocoa powder contains minerals including magnesium (590 mg), phosphorus (960 mg) and potassium, as well as 12.7 g of fat, 19.6 g of protein, 54.3 g of carbohydrates and 5.1 g of fiber.

The cocoa butter in whole beans accounts for 50-60% of their overall energy content. The flavour of cocoa butter (fat) is neutal. In addition to some polyunsaturated fatty acids like linoleic and arachidonic acids, the fatty acids in cocoa also include palmitic, stearic, and oleic acids (Porsgaard and Hoy, 2000). About 1% of cocoa butter is made up of monoacylglycerols, 2% of diacylglycerols, 95% of triacylglycerols, 1% of polar lipids and 1% of free fatty acids (Biehl and Ziegleder, 2003). The lipids in cocoa butter are not absorbed fast or efficiently due to the complex molecular arrangement of the fatty acids in cocoa butter triglycerides, which influences the total amount of time for metabolism and intestinal absorption (Sanders *et al.,* 2003).

Albumins, globulins, prolamins and glutelins, the four principal protein components in cocoa beans, account for 95% of the total protein in the seeds (Zak and Keeney, 1996). About 52% of total protein is made up of albumin, which is not deteriorated during fermentation (Dodo *et al.,* 1992). During fermentation, the proteins are broken down into peptides and free amino acids, which are crucial for the emergence of the cocoa flavour.

The crude protein level ranged between 16-22% during fermentation and bean storage (Afoakwa *et al.,* 2013). Depending on the type of chocolate product, the protein level might range from 3-26% (USDA, 2016). Chemical value for cocoa protein is less than 25 due to the low methionine content (Young *et al.,* 1999). During fermentation, the mature and ungerminated cocoa seeds exhibit high levels of proteolytic activity that break down the vascular storage protein and liberate oligopeptieds and hydrophobic amino acids, which were the primary building blocks of cocoa flavour (Beihl *et al.,* 1995).

Depending on the composition of cocoa, milk and other ingredients different amounts of carbohydrates can be found in chocolate. As per Nutrient Data Base (2018), the nutritional composition of cocoa powder and various chocolates ranges from 24-63%.

Freshly harvested cocoa beans have a carbohydrate content of 12-14% digestible and a significant amount of non-digestible or fiber (Minifie, 1989). The fermentation process breaks down the cocoa pulp, resulting in the production of long-chain sugars, acetic acid, ketoacids and alcohol (Dei, 2006). According to Afoakwa (2009), the three main sugars in cocoa are sucrose, fructose and glucose, with sucrose constituting the majority of total sugars (90%), followed by glucose and fructose (about 6%). Fermented samples contain significantly more carbohydrates than unfermented samples.

Essential minerals like calcium, iron, copper, manganese, magnesium, zinc, phosphorus and potassium are abundant in cocoa (Lefeber *et al.,* 2010). According to Afoakwa *et al.* (2013), the amount of micronutrients decreases as cocoa pods are stored and fermented. Cocoa powder is recognized as a valuable source of magnesium, sodium, potassium and phosphorus, with magnesium levels ranging from 2-4 mg/g dry powder. Dark chocolate contain 40 mg of magnesium.

2.1.2 Secondary metabolites in cocoa

Bioactive chemicals are secondary metabolites that are biosynthesized from primary metabolites and include alkaloids, phenolics, glycosides, terepenoids etc. (Bernhoft, 2010). The biologically active substances flavonoids, theobromine and anthocyanin found in cocoa may have negative health effects on people (Wollgast and Anklam, 2000). There is a plentiful supply of bioactive substances like polyphenols in cocoa and its products (cocoa powder, cocoa liquor and chocolate) (Hi *et al.,* 2009).

Polyphenols and methylxanthines are two categories of bioactive substances found in cocoa. The principal flavanoids in cocoa are catechins, polymeric procyanidins and monomeric epicatechin, while polyphenols are made up of both flavanoids and non-flavanoids (Kim *et al.,* 2014). Wollgast and Anklam (2000) discovered three types of polyphenols, including proanthocyanidins (58%), flavan-3-ols or catechins (37%) and anthocyanins (4%) from cocoa beans. Due to the production of complex polyphenols with proteins and polysaccharides, polyphenols have a significant influence in the sensory

qualities of cocoa beans and products generated from them (Ferrazzano *et al.,* 2009). Procyanidins with a concentration range of 1.08 to 85.36 mg/g were found to be the most prevalent polyphenol in cocoa and chocolate products. The second most common polyphenols in cocoa were catechins and epicatechins (Manach *et al.,* 2004).

Catechin, epicatechin and procyanidins are found in high concentrations in cocoa. Dark chocolate has higher flavonoid concentrations than milk chocolate. Compared to milk chocolate, black chocolate has more biological benefits from flavonoids (Lee *et al.,* 2003). In 100 g of dark chocolate, there are 28.30 mg of total flavanoids (Miller *et al.,* 2009).

Methylxanthines are phytochemicals formed from the purine base xanthine, including caffeine, theobromine, and theophylline. The two main methylxanthines found in cocoa and chocolate products are caffeine and theobromine (Kim *et al.,* 2014).

2.2 RHEOLOGY OF DARK CHOCOLATE

Saputro *et al.* (2019) conducted a study on the rheological and microstructural properties of dark chocolate produced using a liquefier device and a ball mill. The impact of processing parameters such ball size, milling time and lecithin content was examined in the study. The findings demonstrated that the lecithin concentration, milling duration and ball size had a significant impact on the rheological properties of the chocolates. The Casson yield value and Casson viscosity of the chocolates made using the alternative processing method were higher than those made using the traditional processing method. The alternate processing method appeared to be satisfactory from a micro structural and rheological perspective and the optimal flow properties were obtained using 0.4% lecithin and a milling period of 30 minutes.

A study on the rheological, textural and calorimetric changes in dark chocolate during various processing steps was carried out by Glicerina *et al.* (2013). It was discovered that the samples showed noticeable shear thinning behaviour with yield stress during various processing step and the power-law model was well suited for the values. Results

7

revealed that all fundamentals, including apparent viscosity, yield stress, G', G" and K index, saw extreme increases in samples.

Afoakwa *et al.* (2007) studied the factors influencing rheological and textural qualities in chocolate. Results revealed that processing methods, particle size distribution, and ingredient had an impact on the rheological features and physical qualities of chocolate.

Feichtinger *et al.* (2020) investigated the effect of particle size distribution (PSD) and addition of lecithin on rheological properties of chocolate. The purpose of the study was to assess the impact of the PSD of the two main components of chocolate (cocoa powder and sugar) on viscosity at various fat concentrations. It was discovered that the highest viscosity difference occurred at a coarse fraction proportion of 0.6, while the proportion with coarse fractions of 0.8 or 1 had the lowest viscosity values. Lecithin was added and the viscosity was reduced as a result of fewer particle-particle interactions.

Shourideh *et al.* (2012) conducted a study on the effects of D-Tagatose and Inulin on some physicochemical, rheological and sensory properties of dark chocolate. The findings demonstrated that a low inulin concentration improves yield stress and linear shear stress while decreasing plastic and perceived viscosity. Low moisture contents of the chocolate and higher Aw are caused by a rise in D-tagatose and a decrease in inulin. Dark chocolate samples containing inulin showed that D-tagatose ratios of 25-75% and 100% were effective replacements for sucrose.

Afoakwa *et al.* (2009) compared the rheological models for determining the viscosity of dark chocolate. For the rheological characteristics of dark chocolates with varied fat, lecithin content and PSD, the Casson model as well as the International Confectionery Association (ICA) approach were compared and correlated. A shear rate controlled rheometer was used to study the rheological properties and studies revealed high correlation (r = 0.89-1.00) and regression coefficients (R^2 = 0.84-1.00). The most recent ICA recommendations (yield stress and apparent viscosity) for assessing the viscosity of

chocolate were very closely related to the Casson reference parameters, such as yield value and plastic viscosity. The Casson model, which has problems with variations in chocolate viscosity, proved less effective than the ICA technique.

Schantz *et al.* (2005) investigated the influence of lecithin-polyglycerol polyricinoleate (PGPR) blends in a concentration up to 14 g/kg on the rheological properties of chocolate. Rotational rheometry was used to analyze the flow characteristics of melted milk and dark chocolate. The findings demonstrated that, regardless of the emulsifier's concentration, applying combinations of 30% lecithin and 70% PGPR effectively reduced the yield stress of both milk and dark chocolate. For milk and dark chocolate, respectively, lecithin-PGPR blends of 50:50 and 75:25 were found to have low viscosity values.

Afoakwa *et al.* (2008) conducted a study on the relationship between rheological, textural and melting properties of dark chocolate as influenced by particle size distribution and composition. Lecithin (0.3 and 0.5%), PSD (D90 of 18, 25, 35, and 50 m) and fat (25, 30 and 35%) were varied in a 4×3×2 factorial study. A shear rate-controlled rheometer was used to test rheological characteristics. It was discovered that the rheological, textural and melting qualities are significantly influenced by the fat, lecithin and PSD contents. The rheological, textural and melting indices showed strong correlations (r = 0.78-0.99) and regression coefficients (R^2 = 0.59-0.99).

2.3 DIETARY FIBER ENRICHMENT OF CHOCOLATE

Due to its high nutritional value, easy digestion and quick metabolism, chocolate is one of the most extensively consumed foods in the world. Its inclusion of cocoa, milk and sugar can ensure that the right amount of carbohydrates, lipids, proteins, vitamins and minerals are consumed.

Ozguven *et al.* (2016) fortified dark chocolate with spray dried black mulberry (*Morus nigra*) waste extract encapsulated in chitosan-coated liposomes with alkalization

degrees (pH 4.5, 6, 7.5) at conching temperatures of 40ºC, 60ºC and 80ºC. Chitosan-coated liposomes were discovered to offer superior anthocyanin content protection in high pH and temperature conditions. Depending on the conching temperature and pH, chocolate was supplemented with encapsulated anthocyanins (76.8%).

Belscak-Cvitanovic *et al.* (2012) studied the effects of formulations of chocolates enriched with plant polyphenols from red raspberry (*Rubus idaeus L.*) leaves. Milk, semisweet and dark chocolate's bioactive content, as well as their physical and sensory characteristics, were evaluated in relation to the addition of concentrated (1% and 3%) and freeze dried (1%) red raspberry leaf extract. The total phenol content in all chocolates increased when concentrated extract at a concentration of 3% was added. However, the concentrations of extract currently being used are ineffective for increasing the bioactive content of chocolates; instead, a freeze-dried raspberry leaf concentrate should be used.

Kobus-Cisowska *et al.* (2019) enriched novel dark chocolate with *Bacillus coagulans* as a way to provide beneficial nutrients. The preservation of bacterial counts during the storage period, as well as the physicochemical and sensory properties was examined. Dark chocolate serves as a suitable matrix for B. coagulans probiotic bacteria as a new dietary supplement, particularly for children and it was shown that the properties of produced chocolate are similar to those of the traditional product.

Barisic *et al.* (2019) studied the effect of addition of fibers and polyphenols on the properties of chocolate. The goal of the experimental study was to ascertain how various supplements affected rheology, particle size distribution, hardness, water activity, colour, sensory qualities and polyphenol content. The findings demonstrated that the product's enhanced viscosity and hardness were dependent on the moisture of the added ingredient. Fiber added chocolates were darker and had less water activity.

Erdem *et al.* (2014) developed novel synbiotic dark chocolate enriched with *Bacillus indicus* HU36, maltodextrin and lemon fiber. To ascertain the influence of

variables and quality attributes sensory and colour characteristics of the products were investigated. The RSM model produced the best formulas. It was discovered that the addition of dietary fiber had no adverse effects colour, organoleptic qualities and flavour of the samples. According to the findings, in order to get the best organoleptic qualities for the product, the concentration of lemon fiber should be maintained at 1.5 (g/100 g), while the concentration of maltodextrin should be in the range of 3.20 and 3.91 (g/100 g).

Tolve *et al.* (2018) conducted a study on the fortification of dark chocolate with microencapsulated phytosterols. The developed products were chemically stable and had a particle size less than 30 m. It was shown that the fortifying of microcapsules had no effect on how intense the sensory qualities were when compared to the cocoa content.

Acan *et al.* (2020) studied the effect of grape pomace usage in chocolate spread formulation on textural, rheological and digestibility properties. The mixture design method was used to create the formulations. Additionally, spreadability and hardness parameters were determined in the range of 2.15-4.24 N mm and 0.80-1.42 N correspondingly. It was discovered that the consistency coefficient (K) and flow behaviour index of chocolate spread samples varied between 8.10 and 28.50 $Pa.s^n$ and 0.52-0.71. Between 25% and 84% of the sample was digestible. The study sheds light on the use of dried pomace as a cheap and nutritious partial replacement for powders made from sugar and milk in chocolate spread manufacturing.

Bouaziz *et al.* (2017) evaluated the effect of addition of Tunisian date seed fibers on the quality of chocolate spreads. When compared to the control, chocolate spread that had been supplemented with 5% date seed soluble fiber concentrate showed the highest OBC (304.62%). Date seed soluble fiber concentrate (DSSFC) and date seeded insoluble fiber concentrate did not significantly differ from controls in terms of the firmness, chewiness, and adhesiveness of prepared chocolate spreads (DSIFC). By adding date seed dietary fiber up to 5% level, functional chocolate spread of excellent quality may be made without negative consequences.

2.4 3D FOOD PRINTING

A unique idea known as 3D printing is based on the additive manufacturing (AM) technology. Layer by layer, fabrication of materials takes place in accordance with the design to create a complete 3D object and it also makes it possible to realize a digital prototype model. It distinguishes itself from conventional or subtractive manufacturing processes. In recent years, it has developed a wide range of industrial uses, including those in the fields of medical, the military, civil engineering, textiles, automobile and food application (Severini *et al.,* 2016). The technology is known as "food-layered manufacture" when used in the food business (FLM).

Consumer expectations and food choices have been significantly impacted by changing lifestyles and diverse eating habits. By providing foods with personalized shape, flavour, nutrition, cost and convenience, AM technology was thought to define as the emerging styles in food processing. Customization continues to be the driving force behind 3D food printing, with other factors including complicated geometry as well as on production (Nachal *et al.,* 2019). This technology makes it feasible to precisely regulate the ingredients of food based on consumer preferences and health (Lupton, 2017). As a promisingly creative technology, 3D food printing opens up new facets of food culture by addressing convenience, novelty, leisure and entertainment, nutrition and global food in addition to sustainability, flexibility, creativity and effective raw material use (Lupton and Turner, 2018).

This strategy can be carried out by combining various macro and micronutrients in a synergistic manner while taking into account their inherent qualities to aid in layer binding and deposition. Due to its unique capability to create foods based on a person's age, diet, and medical problems, these factors have expanded the market potential for 3D printed food goods.

2.5 3D FOOD PRINTING TECHNOLOGIES

Extrusion 3D printing, inkjet printing, powder-binding deposition and bio-printing are some of the current 3D food printing processes. Depending on the kind and makeup of the supply material, the driving mechanism etc. several printing technologies are used. The following section goes over the above mentioned methods.

2.5.1 Extrusion 3D food printing

The most extensively used 3D printing technology is extrusion printing. This technique requires moving a print head equipped with a cylinder that extrudes material ink to the deposition platform through a nozzle. A 3D model directs the layer deposition in accordance with the preferred design (Liu *et al.,* 2017). Liquid and semi-solid materials can be printed using this method. The three most widely utilized extrusion mechanisms are air pressure extrusion, screw-based extrusion and syringe-based extrusion. The designed ink must be able to be extruded and after it has been deposited, it must have enough mechanical integrity to maintain the structure (Lipton, 2017). Individual layers had to be bound together via pre-processing, post-processing and cooling or hydrogel formation depending on the food components chosen (Wegrzyn *et al.,* 2012). Recent reports include the extrusion printing of soft cheese, fresh ingredients, hydrocolloid composites comprising starch and protein.

2.5.1.1 Hot Melt Extrusion (HME)

Crump *et al.* (1991) described the technology initially and the method is also known fused deposition modeling (FDM). In hot-melt extrusion, ink that has been heated to a temperature slightly over its melting point is forced into the nozzle. Following extrusion, the product quickly solidifies and adheres to the earlier layers (Sun *et al.,* 2017). Personalized 3D chocolate goods with various patterns were frequently made using this technique. HME based 3D printers are small and require little upkeep.

2.5.1.2 Room Temperature Extrusion (RTE)

Extrusion at room temperature is used to print materials that are naturally printable, such as cheese, creamy peanut butter, chocolate paste, blends with starchy gels, dough, jelly, hummus and similar items (Periard *et al.,* 2007; Lille *et al.,* 2018; Chuanxing *et al.,* 2018). RTE approach makes it possible to produce intricate confections with excellent repeatability, which was challenging to execute by hand (Periard *et al.,* 2007). RTE has used proteins, carbohydrates and other nutrients extracted from non-traditional sources like algae and insects (van der Linden, 2015).

2.5.1.3 Hydrogel-Forming Extrusion (HFE)

Using a syringe pipette and other tools, hydrocolloid solutions are printed into a gel-setting bath during hydrogel-forming extrusion (HFE). Typically, gel droplet diameter was between 0.2 and 5 mm and accurate and stable shape formation in HFE required careful temperature control of the solution (Sun *et al.,* 2018). This process is dependent on the rheological characteristics of the polymer and the mechanism of gel formation. To deal with various food material design and fabrication, it can also use different print heads and interchangeable extruders. HFE has been used to create fruit-based soft meals specifically for a certain age group having swallowing issues (Serizawa *et al.,* 2014).

2.5.2 Ink-jet Printing

Powder based ink-jet printing uses a piezoelectric or thermal mechanism to build up droplets of the substance on the surface of substrate (Gross *et al.,* 2014). Instead of building intricate designs, it is typically used to print drawings with low viscosity materials. These printers either operate continuously or drop on demand (DoD).

(A)

(B)

(C)
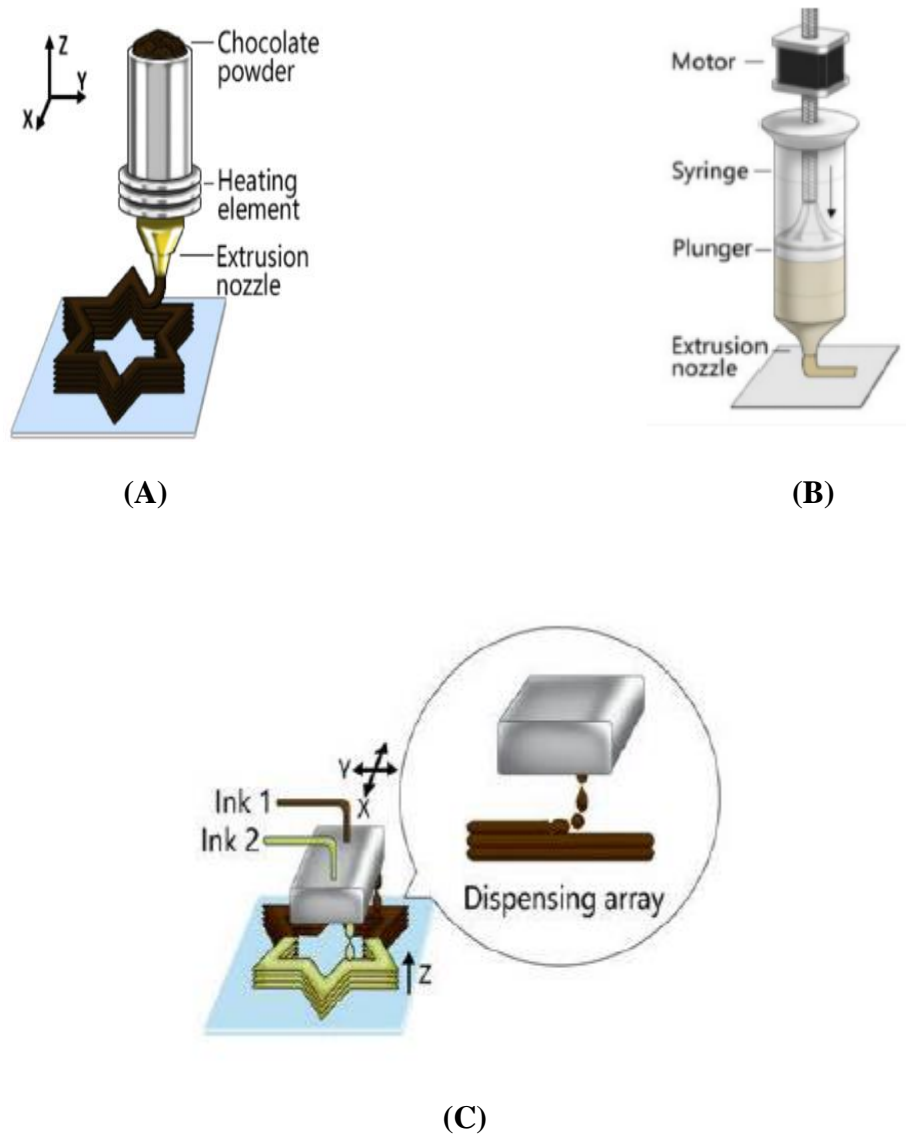
Fig. 2.1 Extrusion food printing: (A) Hot-melt extrusion, (B) Room-temperature extrusion, (C) Ink-jet Printing (Source: Sun *et al.,* 2018)

Formulated ink is continually expelled through a piezoelectric head in a continuous jet printer. At regular intervals, the piezoelectric head separates the ink into droplets using sonic waves (Murphy *et al.,* 2014). The ink is charged by certain conductive substances to achieve the proper flow. In DoD printers, ink is ejected through the print head under

pressure from a valve. Although DoD printers have good resolution and precision, continuous jet systems often have faster printing rates. Because it can alter the surface energy and rheological characteristics of the inks, temperature is regarded as a crucial element in ink jetting (Liu *et al.,* 2017).

2.5.3 Powder Binding Deposition

Another well known method for printing 3D foods is powder binding deposition. Based on the technology used to bind layers of powder, the procedure is divided into three categories: selective laser sintering (SLS), selective hot air sintering and melting (SHASAM) and liquid binding (LB). Each method involves depositing powder on the surface of bed (Feng *et al.,* 2019).

The SLS approach uses an infrared laser as the heat source to bind particles together and this process produces multi-layered 3D food. SLS can be used in the production of foods like sugar and curry cubes. Researchers have created 3D sugar-based sculptures using SHASAM, which uses hot air to fuse powdered material, while LB printing involves building up powder layers through direct fusion (Wegrzyn *et al.,* 2012). Each layer is covered with a liquid binder, which is applied without the need of heat. Therefore, during layer solidification, there is no phase change (Sun *et al.,* 2015). Based on DoD methodology, LB functions by depositing a binder on a layer, which causes the powder particles to sinter together. Food fluids like hydrocolloids and protein-based substances can be sprayed onto a surface to create 3D sculptures.

2.5.4 Bio-Printing

Without using a biomaterial substrate, tissues can be created using the bio-printing approach. Living cell cultures and biomaterials are layered on top of one another in this method. Bio-mechanical properties were developed during this maturation period when the bio-materials were deposited on an appropriate bio-compatible surface and moved to a bioreactor (Godoi *et al.,* 2016). The extensively used techniques for bio-printing are micro-extrusion and laser-assisted printing (Murphy *et al.,* 2014). Despite being regarded as a

sustainable meat production alternative, the method has certain implication on society, religion and ethics view on eating animal meat.

(A)   (B)
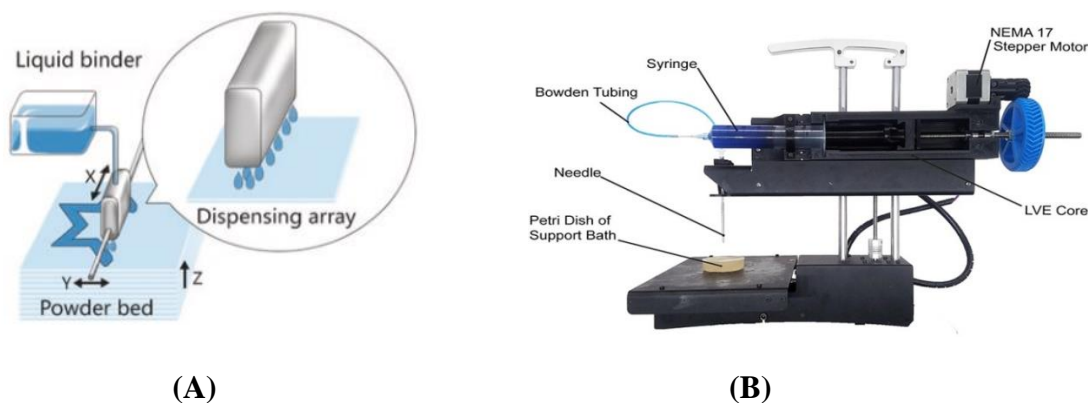
Fig. 2.2 (A) Powder Binding Deposition, (B) Bio-Printing

2.6 EXTRUSION MECHANISMS

Semisolid and liquid materials have been extruded using three different mechanisms: syringe-based extrusion, air pressure driven extrusion and screw-based extrusion.

2.6.1 Syringe-based extrusion

The step motor and syringe in the syringe-based extrusion mechanism are used to drive the extrusion process and store the formed ink, respectively. The step motor is programmed to control the position of the syringe plunger, force the formed ink out of the nozzle and move the liner. Changing the motor speed makes controlling the extrusion rate simple (Sun *et al.,* 2018). When additional power is required to extrude high viscosity materials, this technology is appropriate for printing mechanically strong, semi-solid or solid food items. With this design, each print head just needs one motor, considerably increasing the printing payload for multiple materials (Peng, 2015). It has been used in

designs such as Choc Creator (Choc Edge, 2014), and CocoJet 3D Printer (3D Systems, 2015).

2.6.2 Air pressure driven extrusion

A pneumatic pump and an enclosed food cartridge system make up the air pressure driven extrusion device. The material in the encapsulated food cartridge is forced out of the nozzle by a pneumatic pump, which generates the necessary amount of air pressure. Through customizable valves, the pump may simultaneously run several print heads with various extrusion rates. Due to the ease with which semi-solid and solid materials can adhere to the interior of the food cartridge, this mechanism is better suited for liquid ingredients. It has been used in the design of machines like the BeeHex 3D printer and Barilla's pasta-making 3D printer. The risk of food contamination is decreased by the fact that none of the two extrusion techniques previously discussed involves mechanical equipment coming into touch with food ingredients. To minimize contaminations of the printing material, a filtration system must be connected to the pneumatic pump.

2.6.3 Screw-based extrusion

The thin tube structure and the extrusion nozzle are placed after the cartridge with a large loading hole for food items in the screw-based extrusion. For continuous printing, food-related materials are driven through the nozzle by an auger screw after being supplied into the cartridge. The food items are brought downward during the process to pass through the nozzle with the least amount of air bubble contact (Sun *et al.,* 2018). For autoclaving, the screw and cartridge should be made of stainless steel that is approved for use in food because they will be in direct contact with food. The printed samples, however, lack the necessary mechanical strength to support the subsequent deposited layers since the screw-based extrusion is inappropriate for foods with a high viscosity and high mechanical strength (Liu *et al.,* 2017).

(A)   **(B)**   **(C)**
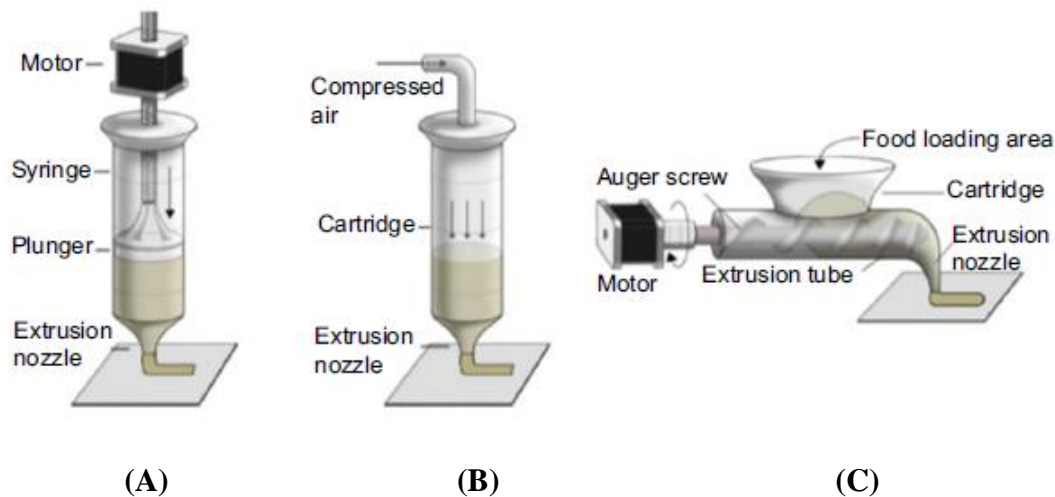
Fig. 2.3 Extrusion mechanism in the 3D food printing process (A) Syringe-based extrusion, (B) Air-compressed extrusion, (C) Screw-based extrusion.

2.7 3D FOOD PRINTING MATERIALS

Printability is the capacity of a formulated ink to be handled and deposited by a 3D printer in accordance with a design while maintaining its structural integrity after deposition. Food ingredients are divided into three categories based on their printability: naturally printable materials, non-printable materials and alternative ingredients.

2.7.1 Natively printable materials

Without the use of any flow boosters, food substances including chocolate, cake icing, hummus, soft cheese and hydrogels can smoothly extrude via a syringe (Cohen *et al.,* 2009). Products made with natively printable food materials can be completely altered in terms of flavour, texture and nutritional value. However, the majority of these foods are not thought of as main courses. They are therefore more motivated by applications in medicine and space. Some materials that are naturally printed may maintain the structure after deposition and don't need any additional processing. Without any post-cooking steps, powder materials made of mashed potatoes, starches and sugars were used to create sugar

19

teeth (Southerland *et al.,* 2011). Marmite and Vegemite are regarded as appropriate materials for 3D printing since they are strong enough to maintain their shape after printing (Hamilton *et al.,* 2018). Protein pastes and batters are examples of formulations that call for some post processing (Lipton *et al.,* 2010), making it challenging to maintain their printed geometry.

2.7.2 Non-printable Traditional Food Material

This category includes staple foods including rice, meats, fruits and vegetables that cannot be printed. By altering the materials' rheological and mechanical properties, flow enhancers like hydrocolloids and naturally printed materials are introduced to make extrusion easier (Dick *et al.,* 2019). Using simple additives, Lipton *et al.* (2010) altered conventional meal recipes and created intricate geometries. The most often used hydrocolloids are agar, gelatin, xanthum gum and guar gum. Choosing an appropriate concentration of hydrocolloids will explore a range of textures. According to studies, the addition of hydrocolloids affects the flow properties and gives it shear thinning behaviour (Huang *et al.,* 2019). Traditional culinary ingredients typically require post-process cooking including baking, frying or steaming.

2.7.3 Alternative Ingredients

Insects can be used as substitute ingredients in food items to address the global dilemma of food shortage. Insects, algae, fungi, seaweed and lupine are examples of novel sources of protein and fiber in this category. It was discovered that the protein content of insect powder was significantly higher than that of conventional meat products (Sun *et al.,* 2015). When used to create sustainable and personalized foods, these ingredients establish a new trend (Nachal *et al.,* 2019). Protein-rich snacks made from yellow mealworms (*Tenebrio molitor*) were created by Severini *et al.,* (2018). It was discovered that adding yellow mealworm powder greatly enhanced the protein content and affected the dough's capacity to be printed. As a substitute source for 3D food printing, agricultural wastes and byproducts can readily be transformed into enzymes, metabolites and flavors (Silva *et al.,*

2007). The use of these elements in 3D food printing will result in the manufacture of healthier (e.g. low-fat) food products and play a significant role in making the cultural background of insects more appealing to customers.

2.8 DESIGN AND CONFIGURATION OF PRINTING PLATFORM

The section explains the two different printing platform designs such as universal 3D printers and specialized food printers with the ability to print food, followed by a discussion on printing stage configuration.

2.8.1 Universal 3D printers and specialized food printers

To speed up the development process and it's time for the purpose of printing food, researchers have modified open source universal 3D printers. A general desktop printer that prints food materials, the Fab@Home system, was not created expressly for culinary purposes (Cohen *et al.,* 2009). Additionally, MakerBot was modified to print food by adding a Frostruder MK2 print head (Millen, 2012).

These industrial 3D printers that also have the ability to produce food are reasonably priced considering that functionality. Researchers utilized it to make 3D food models and examine the qualities of food ingredients, but only a small number of raw materials are relevant, making it impossible to conduct in-depth research. The majority of printers are composed of plastics, which during the printing of food may emit harmful ultra-fine particles and have adverse health effects. It is difficult to certify these type of printers as safe and general food safety is also a worry. For instance, bacteria can accumulate in the extruder when food becomes blocked between tiny gaps and fractures (Sun *et al.,* 2018).

To support research goals, specialized food printers were created depending on specific criteria such as dispensing mechanisms, material properties etc. (Hao *et al.,* 2010). These parts of printers are made of food safe materials, so they are secure when they come into touch with food. A component cleaning method is also added to prevent food

contamination. The best example of specialized food printers is Foodini, which uses a reusable stainless steel extruder and a nozzle that is simple to clean by hand. Although relatively pricey, these printers perform better during fabrication. Both general-purpose 3D printers and specialized food printers with a printing capability for food are offered for sale in the market.

2.8.2 Interchangeable and Multi-Print head Extruders

Food printing has used interchangeable and multi-print head extruders, which can produce multi-material production with complicated geometric design more quickly than by hand. The printing process is what determines the quality of developed food products not the operator's skills.

The universal 3D printers that can print food include interchangeable extruders that can be switched out simultaneously for printing polymers and foods. These extruders are used by the Focus 3D Printer to manufacture food paste, PLA and ABS filaments. This 3D printer can recognize and alter its settings for a variety of interchangeable extruders automatically (Grunewald, 2015).

Specialized food printers also use interchangeable extruders to switch between different food materials. In order to showcase several materials utilizing interchangeable extruders, Sun *et al.,* (2015) created multi-material butterfly cookies using the same dough material with different food colours. In order to decorate food products or produce functional food with enriched nutrients, this can also be utilized to replace an existing print head with a continuous inkjet print head.

Both general-purpose 3D printers with food printing capabilities and specialized food printers have utilized multi-print heads. The activation of data from each layer and its direction to the platform controller's associated motors for moving the relevant dispensing head with an exact feeding rate and deposition area allowed for the controlled deposition and distribution of fabrication materials. Multi-print heads provide computer-controlled,

beautiful printing of multiple materials from a variety of sources. To create customized pizza, the BeeHex 3D printer used a multi-print head design that dispersed cheese, sauce and pizza dough separately through a number of nozzles (Garfield, 2016). Interchangeable and multi-print head extruders are frequently coupled based on customer expectations.

2.8.3 Printing Stage Configurations

Cartesian, Delta, Polar and Scara configurations are the multi-axis stages used for 3D food printing. The above mentioned types are discussed in the following section.

2.8.3.1 Cartesian Configuration

Cartesian configuration is frequently used in the development of first generation 3D food printers because it is easy to calibrate, create and maintain. The X, Y and Z axes of this machine design can move in three different directions: left to right, front to rear and up and down, respectively. It may have a print head that moves along the X-Z axis and a square stage positioned on the Y-axis or a print head that moves along the Z axis and a square stage positioned on the X-Y axis (Sun *et al.,* 2018).

The print head is heavy when loaded with ink, which slows down printing in various directions, causes a persistent jerking motion and may cause the collapse of a large-height end product. Due to the need for a large operating area for printing, this arrangement is not regarded as a consumer end device. To make the design and development under this arrangement, hardware resources and sophisticated tools, such as slicing software, dual print head design and printing route planning are available. Foodini (Natural Machines, 2014), Choc Creator (Choc Edge, 2014) and BeeHex Robot pizza printer are examples of this arrangement (BeeHex, 2016).

2.8.3.2 Delta Configuration

In the delta design, a print head is suspended by three arms above the fixed circular print stage. The Delta configuration printers are quicker, more affordable and capable of

producing higher volumes of product faster than the Cartesian configuration. The less number of component in the configuration results in very low maintenance and equipment expenses. This setup works well for fabricating digitally but is less accurate for controlling positions. The printing process may become unstable when liquid food material (melted chocolate) is printed at a quicker speed due to liquid vibration caused by acceleration and deceleration inside the feeding unit. For liquid foods, it is advised to utilize a modified Delta setup with a fixed print head and a moving print stage. Both the Pinya3 food printer (Alcalde, 2016) and the Tytan 3D delta printer (Krassenstein, 2014) are currently under development and have a Delta configuration.

| (A) | (B) | (C) | (D) |
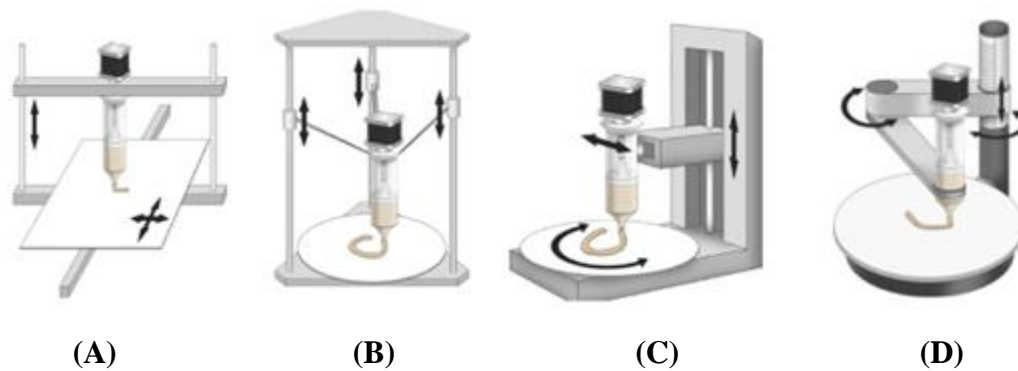
Fig.2.4 3D Food printer configuration: (A) Cartesian, (B) Delta, (C) Polar, (D)SCARA

2.8.3.3 Polar Configuration

In polar configuration, rather of a square grid, points are described by polar coordinates. A spinning stage and a print head that can move left to right to cover the X and Y axes and up to down to cover the Z axis are typical components of this setup. In comparison to other setups, this 3D food printer uses less space and can generate larger volumes more quickly. Polar arrangement can function identically in all directions and can produce a complete circle with less mechanical defects and minimal calibration. The greatest examples are the TNO food printer (van der Linden, 2015) and the XOCO 3D printer (Michiel Cornelissen Ontwerp n.d.).

2.8.3.4 SCARA Configuration

Since the 2011 passage of the Food Safety Modernization Act (FSMA), Selective Compliant Assembly Robot Arm (SCARA) has attracted increasing interest from the food industry (Nowak, 2015). It comprises of a robot arm that moves along the X-Y plane and an actuator that moves along the Z-axis. SCARA configuration has been adapted for 3D printing and is simple to construct. This configuration was utilized by "Sanna: the food printer of 2020" created by Columbia University (Creative Machines Lab, 2016) to transform frozen, unprocessed, raw food purees into cooked, flavorful and texturized dishes.

2.9 FACTORS INFLUECING 3D FOOD PRINTING

The composition of materials and printing process parameters are two important factors influencing in the optimization of the 3D food printing.

2.9.1 Composition of material and feasibility of printing

The food materials chosen for 3D printing must adhere to rules and requirements for food safety. Therefore, it is necessary to comprehend the physical, structural, rheological, mechanical and sensory aspects of the material. Porosity, density, thermal properties, heat resistance, thermal conductivity, crystallization temperature and thermal diffusivity are the engineering characteristics of the materials that have a significant impact on the final 3D-printed product (Godoi *et al.,* 2016). Compressibility, viscosity, glass transition and wet ability are some of the important thermo-rheological parameters that must be measured (Yang *et al.,* 2017).

Hao *et al.* (2010) compared the physical structure of seeded chocolate in the lab with commercially tempered chocolate using Differential Scanning Calorimetry (DSC).The findings indicated that both forms of chocolate had melting peaks in the same range of

temperatures (26-36℃) and they indicated that seed tempering was a crucial procedure to be used on chocolate.

Viscosity is one of the important rheological parameters to be considered during 3D food printing. Dankar *et al.* (2018) studied the effect of four food additives like agar, glycerol, alginate and lecithin on the rheological properties of potato puree. It was found that all of the samples had non-Newtonian pseudo-plastic properties that were beneficial for extrusion through a nozzle. Only agar and alginate stabilize more potato puree, with the amounts having an effect on whether or not the viscosity increases or decreases. Prior to printing with the ChocALM printer, Hao *et al.* (2010) used a parallel plate rheometer to measure the viscosity of chocolate. According to the study, chocolate exhibits a constant viscosity with a temperature range of 3.5-7 Pa s between 32 and 40°C.

Anukiruthika *et al.* (2020) investigated the printability of egg yolk and egg white using rice fractions, in which consistency index (k) and flow behavior (n) were found to be important parameters affecting the material for 3D printing.

The flow and stability of the supply material are significantly influenced by temperature. When printing chocolate, the temperature must be kept in the low range to facilitate the chocolate's post-extrusion hardening. Mantihal *et al.* (2017) investigated the thermal and flow characteristics of printing chocolate under various settings, with the nozzle temperature calibrated at 32°C to facilitate the smooth flow of melted chocolate. To solidify the chocolate, the deposition bed temperature was kept within a range of 15-22°C.

Hamilton *et al.* (2018) suggested that, high temperature (65℃) reduces the consistency and yield stress of vegemite and marmite hence, the pressure should be reduced during extrusion. At room temperature (25℃), the structural integrity of printed vegemite and marmite was better retained to due to higher levels of yield stress.

Dianez *et al.* (2019) conducted a temperature induced gelification of κ-carrageenan to study the effect of printing variables on visco-elastic properties of the gel using 3D

printing. Results indicated that as printing speed and layer height decreased, gel strength increased. As an alternate way for gel preparation, a new technique has been devised that can lower temperature and process time for gel printing with pre-defined rheological parameters.

Tohic *et al.* (2017) studied the effect of 3D printing on textural properties of processed cheese and found that the printing process reduced the hardness of printed cheeses compared to unprinted ones. The textural characteristics of processed cheese were not changed by 3D printing at high or low speeds.

Severini *et al.* (2018) evaluated the sensory attributes of 3D printed blends of fruits and vegetables. It was discovered that smoothies printed in 3D had improved visual appeal while smoothies not printed in 3D had no difference in flavour, colour and aroma. The appearance of finished products and food preservation are both enhanced by 3D printing technology.

2.9.2 3D printer parameters

The process variables that affect the creation of edible 3D food include nozzle size, height, extrusion rate, pressure, motor speed and air gap between layers. Using computer control systems, it is important to optimize printing parameters such as form and layer thickness, printing speed, line distance, laser power, number of layers and heating and cooling rates. These variables regulate printing accuracy, which affects the resulting quality of the product.

According to studies, printing with a small nozzle size achieves more precision and resolution than printing with a big nozzle size. While a smaller nozzle diameter produces finer layers and better precision, a larger one produces thicker layers and can occasionally cause over extrusion (Periard *et al.,* 2007). Lower printing precision is the outcome of faster printing speeds. It is advised to have a nozzle height equal to that of the nozzle diameter as this is another significant factor that influences the printing of food (Hao *et al.,*

2010). Lower nozzle heights result in faulty printing and higher nozzle heights result in improper layering of material.

Wang *et al.* (2017) developed 3D printed fish surimi gel to study the printing variables. It was discovered that the finished product had superior dimensional resolution and surface quality with smaller nozzle diameters. An extremely small nozzle diameter may cause irregularity in both length and width (0.8 and 1.5 mm).

Yang *et al.* (2018) studied the printing variables of baking dough at different compositions and suggested that it is better to kept the nozzle height as same as the nozzle size. According to the findings, the best quality product could be produced using nozzles with a diameter of 1 mm, 24 mm^3/s extrusion rates and a movement speed of 30 mm/s.

Severini *et al.* (2016) studied the printing variables in wheat dough. They came to the conclusion that an ideal layer height of 0.4 mm was achieved utilizing a nozzle diameter of 0.6 mm, a print speed of 30 mm/s and a travel speed of 50 mm/s. When layer height values were less than 0.4 mm, the diameter of the samples decreased, and if it was more than the ideal value, the samples extruded unevenly and have high diameter.

Derossi *et al.* (2017) developed 3D printed fruit based snack for children and studied the effect of flow level and print speed on the printability of the product. The study came to the conclusion that as the flow level is raised, the total volume of deposited material rises and the porosity fraction decreases. Up to a print speed of 50 mm/s, the product's growth rate increased in terms of height and flow level and print speed had an impact on deposition rate.

Yang *et al.* (2017) studied lemon juice gel as 3D printing food material with the effect of potato starch with different combinations (10, 12.5,15, 17.5 and 20 g/100g). The findings demonstrated that high nozzle movement speed causes the extruded filaments to drag because it does not provide enough time for deposition on the bed. Before the breaking happened, the nozzle movement speed had to be increased to 35 mm/s.

Theagarajan *et al.* (2020) conducted a study on rice starch for 3D food printing to study the effect of nozzle diameter (1.2-1.7 mm), extrusion motor speed (120-240 rpm) and nozzle movement speed (800-2200 mm/min). Shape, texture, appearance, dimensional stability, finishing, thread quality, layer definition and binding property of the printed final product were also studied. Rice starch had greater printability when printed at slower printing speeds (800-1500 mm/min) and higher motor speeds (180-240 rpm).

Liu *et al.* (2019) developed 3D printed food composed of wheat flour, water and olive oil with an optimized material composition (55:2.75:30). The many process variables that affect the printing of food were investigated. The internal filling ratio, needle velocity, compressive pressure and needle diameter were all found to be best at 50%, 6 mm/s, 600 k Pa and 0.58 mm respectively. The finished product had a well-organized packing structure, minimal distortion and a good internal texture.

Wilson *et al.* (2020) studied the printability of ground chicken meat with refined wheat flour in 2:1 formulation. The study found that 0.82 mm nozzle size, 0.64 mm nozzle height, 1000 mm/min printing speed, 360 rpm extrusion motor speed and 4 bar extrusion pressure were the ideal printing settings. Deep frying was done after hot-air drying, which was the final post-processing step.

Huang *et al.* (2019) evaluated the printability of brown rice and the effects of printing variables such as nozzle size (0.84,1.20 and 1.56 mm), perimeters (3, 5, 7), and infill densities (15%, 45%, 75%) on the quality attributes of the products. Researchers also looked at textural characteristics including hardness and gumminess. The findings showed that the diameter and height of printed samples were comparable to the design model when the nozzle diameter was reduced from 1.56 to 0.84 mm. While the nozzle diameter changes both the void rate and number of layers deposited got changed, which indirectly influenced the texture characteristics, the textural features were closely related to infill density.

2.10 ROLE OF FOOD CONSTITUENTS IN FOOD PRINTING

Ink for 3D printing can be created using food ingredients such dietary fiber, protein, fat and carbohydrates. The materials should flow easily during deposition and support the structure following deposition. Due to the importance of material composition in food printing, each component of a food item has an impact on the printing process. During both powder-based and liquid-based 3D printing procedures, the differences in the amounts of carbohydrates, proteins and fat will undoubtedly affect the melting behaviour, plasticization and glassy state of the food materials (Slade and Levine, 1994).

2.10.1 Carbohydrates

Carbohydrates and starches when used above the gelatinization point will aid in extrusion and retain the structure of food after printing. Lille *et al.* (2018) conducted a study with skim milk powder (SMP) and semi-skim powder (SSMP) as protein sources. SMP was not suited for extrusion because of its high viscosity. The SSMP's low carbohydrate and high fat content lowered the stickiness of final products while improving printability and structure holding.

The glass transition temperature (Tg) of materials is another crucial consideration for carbohydrates. With the addition of water or a gelling agent, high molecular weight carbohydrates can be printed (such as hydrocolloids). According to studies, the best hydrocolloid concentrations are between 0.2% and 1.0% of the composition's total dry weight. Maltodextrins, for example, have a greater Tg than simple sugars because of their high molecular weight. To maintain the structure of the material after printing, Tg control is crucial (Bhandari *et al.,* 1999). Chen *et al.* (2019) concluded that the relationship between printability and rheological properties of three starches (potato, rice and corn) exhibited shear thinning and strain responsiveness characteristics enabling it suitable for printing by extrusion process.

2.10.2 Proteins

The texture and microstructural characteristics of printed food are influenced by the proteins in the source material. When proteins were the main source of material supply, pH and iso-electric point (pI) became the important characteristics. In liquid-based AM methods governed by hydrogel-forming mechanisms and particle-based-gelation, proteins exhibit aggregation at pI and were an appealing feature.

During the production process, proteins can be added in addition to polysaccharide materials like gelatin and alginate to alter the texture of the final product. Due to external stress (such as temperature) or chemicals, proteins will get denaturized or agglomerate (such as acids or bases). Lipton *et al.* (2010) maintained the rheological properties of meat by incorporating transglutaminase to meat puree. It was accomplished because to the protein conformation's self-supporting structure and the addition of enzymes change the process.

A crucial component of 3D printing is gelatin. The protein molecule gelatin has the ability to alter the viscosity of a substance and viscosity values exhibit a decreasing trend at greater shear rates (Godoi *et al.,* 2016). In situations other than when extended by charged groups, gelatin exhibits Newtonian flow in diluted solution. Protein structure is changed and disrupted during food printing, creating the "melt-in-your-mouth" sensation.

2.10.3 Fat

The physical and organoleptic qualities of printed foods are impacted by the amount of fat contained in the material supply. The structure and makeup of triglycerides (TAG) control material characteristics such crystal structure, melting point and solid fat index. The melting point of the supplied material is crucial to the melt extrusion process. Pre and post-processing parameters might be altered according to the melting point of deposited layers and the triglyceride composition (Godoi *et al.,* 2016).

According to studies, variations in the melting points of fatty acids have an impact on the softness or firmness of the fat in meat, which in turn affects the qualities of meat in

terms of colour, texture and shelf-life. Because solid fat with a high melting point appears whiter than liquid fat, the amount of fatty acids in food has an impact on its colour. Because unsaturated fatty acids are rapidly oxidized, the fatty acids also affect how long meat will last (Wood *et al.,* 2004). Fat crystallization affects the structural integrity of printed chocolate items and larger fat globules result in printed cheese's darker hue.

2.10.4 Dietary fiber

Although dietary fibers are good for human health, they cannot be directly employed as 3D printing materials. Because most of the dietary fibers lack flexibility and have weak self-supporting characteristics. As a result, fibers are frequently combined with other materials or utilized as additives in 3D printing. Fiber addition causes a number of modifications, ranging from the material characteristics to textural adjustments made during post-printing activities (Lille *et al.,* 2018).

Severini *et al.* (2018) used mix of vegetables-fruits paste and collagen of fish for printing edible objects and observed that there was no significant change in sensorial characteristics, total phenolic content and antioxidant capacity of the resultant samples. There were significant geometric differences between model and final products.

Lille *et al.* (2018) studied the extrusion printability of protein and fiber mixtures. The best results were obtained with a material supply of 10% cold swelling starch, 15% skimmed milk powder, 30% rye bran, 35% oat protein concentrate, 45% faba bean protein concentrate and 60% semi-skimmed milk powder. Printability was impacted by the fiber content of the material source.

2.11 3D PRINTING OF CHOCOLATE

Chocolate is the most widely used material for 3D food printing. Because it can be easily modulated to any formulations and in most cases it doesn't requires any post processing. By choosing chocolate as the raw material, ready to eat end products can be obtained. Chocolate is commonly printed using hot melt extrusion technology.

Rando and Ramaioli (2020) studied the effect of heat transfer on print stability of chocolate. They investigated the rheological, heat-transfer and manufacturing parameters of dark chocolate. IR Thermography was used to measure how the temperature changed throughout the procedure. It was discovered that the build plate temperature, external air temperature and printing velocity all affected the material temperature after deposition. Environmental temperatures of 20°C with a printing velocity of 4 mm/s and 18°C with a printing velocity between 4-12 mm/s produced stable structures.

Mantihal *et al.* (2018) studied the textural modification of 3D printed dark chocolate by varying internal infill structure. By varying the infill percentage to 5%, 30%, 60%, and 100% for patterns such the Hilbert curve, honeycomb and star, this study examined complex interior structure. Thus noted that for all three designs with infill density 5%, voids ranged from $60.8 \pm 2.1\%$ to $72.2 \pm 1.8\%$ and for samples with infill density 30% it varies from $20.9 \pm 2.1\%$ to $49.2 \pm 3.6\%$ while with 60% it ranged from $11.6 \pm 2.3\%$ to $19.4 \pm 4.2\%$. For 100% infill density, printed chocolate was less hard in snap test.

Lanaro *et al.* (2017) evaluated the melt extrusion 3D printer to enable printing complex 3D objects from chocolate. Spanning distance ability of extruded chocolate without collapsing was also studied. The outcomes demonstrated that extrusion rate was 10-20% leaner and that spanning distance was unaffected by printing speed, which ranged from 300-700 mm/min. It was also discovered that blowing air at the printing component increases spanning distance and lowers temperature by about 3.5°C.

Mantihal *et al.* (2017) conducted a study on optimization of chocolate 3D printing by correlating thermal and flow properties with 3D structure modeling. With various support systems, including cross support, parallel support and no support, the study examined the snapping characteristics of chocolate. The product's dimensions, weight and physical characteristics, such as melting characteristics, flow behaviour and snap ability, were examined. The outcomes demonstrated that the wall thickness varied along the height

as a result of the uneven deposition of the chocolate layer. Support structures give the samples more breaking strength and cross-supported samples take a lot of force to shatter.

Mantihal *et al.* (2019) studied the effect of additives on thermal, rheological and tribological properties of 3D printed dark chocolate. Food additives like plant sterol (PS) powder and magnesium stearate (Mg-ST) were used. The melting temperatures of the control and printed chocolate samples with the addition of food additives did not differ significantly and the yield stress of the product was comparatively greater than the control samples. As coefficient of friction of sample increased and reduced slippage during auger extrusion, additives had a significant impact on lubrication behaviour.

Hao *et al.* (2010) developed an additive layer manufacturing process for chocolate (ChocALM) to study the extrusion behavior of chocolate. The findings demonstrated that key parameters for smooth deposition, including nozzle diameter, nozzle height, nozzle velocity and extrusion rate, must be optimized in order for the system to produce 3D chocolates of the desired quality.

Karavasili *et al.* (2020) developed 3D printed chocolate-based oral dosage forms with the addition of hydrophilic and lipophilic drugs for pediatrics using extrusion-based 3D printing. Along with physicochemical research like Fourier-Transform infrared spectroscopy, X-Ray diffraction, particle size distribution and differential scanning calorimetry, texture profile analysis, rheological studies and in vitro digestion experiments were carried out. It was discovered that the technique enables precise dosage level adjustments and patient participation in the customization of the finished product's design, organoleptic features and textural qualities.

CHAPTER III

MATERIALS AND METHODS

This chapter involves the materials and methods used for the 3D printing of chocolate enriched with the dietary fiber of coconut. The section describes the methods for the formulation of printing ink, the optimization of 3D printing process parameters and the procedures used for the quality analysis of the developed 3D printed coconut-based chocolate.

Ingredients

↓

Pre-Processing

↓

Formulation of Ink

↓

Supply Material

↓

Feeding to Tank

↓

Printer Head

↓

Nozzle Tip

↓

Deposition Platform

↓

3D Printed Product

↓

Post- Processing

↓
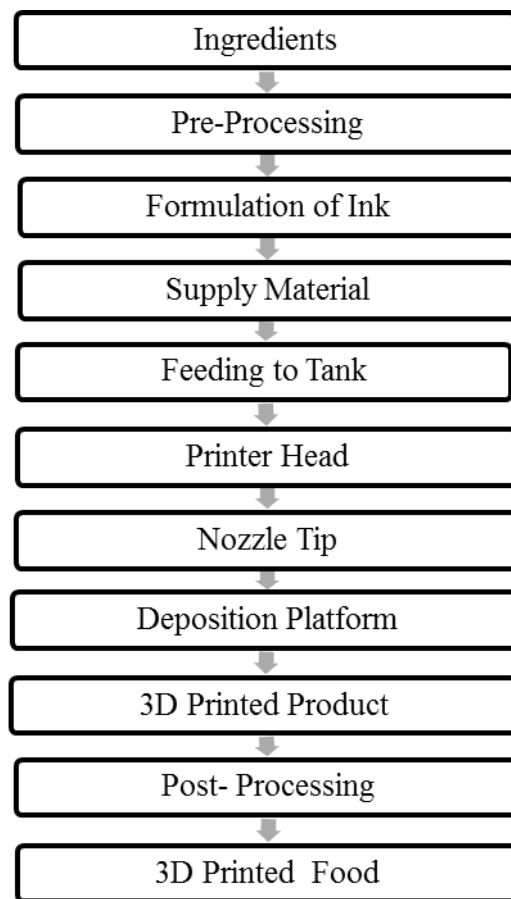
3D Printed Food

Fig. 3.1 Schematic flow diagram of 3D food printing process

3D printing of foods follows a well-defined sequential process (Fig.3.1). This begins with the designing of a 3D model of the required geometry and slicing software to

slice this 3D design into machine-readable codes for the 3D food printer. Natively printable materials like chocolate can be easily got printed and for some other ingredients pre-processing techniques have to be applied. These ingredients along with flow enhancers are mixed to obtain a suitable supply material with uniform particle distribution and flow ability. The formulated supply material was filled into the feed tank of the 3D printer and transferred to the extrusion head using connecting tubes. Based on extrusion technology the supply ink gets extruded through the nozzle tip to the deposition platform under proper machine conditions according to the 3D design attached. Some products have to be post-processed (baking, frying, and cooling) to obtain the final product (Brown *et al.,* 2014).

3.1 MATERIALS

The printing supply material (ink) was prepared using Mello dark compound chocolate (3F Industries Ltd. Telangana), obtained from the local dealers at Thrissur. Similarly, coconut, sugar and flow enhancer (soya lecithin) were also purchased from the local dealers.

The dark compound chocolate was composed of 58% cocoa solid (non-fat), 33% cocoa butter, anhydrous milk fat (5%), soy lecithin (0.5%) and salt (Mantihal *et al.,* 2017). Soya lecithin (E322) was a food-grade emulsifier added to melted chocolate to make a silky smooth texture. Coconut meal was obtained by removing the fat in the grated coconut. Grated coconut was defatted manually two or more times using a muslin cloth to remove maximum amount of fat content. Defatted coconut was dried at 60ºC for 60 to 90 minutes using a tray drier and powdered using a mixer grinder. Defatted powered coconut meal was sieved with a 60 ASTM sieve for obtaining uniform particle size.

3.2 3D FOOD PRINTER

Simplify 3D software was used to design the 3D structure for printing (Fig. 3.2). The model was fabricated in the shape of 'gear' with dimensions 41.50 mm × 41.50 mm × 10.00 mm. Stereolithography (STL.) files were obtained from the software and this slicing

software was used to slice the 3D design into layers by generating G-codes and M-codes that suit the 3D food printer. G-codes refer to the numerical control language to direct printing motors, printing speed and printing axis. M-codes refer to auxiliary commands that assist the functioning of the machine.
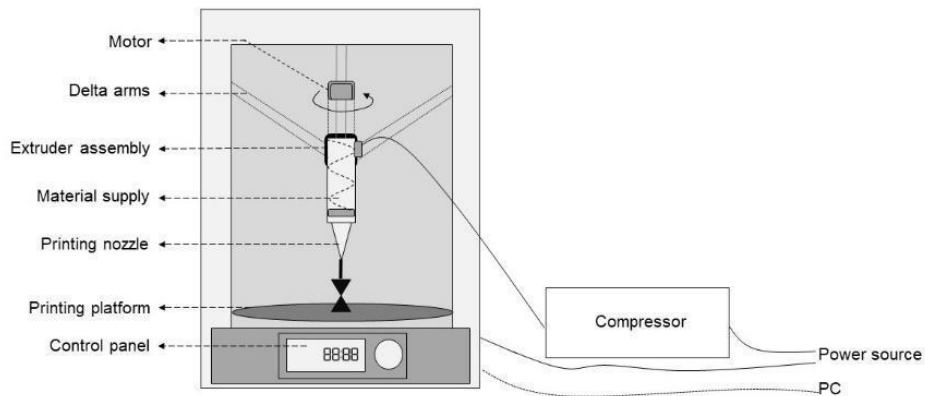
Fig. 3.2 Schematic diagram of 3D food printer

(Source: Anukiruthika *et al.,* 2020)

FABFORGE 3D food printer was used to print chocolate samples. The printer was operated at 230 V AC, 50/60 Hz, and involved instantaneous movement of the print head in X, Y and Z axes based on the design uploaded. X and Y-axis movement speeds were kept at 100 mm/s and the Z-axis movement speed was at 5 mm/s. The design was in STL format and was uploaded into the slicing software, Simplify 3D (ver. 4.1.0) that it converts the information of the 3D design into machine-readable G and M codes. A 3D design of 'gear' with dimensions 41.50 mm $\times$ 41.50 mm $\times$ 10.00 mm was used for 3D printing studies (Fig.3.3). All the printing trials were conducted at ambient temperature ($30 \pm 2°C$).
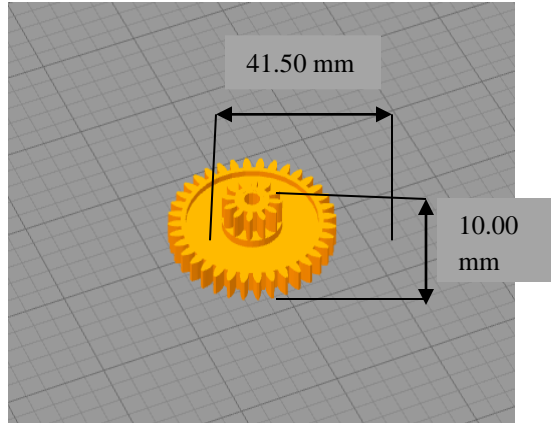
Fig. 3.3 3D Model of Gear

3.3 EXPERIMENTAL DESIGN FOR COCONUT BASED CHOCOLATE

3.3.1 Preparation of printing ink

Independent variables

1. Coconut: chocolate ratio
2. Flow enhancer percentage

3.3.2 Optimization of 3D printing process parameters

Fixed variables

1. Printing formulation
2. Shape geometry/ dimension
3. Extruder temperature
4. Infill percentage
5. Layer thickness
6. Bed temperature
7. Post-processing
8. Melting point

Independent variables

1. Extruder motor speed (S1, S2, S3)

2. Conveying air pressure (P1, P2, P3)

3. Nozzle diameter (R1, R2, R3)

4. Printing speed (PS1, PS2, PS3)

3.3.3 Quality analysis of printed products

1. Proximate composition
2. Sensory analysis

3.4 PREPARATION OF PRINTING INK

Dark compound chocolate was melted by double boiling. Coconut meal (6-12%), sugar powder (3%) and soya lecithin (0.1-0.5%) was added to melted dark compound chocolate to obtain the supply material for printing. The supply material was thoroughly mixed to make a semi-solid form without any lumps. The composition optimization was based on Response Surface Methodology (No. of runs: 13) with two variables (Table 3.1).

Table 3.1 Experimental condition for the optimization of composition for printing ink

Run	Coconut meal (%)	Flow Enhancer (%)
1	9	0.30
2	9	0.30
3	9	0.30
4	9	0.02
5	6	0.10
6	13.24	0.30
7	12	0.50
8	4.76	0.30
9	9	0.58
10	12	0.10
11	6	0.50
12	9	0.30
13	9	0.30

The supply material was filled into the cylindrical syringe barrel (tank) of 30 cc capacity and fed to the FABFORGE 3D food printer. The extrusion type 3D food printer consists of a print head with an extrusion assembly, an XYZ printing axis equipped with individual stepper DC motors, a feed syringe barrel system, a printing stage and a compressor unit (hp).

Plate 3.1 FABFORGE 3D FOOD PRINTER

Printing parameters such as printing speed (50 mm/s), motor speed (30 rpm), nozzle diameter (1.2 mm) and air pressure (2 bar) were set based on correlations between the thermal and flow behaviour of the chocolate. The printed samples were stored in refrigeration at around 15°C until quality assessment analysis. Optimization of supply material was carried out based on the sensory scores such as colour, appearance, flavour and overall acceptability.
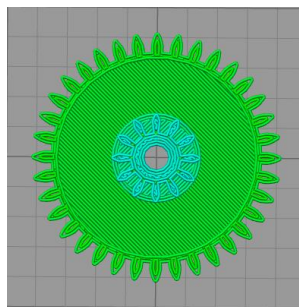
Fig. 3.4 3D Design of 'Gear' used for prototype

3.5 OPTIMIZATION OF 3D FOOD PRINTING PROCESS PARAMETERS

The printability was assessed by considering printing parameters like nozzle size, extrusion motor speed, printing speed and conveying air pressure. For the optimization of printing parameters, the supply material was manually fed into the syringe barrel and subjected to various printing speeds of 50, 60 and 70 mm/s using three different nozzle diameters (0.82, 1.20, and 1.55 mm), at extrusion motor speed of 20, 30, 40 rpm and varying air pressure of 2, 3 and 4 bar. A 3D design of 'gear' with dimensions 41.50 mm × 41.50 mm × 10.00 mm (Fig. 3.4) was used for 3D printing studies. The dependent parameters for which the optimization of process parameters was done include extrusion rate, printing rate, texture, color, moisture content, weight and dimension. The printing experiments were conducted at room temperature. Good hygienic practices were maintained throughout the printing process to avoid contamination during the experiments. The process parameters optimization was based on Response Surface Methodology (No. of runs: 29) with four variables (Table 3.2).

Table 3.2 Experimental condition for the optimization of 3D food printing process parameters

Run	Motor speed (rpm)	Air Pressure (bar)	Nozzle Diameter (mm)	Printing Speed (mm/s)
1	20	2	1.2	60
2	40	2	1.2	60
3	20	4	1.2	60
4	40	4	1.2	60
5	30	3	1.2	60
6	30	3	1.2	60
7	30	3	1.2	60
8	20	3	1.2	50
9	40	3	1.2	50
10	30	2	1.2	50
11	30	4	1.2	50
12	30	2	1.55	60
13	20	3	1.55	60
14	40	3	1.55	60
15	30	4	1.55	60

16	30	3	1.55	50
17	30	3	1.55	70
18	30	2	0.84	60
19	30	4	0.84	60
20	20	3	0.84	60
21	40	3	0.84	60
22	40	3	1.2	70
23	20	3	1.2	70
24	30	2	1.2	70
25	30	4	1.2	70
26	30	3	0.84	50
27	30	3	0.84	70
28	30	3	1.2	60
29	30	3	1.2	60

3.6 QUALITY EVALUATION OF THE DEVELOPED 3D PRODUCT

Quality evaluation included the study of sensory characteristics, textural properties, rheological properties and determination of biological, physical, and chemical quality parameters.

3.6.1 Analysis of quality parameters

Quality parameters were analyzed based on the objectives of the study. During the printing ink formulation, sensory scores like texture, colour, appearance, flavor and overall acceptability were assessed by sensory analysis and parameters such as moisture content, water activity and viscosity were also determined. Extrusion rate, printing rate, texture, colour, moisture content, weight and dimension of printed products were evaluated during the optimization of process parameters. Further, the final 3D printed product was subjected to quality analysis like texture, colour, water activity and moisture content.

3.6.1.1 Textural characterization of 3D printed chocolate

A texture analyzer (SHIMADZU, EZ Test, E Z-SX, Japan) was used to evaluate the textural properties of the samples. The instrument was calibrated with a 500 N load cell and fitted with a cutting probe. The parameters for testing were as follows: pretest speed 1

mm/s, test speed 0.5 mm/s, post-test speed 1 mm/s, trigger force 0.1 N, at room temperature (25 ± 1°C) (Yang *et al.,* 2017).

3.6.1.2 Colour

Colour analysis is the most important determinant of the acceptability of the product. It was determined by using a Hunter lab colorimeter (Serial Number: MSEZ2294, Model Number: 4500L, Hunter Associates Laboratory, USA) and colour of the optimized supply material was compared to the colour of the control chocolate (Anukiruthika *et al.,* 2020).

The readings were made in *L*, a* and b** colour scale. The colour value change between control chocolate and optimized supply material was determined using the equation:

$$\Delta E = \sqrt{\Delta L^{*2} + \Delta a^{*2} + \Delta b^{*2}} \qquad (1)$$

3.6.1.3 Water activity measurement

Water activity (a_w) is a significant factor affecting the shelf life of the product. The water activity of the supply material was determined using the Pre Aqua Lab water activity analyzer (SN: PRE001205, Decagon Devices, Inc. Pullman, WA, USA) with ± 0.001 sensitivity (Theagarajan *et al.,* 2019).

3.6.1.4 Moisture Content

The moisture content of each chocolate sample was determined by using an electronic moisture analyzer (Sartorius Moisture Analyzer, Model: MA 37, Germany). Samples of 2 g weight were placed in a pan at 100ºC and the measurements were noted (Ibrahim *et al.,* 2020).

3.6.1.5 Rheological characterization

Rheological measurements were performed in a shear-controlled Physica MCR 52 rheometer (Anton Paar GmbH, Graz, Austria) with a concentric cylinder system/CC27 having a diameter of 26,662 nm, length 40,013 and a concentricity of 6 µm. Before

measurements, samples were liquefied in the water bath and kept at $50 \pm 3°C$ for one hour to ensure that no fat crystals remained in the sample. The measurement was according to the IOCCC 2000, with an additional waiting time of 300 s before the actual measurement started, to ensure temperature equilibration. The temperature was set to 30°C. Shear stress was measured at 30°C ($\pm 0.1°C$) as a function of increasing shear rate from 2 to 50/ s 1 with 18 positions 180 s (upward), then decreasing from 50 to 2/ s duration 180s (downward). The Casson model was used to calculate Casson yield values from interpolation data using rheoplus software (Feichtinger *et al.*, 2020).

3.6.1.6 Extrusion Rate

The extrusion rate (mm^3/s) was calculated according to Yang *et al.*, (2017) using the equation:

$$V_d = \pi/4 \, v_n D_n{}^2 \tag{2}$$

where,

V_d is the volume of material extruded (mm^3/s), v_n is the nozzle moving speed (mm/s) and D_n is the nozzle diameter (mm).

3.6.1.7 Printing rate

The printing rate was calculated by dividing the weight of the 3D printed product by printing time to determine the amount of chocolate printed per minute (Mantihal *et al.*, 2017).

$$\text{Printing rate} \left(\frac{g}{min}\right) = \text{Total weight of printed object (g)/ Printing time (min)} \tag{3}$$

3.6.1.8 Dimensional evaluation of 3D printed chocolate

A digital weighing balance was used to determine the weight of each printed chocolate. A digital caliper (0-150 mm, ± 0.002 accuracy, Absolute AOS, DIGIMATIC, Japan) was used to measure the diameter and thickness of 3D printed chocolate

(Mantihal *et al.*, 2019). The measurements (diameter and thickness) were done in three different locations on each printed samples and the average value was reported.

3.6.1.9 Sensory evaluation

3D food printing technology has the unique capability to construct designs with complex internal patterns and customized shapes (Liu *et al.*, 2019). In this study, 3D printed chocolate products were subjected to sensory analysis for their texture, colour, appearance, flavour, taste and overall acceptability. Around 20 semi-trained panel members assessed the printed products attributes against a 9-point hedonic scale with 9 representing 'like extremely' to 1 representing 'dislike extremely' (Saldana *et al.*, 2019).

3.6.1.10 Proximate Analysis

The nutritional profile of the end product was analyzed through a proximate analysis. The carbohydrates, crude protein, fat, ash and crude fiber content of the end product were analyzed using AOAC methods (AOAC, 21st edition, 2019).

3.7 STATISTICAL ANALYSIS

Response surface methodology (RSM) was done in Design-Expert software for evaluating the experimental data and optimizing the conditions for product development. Central Composite Design (CCD) was used for the preparation of printing ink and Box-Behnken Design (BBD) was used for the optimization of 3D printing process parameters.

CHAPTER IV

RESULTS AND DISCUSSION

The study was undertaken to develop coconut based chocolate by 3D printing technology. The methodology was formulated to optimize the printing ink and the process for the hot melt extrusion 3D printing of chocolate enriched with coconut dietary fiber. Accordingly, the experiments were carried out and the results are included in this section. The optimal process for the coconut based chocolate by 3D food printing technology has been discussed.

4.1 PRINTING INK FORMULATION

Supply material composition is an important factor that decides the final quality of the 3D printed chocolate products. Since, chocolate is a natively printable material, it gets easily printed by hot-melt extrusion process. For the optimization of printing ink based on the central composite design by response surface methodology (RSM), thirteen different sample compositions were prepared using dark compound chocolate, coconut meal, soya lecithin and sugar. According to the preliminary tests (line test), each sample were printed at 2 bar air pressure, 60 mm/s printing speed with 20 rpm motor speed, using 1.2 mm nozzle diameter which produce stable 3D printed products sufficient to represent the 3D design geometry (with desired accuracy and precision).

The study showed that the material composition had significant influence on the 3D food printing quality. A notable effect on printability and viscosity factors were reflected. The sensory scores were utilized to optimize the best composition capable of 3D printing fortified chocolate. The details of the results obtained for optimization of material composition are given in the following sections.

4.1.1 Effect of material composition of printing ink on printability

Commercial dark compound chocolate was able to be printed using this hot-melt extrusion 3D food printer. On fortification with coconut, the dark compound chocolate exhibited complex printing process behavior. Because the dietary fiber content made some changes on the physicochemical properties of the chocolate and becomes solid which leads to the clotting of supply material on the tank, connecting tubes and extrusion screw. To avoid this condition, flow enhancer (soya lecithin) was used to retain the flowability of the chocolate by making it into a semi solid form without any lump. The textural characteristics of the chocolate-coconut meal (dietary fiber) mixture were also influenced by the soya lecithin. Supply material composition with soya lecithin content gave better printability and flow.

4.1.2 Effect of material composition of printing ink on Viscosity

In 3D extrusion food printing, rheological characteristics of the supply material is the critical parameter that explains its visco-elasticity. Dark compound chocolate is a solid food product, which can be made into semisolid form by melting it. The viscosity of the semisolid form of supply material influences the printability of the product. The supply material should have a suitable viscosity for the easy flow and printing of the product. Also, printability is a function of viscosity, concentration, material flow rate, printing speed and nozzle diameter (Anukiruthika *et al.,* 2020).

An ideal 3D food printing material for extrusion based printing should possess viscosity high enough to be cohesive and low enough to the easy flow of material supply, so as to remain stable without any deformation of previous layers during deposition of material (Liu *et al.,* 2017). The viscosity flow curves of supply material with different composition are shown in Fig. 4.1. Results showed that viscosity of supply material decreases with increase in shear rate. This clearly depicts that the material supply exhibits pseudoplastic behaviour which can easily flow through the printing nozzle (Liu *et al.,* 2019). Table 4.1 showed that the viscosity values were ranged between 24.2-6.15 Pa s. The

47

sample with a composition of 9% coconut meal, 3% sugar, 0.02% soya lecithin and 87.98% chocolate showed high viscosity of 24.2 Pa s and sample with 9% coconut meal, 3% sugar, 0.3% soya lecithin and 87.7% chocolate gave low viscosity value of 6.15 Pa s. The control sample (dark compound chocolate) had a viscosity value of 1.33 Pa s. Soya lecithin content had considerable effect on the viscosity of the supply material compositions (Nebesny *et al.* 2005). Supply material with high amount soya lecithin gave low viscosity value and small concentration of soya lecithin didn't have much effect on the viscosity and flow characteristics of supply material.

Fig. 4.1 Viscosity flow curve of supply material with different composition
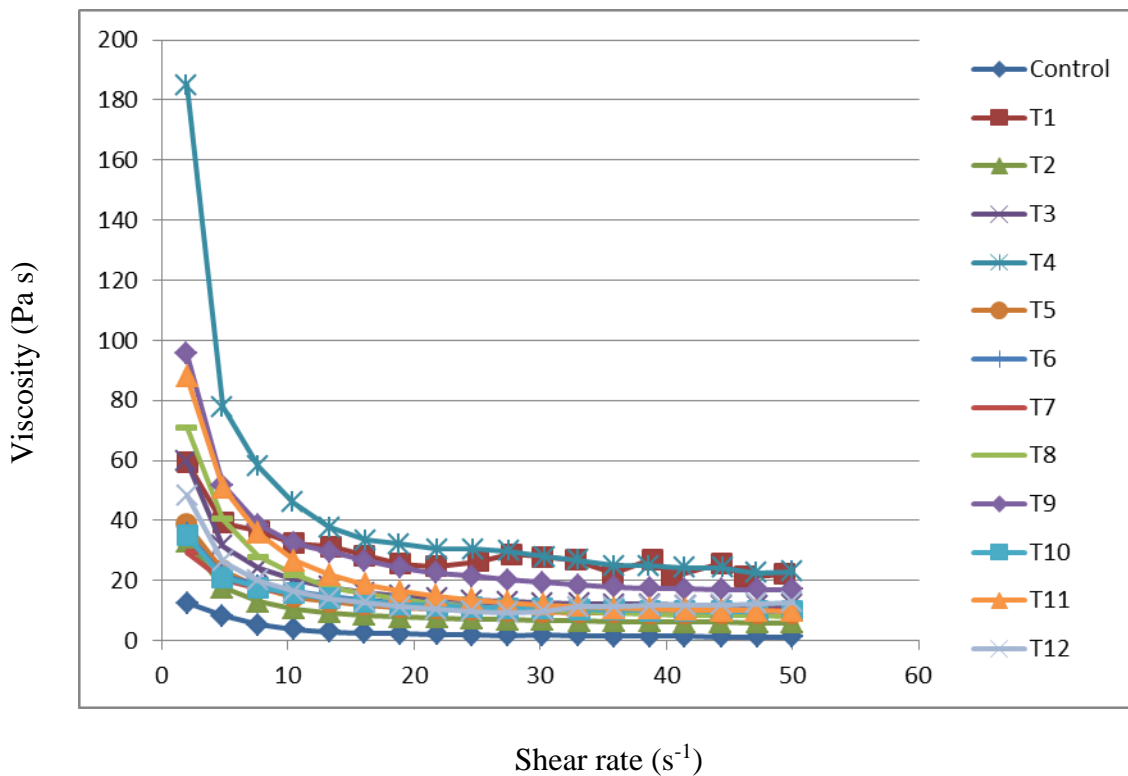
The extrudability of food inks was done by evaluating the yield stress of the supply material. The sample with higher value of yield stress was regarded as the suitable supply material that could maintain their 3D shapes during and after printing (Kim *et al.*, 2018). Yield stress curves of supply material with different composition are shown in Fig. 4.2.

Results showed that yield stress of supply material decreases with decrease in shear rate. The yield stress values ranged between 85.5-372 Pa. The control sample has a yield stress value of 39.9 Pa. The sample with a composition of 9% coconut meal, 3% sugar, 0.02% soya lecithin and 87.98% chocolate showed high yield stress of 372 Pa and sample with 9% coconut meal, 3% sugar, 0.3% soya lecithin and 87.7% chocolate gave low yield stress value of 85.5 Pa.

Fig. 4.2 Yield stress curve of supply material with different composition

Shear rate (s^{-1})
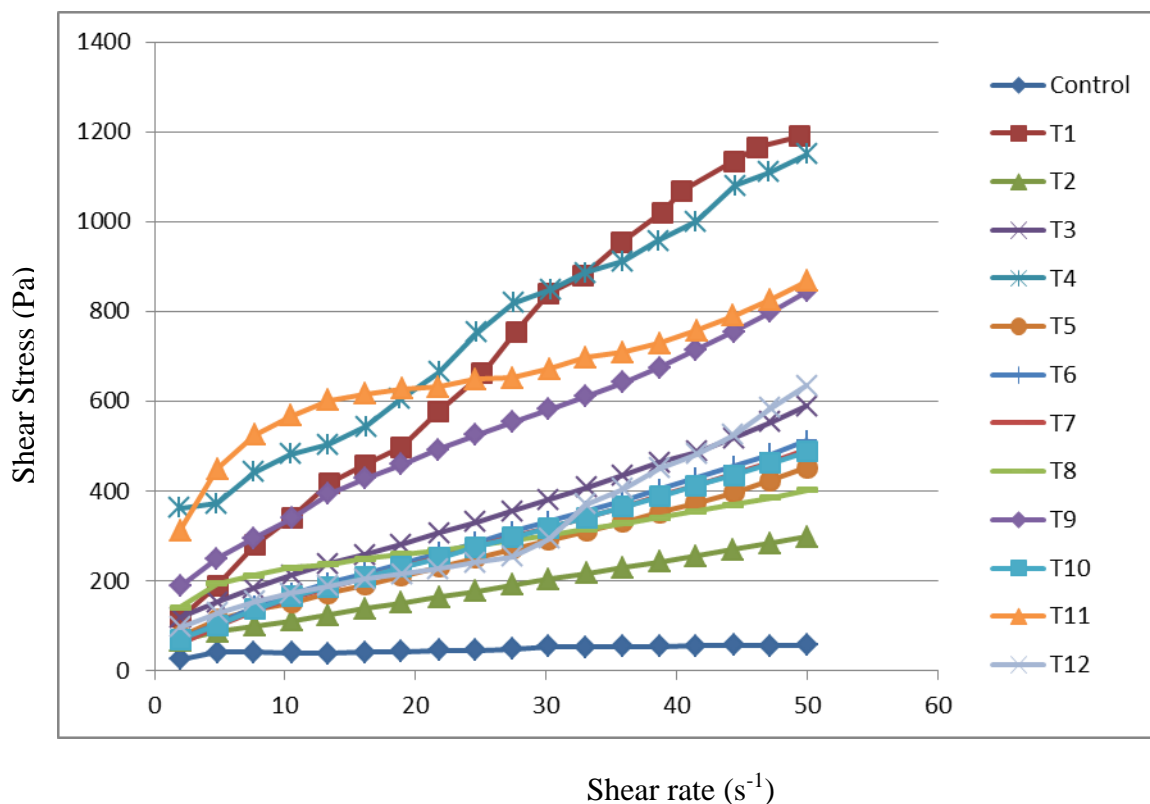
4.1.3 Dynamic Rheological Analysis

The flowability and post-printing stability of supply material ink was measured by evaluating the dynamic visco-elastic properties. The storage modulus (elastic modulus) (G′) and loss modulus (viscous modulus) (G″) measurements were included in this dynamic visco-elastic properties. The mechanical strength and the ability of the supply material to have an elastic solid-like behavior were indicated by the G' values (Wilson *et al.,* 2020). It

represents the deformation energy stored in the sample during the shear process (Angioloni and Collar, 2009).On the other hand, G'' reflects the viscous nature of the supply material that indicates the amount of energy dissipated during each deformation cycle (Theagarajan *et al.,* 2020). Fig 4.3 shows the dependence of storage modulus and loss modulus on the angular frequency.

Fig. 4.3 Dynamic viscoelastic properties of the supply material.

(a) Storage modulus, (b) Loss modulus.
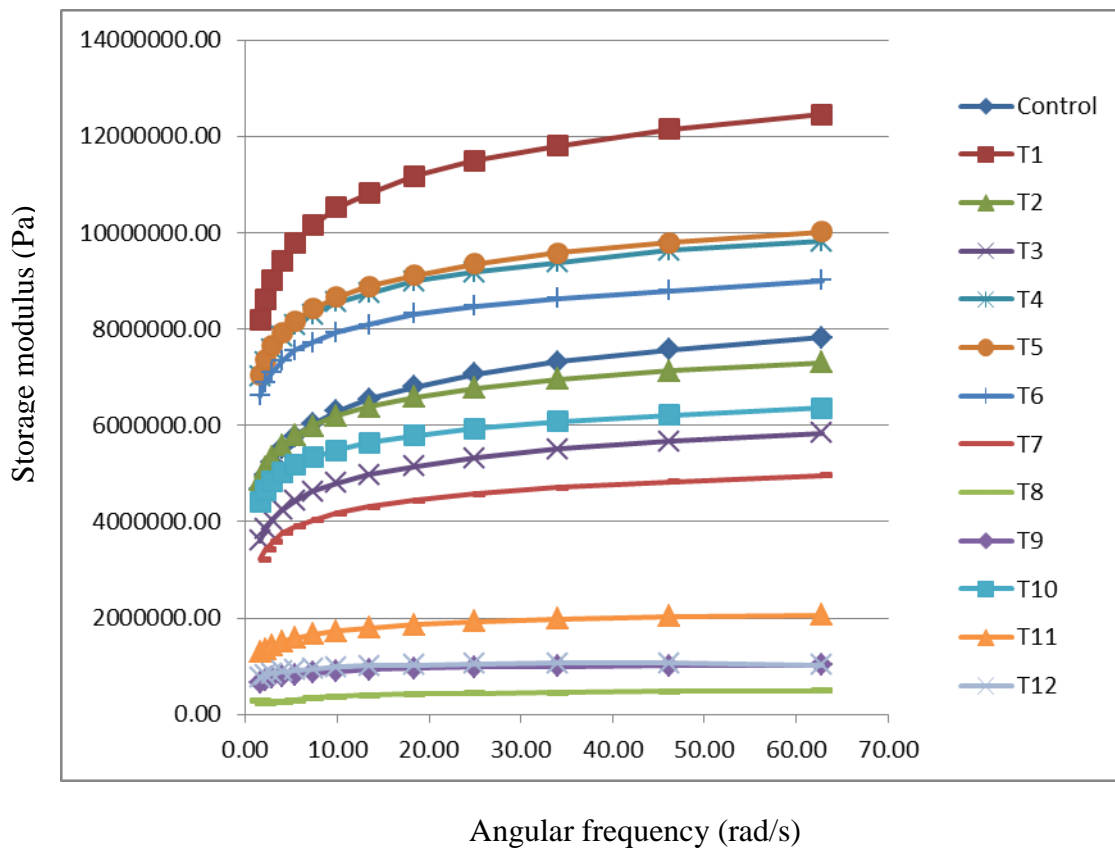
(a)
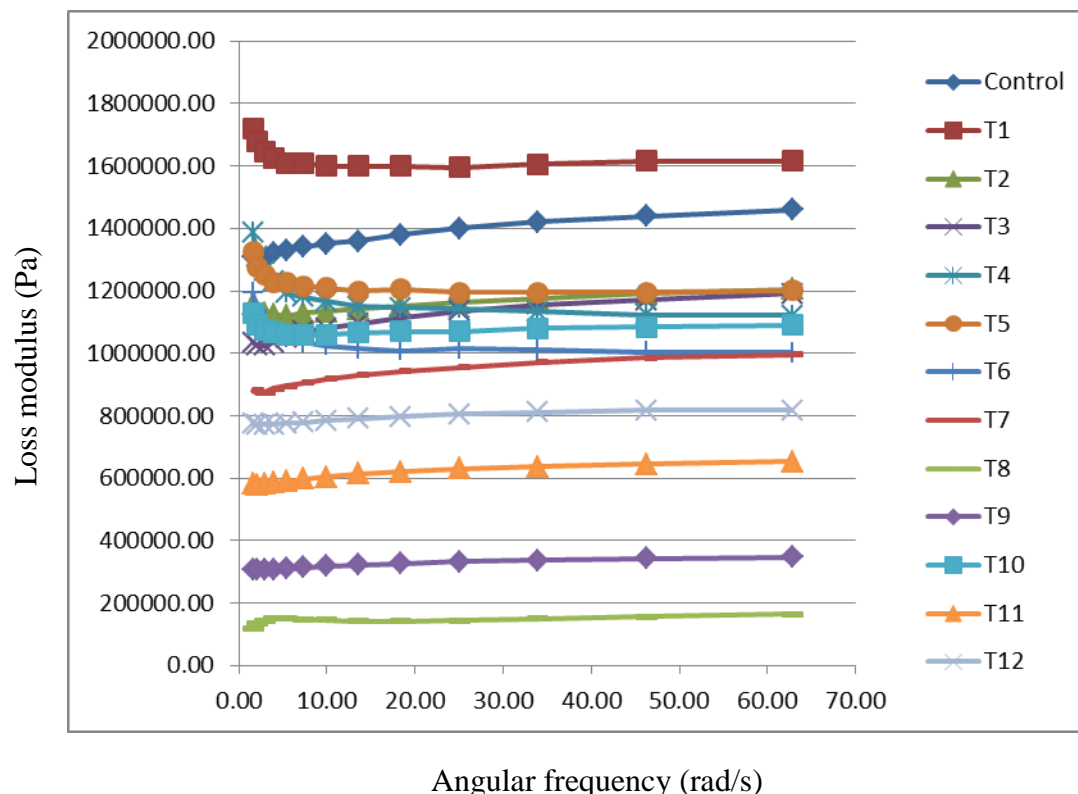
(b)

Results showed that G' increased gradually with increasing angular frequency. It was found that the G' values was higher than G'' for all supply materials explaining the solid-elastic nature of the materials. Under non destructive conditions the elasticity has a predominant effect on viscosity (Peressini *et al.* 2006). This was an important aspect of the supply material ink, having the capacity to hold the 3D-printed shape used in extrusion-based 3D printing (Yang *et al*. 2018). Johansson and Bergensthal (1992) reported that the high value of G' was due to the high level interactive forces between particles, which confirms the high amount of stress requirement to start the flow. The low values of G'' were found on the supply materials due to the high amount soya lecithin content (0.3 and 0.5%). Johansson and Bergensthal (1992) also reported similar results on the effect of emulsifiers on the sugar particles, reducing the changing in the interaction particles and in the network structure ones.

4.1.4 Effect of material composition on sensory scores

Sensory scores such as texture, colour, appearance, flavor and overall acceptability of the different supply material composition was done based on the 9-point hedonic scale. Table 4.1 shows the grades of sensory scores for the optimization of material composition. Almost all compositions didn't have any considerable effect on the sensory scores like colour and appearance. Actually the aim of the study was to develop a 3D printed product enriched with dietary fiber without the taste of coconut meal. The sample with high amount of dietary fiber (13.24% coconut meal) taste and flavored like coconut which may cause non-satisfaction during consumption. Thus the amount of coconut meal in the supply material has to be reduced. Emulsifier such as soya lecithin was commonly used in chocolate products to maintain the texture of the dark compound chocolate along with the additional ingredients to make the supply material (Afoakwa *et al.,* 2008). High quantity of soya lecithin gave smooth texture and small amount of soya lecithin didn't have any effect on the texture and printability of chocolate.

Table 4.1 Effect of material composition on viscosity, sensory scores, moisture content and water activity

Trial	Water activity	Moisture content (%)	Viscosity (Pa s)	Sensory Score					
				Texture	Colour	Taste	Flavour	Appearance	Overall acceptability
T1	0.567	0.27	21.1	9	8	9	7	8	8
T2	0.565	0.22	6.15	8	8	8	7	7	9
T3	0.577	0.4	11.7	9	8	9	9	8	9
T4	0.585	0.34	24.2	7	7	7	9	8	9
T5	0.554	0.26	8.98	8	7	7	6	7	8
T6	0.585	0.35	10.3	6	7	6	6	7	7
T7	0.573	0.41	9.95	6	6	6	6	6	6
T8	0.56	0.18	8.55	8	7	7	7	8	8

T9	0.569	0.39	17.2	7	8	8	8	6	6
T10	0.573	0.23	9.89	6	7	6	6	7	8
T11	0.558	0.527	10.27	7	8	8	8	6	7
T12	0.578	0.42	11.61	8	6	7	7	8	8
T13	0.565	0.38	10.54	7	7	7	8	7	8

4.1.5 Effect of material composition on Water activity and Moisture content

Water activity is the amount of water present in the food material in which the microorganism can grow. The microbiological and biochemical activity within the food product will be prevented if the water activity was lower than 0.6 (Kha *et al.,* 2010). The low concentration of flow enhancer reduced the water activity. From the Table 4.1, the lowest water activity was found for the combination with 6% coconut meal and 0.1% soya lecithin. The sample combination with 9% coconut meal and 0.03% soya lecithin had the highest value of water activity having process parameters such as extruder temperature 32°C, nozzle diameter of 1.2 mm and 2 bar external pressure.

Moisture content is the total amount of water present in the food product which determines the shelf life of the final products. The moisture content of the supply materials was ranged from 0.18-0.52% (Table 4.1). The amount of moisture was lower for the sample formulation with 4.76% coconut meal and 0.30% soya lecithin and the higher moisture content was found for the sample with 6% coconut meal and 0.50% soya lecithin. All samples were printed at 32°C temperature, 2 bar pressure, 1.2 mm nozzle diameter and 30 rpm motor speed. From the results it was concluded that the moisture content increased with increase in the concentration of soya lecithin. Sample with very low amount of soya lecithin showed minimum value for moisture content. Studies were reported on the variation of water activity, moisture content with respect to temperature and no studies have reported the variation of the same according to the changes in the composition of supply materials.

4.1.6 Optimization of supply material for 3D printing of chocolate

Comparing the different supply material composition, the material with soya lecithin showed better flow ability and printability. The supply materials with high proportion of soya lecithin (> 0.50%) exhibit over extrusion due to the higher flowability and made the printed sample difficult to retain the shape of product. On the other hand, the supply material with low proportion of soya lecithin (<0.10%) was found to be ineffective in making considerable changes in the composition of printing samples. Thus, from the three different proportions (0.1, 0.3, and 0.5%) of soya lecithin, 0.3% was selected for final composition. Afoakwa *et al.* (2008) used similar proportion of soya lecithin content in their study of rheological, textural and melting properties of dark chocolate. Actually the aim of the study was to develop a chocolate product enriched with coconut dietary fiber without the taste and flavor of coconut. The results of trials showed that coconut meal content higher than 12% highly influences the taste and flavour of the chocolate products and thus we have to reduce the amount of coconut meal in the supply material within 12%. For balancing the bitter taste of the dark compound chocolate, a fixed amount of sugar powder (3%) having uniform size was added to the final supply material composition.

The printed samples were subjected to sensory analysis such as texture, colour, appearance, flavour and overall acceptability based on 9-point hedonic scale. Moisture content, water activity and flow characteristics of the samples were also determined. Based on the trials and result of these analyses, the supply material composition with 9% coconut meal, 3% sugar, 0.3% soya lecithin and 87.7% dark compound chocolate was finalized for the evaluation of remaining objectives.

4.2 OPTIMISATION OF 3D PRINTING PROCESS PARAMETERS FOR COCONUT BASED CHOCOLATE

3D printing process parameters had a vital role on the appearance and quality of the final printed products. Four important process parameters such as extruder motor speed, nozzle diameter, conveying air pressure and printing speed were considered as independent

variables and the study focused on the effects happening to the final printed products by changing these parameters. For the optimization of printing process parameters, the optimized supply material composition were printed with twenty nine different combination of the four process parameters based on the central composite design by RSM as given in Table 3.2. During the optimization of printing process parameters, variables such as printing formulation, shape geometry, extruder temperature, infill percentage, layer thickness, bed temperature, melting point and post processing were fixed.

4.2.1 Effect of 3D printing process parameters on printability

Optimized supply material composition with 9% coconut meal, 3% sugar, 0.3% soya lecithin and 87.7% dark compound chocolate were used for study the effect of 3D printing process parameters on printability. Based on the preliminary tests, three different variations of four process parameters such as printing speed (50, 60, 70 mm/s), extruder motor speed (20, 30, 40 rpm), nozzle diameter (0.84, 1.20, 1.55 mm) and conveying air pressure (2, 3, 4 bar) were considered. Table 4.2 shows the 3D printed chocolates products at various printing parameters.

Table 4.2 3D printed products with different printing parameters.

Diameter (mm)	Air Pressure (bar)	Motor Speed (rpm)	Printing Speed (mm/s)		
			50	60	70
0.84	2	20			
		30			
		40			
	3	20			

1.20		30			
		40			
	4	20			
		30			
		40			
	2	20			
		30			
		40			
	3	20			
		30			
		40			

	4	20			
		30			
		40			
1.55	2	20			
		30			
		40			
	3	20			
		30			
		40			
	4	20			
		30			
		40			

4.2.1.1 Printing Speed

The effect of printing speed could be determined by considering the time-dependent distance covered by the printing nozzle during 3D printing process. At higher printing speed (up to 75 mm/s), the printing was improper and had some structural defects in the final 3D products. Hence the printing speed was limited to a maximum of 70 mm/s for this study. Higher printing speed resulted in lower thread quality, accuracy and poor overall product finishing. The best print quality was obtained with a printing speed in the range of 50 to 60 mm/s. It provides consistent appearance, uniform layer thickness and good stacking behavior (Liu *et al.,* 2019). Printing at speeds lower than 40 mm/s required more time to complete and produce discontinuous threads. Derossi *et al.* (2018) reported that the distribution of pores in the product was also influenced by printing speed.

4.2.1.2 Extruder Motor speed

Motor speed decides the extrusion of the supply material from the syringe and the auger drive that is attached to the motor. The motor speed influences extrusion rate; higher motor speeds result in higher extrusion rates. In this study, motor speed in the range of 20, 30 and 40 rpm were selected. Higher rpm leads to back pressure. Motor speed between 20 and 40 rpm were found to be better for printability. Motor speed less than 15 rpm resulted in discontinuous threads or the material could not be extruded.

Maintaining reduced printing speeds (50 to 60 mm/min) with a motor speed between 20 and 30 rpm led to good printing quality. Lower motor speed with lower printing speed exhibited poor printability. Similarly, higher motor speed with higher printing speed leads to improper printing. On the other hand lower print speed with increased motor speed gave good printability. Studies conducted by Derossi *et al.* (2018) reported that higher motor speed results in improper structures with high porosity and it affect the characteristics of the end product.

4.2.1.3 Nozzle Diameter

Thread quality of the final printed product was influenced by the nozzle diameter. Three different nozzle diameters were selected for the study (0.84 mm, 1.2 mm, and 1.55 mm). Nozzle diameter of less than 0.84 mm was avoided due to some stuck of the supply material. Larger nozzle diameter (>1.55 mm) extruded thick threads and also the precision was poor. While printing through 0.84 mm and 1.2 mm nozzle diameter, printed product of better structure and shape could be achieved. Similar result was also reported by Theagarajan *et al.* (2020) on the study of 3D extrusion printability of rice starch. Therefore, nozzle diameters of 0.84 and 1.2 mm were preferred. Each nozzle diameters were evaluated by three different printing speeds, motor speeds and three different air pressures.

4.2.1.4 Conveying Air Pressure

Printing was done with the aid of air pressure from an external source. Three different air pressures were used (2, 3 and 4 bars) for the study. Pressure below 2 bar was avoided because it didn't have any influence on the force requirement for printing process. Air pressure between 2 and 3 bars provides better printing quality and good precision without any discontinuous layers. Increasing the pressure above 4 bar resulted in over extrusion of the supply material and made defects in the final structure of product. The extrusion behavior of printing material depends primarily on the type of supply material and the amount of pressure required for extrusion process (Severini *et al.,* 2016).

4.2.2 Effect of 3D printing process parameters on Extrusion rate

The most important parameter that determines the printability of a semi solid material is the extrusion rate, a function of extrusion printing speed and the nozzle diameter (Wilson *et al.,* 2020). The extrusion rate is defined as the volumetric flow of the supply material extruded in a given time which has a considerable effect on the quality of the end-product and printing precision.

There was a linear relationship between the extrusion rate and printing speed. Figure 4.3 shows that the extrusion rate increases with increase in nozzle diameter and printing speed which was statistically significant ($p<0.05$) as shown in the ANOVA table given in Appendix A1. For large nozzle diameter of 1.55 mm, higher printing speed results in higher extrusion rate than that of the small nozzle diameter of 0.84 mm. Thus, Table 4.3 shows the extrusion rate ranged from 94.34 to 132.08 mm^3/s and 27.70 to 38.79 mm^3/s for 1.55 mm and 0.82 mm nozzle, respectively. The addition of flow enhancer had significant effects on the flow ability and printability of the material supply that reflect the stability of printed 3D product (Table 4.3)

Extruder motor speed was directly proportional to the extrusion rate. A greater amount of supply material was extruded as motor speed increased. Diameter of printed material was larger than the actual diameter of nozzle at higher extrusion rates, resulting in spreading of the chocolate over a smaller area. This is due to the over extrusion of chocolate at high extrusion rate with increased nozzle diameter and applied air pressure which resulted in poor resolution of printed object (Wang *et al.,* 2017). Alternatively, at low extrusion rate, thickness of printed line was smaller with insufficient supply material flow and structural accuracy. Regression model fitted to experimental results of extrusion rate and it is given in Appendix A1. Following regression model was obtained to predict the extrusion rate of 3D printed coconut based chocolate is given as below

Extrusion rate $=67.86+39.98C+11.61D+6.66CD+5.37C^2-8.333E-005D^2$ .... (4.1)

where, C is the nozzle diameter and D is the printing speed. The p-value of the model was <0.05, which indicated that the model fitness was significant. By analysis of variance, the R^2 value of this model was determined to be 0.999, which showed that the regression model defined well the true behavior of the system.

Table 4.3 Effect of Printing Parameters on Extrusion rate and Printing Rate

Runs	Extrusion Rate (mm^3/s)	Printing Rate (g/min)
T1	67.858	1.271
T2	67.858	1.182
T3	67.858	1.175
T4	67.858	1.537
T5	67.858	1.346
T6	67.858	1.559
T7	67.858	1.332
T8	56.548	1.660
T9	56.548	1.246
T10	56.548	1.395
T11	56.548	1.298
T12	113.215	1.407
T13	113.215	1.451
T14	113.215	1.958
T15	113.215	1.899
T16	94.34	1.792
T17	132.08	1.338
T18	33.250	1.243
T19	33.250	1.229
T20	33.250	1.108
T21	33.250	1.150
T22	79.168	1.367
T23	79.168	1.473
T24	79.168	1.252
T25	79.168	1.366

T26	27.70	1.076
T27	38.79	1.179
T28	67.858	1.435
T29	67.858	1.356

4.2.3 Effect of 3D printing process parameters on printing rate

Printing rate of the 3D food printer was calculated by dividing the total weight of the printed product by the total printing time required for each sample (Mantihal *et al.* 2017). Table 4.3 shows that there was a considerable difference in printing rate of each sample with respect to the increase in nozzle diameter. Sample printed with 1.55 mm nozzle diameter, offered higher printing rate than sample printed with 0.84 mm diameter. Higher printing speed also influences the printing rate of the products (Mantihal *et al.* 2017). While comparing the printing rate with normal extrusion motor speed and air pressure, the higher motor speed and pressure had a significant effect ($p < 0.05$) on printing rate (Appendix A2). From the Figure 4.4 it was clear that the maximum printing rate (1.958 g/min) was observed with the 1.55 mm nozzle diameter at 60 mm/s printing speed, 40 rpm motor speed and 3 bar air pressure. Minimum printing rate (1.076 g/min) was obtained for the sample printed with 0.8 mm nozzle diameter at 50 mm/s printing speed, 30 rpm motor speed and 3 bar air pressure.

Some inconsistencies occurred during the layer by layer deposition of chocolate, resulting in minor deviations in the total weight of chocolate that have an impact on the chocolate. Another reason might be related with the limitations faced by the "slicing software" which is used for filament 3D-printers. This could affect the extrusion process in terms of extruder movement, printing speed and material deposition (Severini *et al.* 2016).

We can calculate the amount of chocolate required to make a single 3D product by determining printing rate of chocolate. Although printing rate varies between each sample, it was found that the printer is able for printing 3D products which were similar to design

from 3D software. Regression model fitted to experimental results of printing rate and it is given in Appendix A2. Following regression model was obtained to predict the printing rate of 3D printed coconut based chocolate.

Printing rate $=1.35+0.039A+0.011B+0.25C+0.052D+0.14AB+0.11AC-0.010AD-0.061BC-0.047BD-0.051CD-0.014A^2+0.24C^2-0.097D^2$ ……………..(4.2)

where, A is the extruder motor speed, B is the conveying air pressure, C is the nozzle diameter and D is the printing speed·

The p-value of the model was <0.05, which indicated that the model fitness was significant. By analysis of variance, the R^2 value of this model was determined to be 0.8450, which showed that the regression model defined well the true behavior of the system.
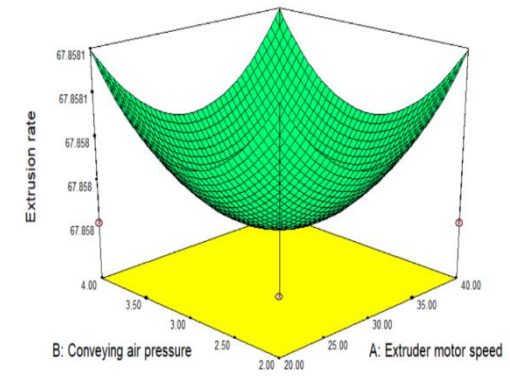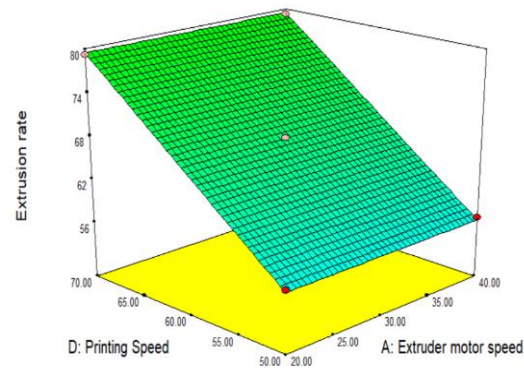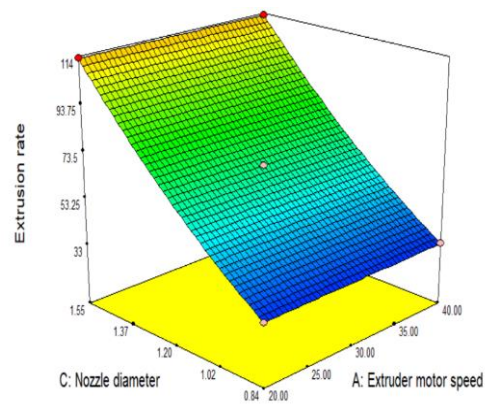
Fig. 4.4 Effect of Printing Parameters on Extusion rate
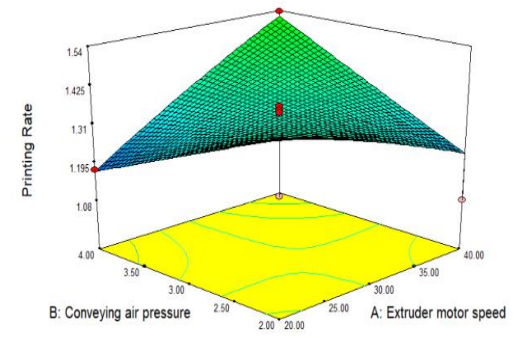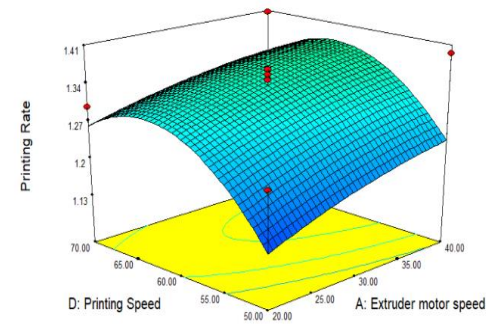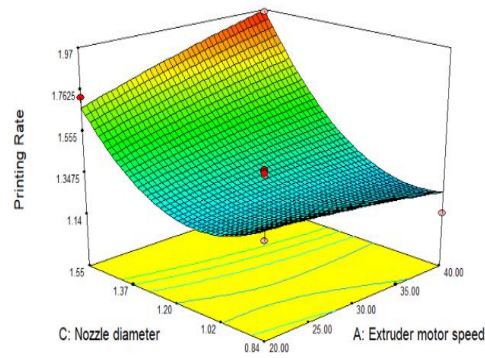
Fig. 4.5 Effect of Printing Parameters on Printing rate

64

4.2.4 Effect of 3D printing process parameters on Colour

Colour is an important aspect affecting the acceptability of a product. The ΔE values obtained using Hunter lab colourimeter by analyzing L*, a* and b* values were shown in the Table 4.4. The values of a* of all printed chocolate products ranging from 2.33 to 4.00 were higher than all b* values, which varied between 1.65 and 3.75, indicating that the color performance of printed chocolate products exhibited brown. Similar results were also reported by Liu *et al.* (2019). Addition of coconut meal and soya lecithin resulted in the increase of redness (a*) value of dark chocolate. ΔE values vary from 0.7081 to 2.9905 for the 29 samples with different printing parameter combination obtained by RSM. Maximum ΔE value (2.9905) was showed by the treatment combination having 1.2 mm nozzle diameter, 20 rpm motor speed, 60 mm/s printing speed and 4 bar air pressure. Minimum ΔE value (0.7081) was obtained by the treatment combination with 1.2 mm nozzle diameter, 40 rpm motor speed, 50 mm/s printing speed and 3 bar air pressure. It is observed from the Figure 4.5, that there was a slight increase in the colour scale which was negligible. Data of colour analysis showed that there was no significant difference (p>0.05) in colour scale among the different combination of printing parameters. The statistical analysis ANOVA (Appendix A3) also revealed that printing parameters didn't have any significant effect on colour.

Table 4.4 Effect of Printing Parameters on Colour

Trials	L*	a*	b*	ΔE
T1	20.58	2.33	2.09	2.5912
T2	22.30	2.81	1.83	2.9636
T3	22.41	2.75	1.92	2.9905
T4	21.30	3.02	2.17	1.2761
T5	21.96	3.25	2.50	1.5673
T6	22.34	2.82	1.97	2.7601
T7	20.76	2.74	1.79	1.5805

T8	20.67	2.78	1.90	1.247
T9	20.79	2.96	2.63	0.7081
T10	20.65	2.66	2.34	0.8462
T11	22.26	2.69	2.20	2.5433
T12	21.14	3.49	2.59	0.714
T13	20.99	2.79	2.03	0.9564
T14	22.55	3.18	2.40	2.235
T15	21.61	3.09	2.21	1.4988
T16	22.68	3.73	3.17	2.5432
T17	22.82	3.64	2.92	2.469
T18	22.48	3.26	2.52	2.0762
T19	22.63	3.47	2.16	2.1944
T20	21.62	3.02	2.35	1.4253
T21	22.25	3.77	2.43	1.8585
T22	20.68	4.00	3.75	1.6573
T23	20.92	3.68	3.62	1.269
T24	21.87	3.80	3.52	2.219
T25	21.53	2.66	2.22	1.8342
T26	22.82	2.98	2.15	2.842
T27	22.64	2.66	2.62	2.6962
T28	20.45	2.48	1.65	1.9785
T29	20.92	2.63	1.87	1.7472

4.2.5 Effect of Printing Parameters on Weight and Dimension of 3D printed chocolate

The measurement of weight, diameter and thickness of the printed products are necessary to determine the precision of 3D food printer in developing the chocolate object. The average weight, diameter and thickness of the 3D printed products are represented in

Table 4.5. As the printing process continues, layer-by-layer deposition of chocolate overlay holding its structure as it builds a complete product. The average weight of final product with small nozzle diameter was ranged between 6.335 g to 7.743 g while weight of product with large nozzle diameter varied between 8.74 g to 9.77 g. It is noted that printed chocolate products with large nozzle diameter tent to be heavier as compared to products printed with small nozzle diameter (Mantihal *et al.,* 2017). The nozzle diameter of the extruder influences the total weight of chocolate product. Figure 4.6 showed that the weight of printed products has a significant increase with increase in nozzle diameter, motor speed, air pressure and printing speed. As the values of printing parameters increases, the printing process becomes much more rapid and more printing material get extruded through the nozzle which resulted in heavier final product. ANOVA table (Appendix A4) also agreed that printing parameters have significant effect ($p<0.05$) on the weight of the final printed product. The printing nozzle wants to move to the outset after completing the layer printing, the material extruded during this period was not under control and get deposited on the adjacent layer. When larger size nozzle (1.55 mm) was used for printing, excessive amount of supply material get extruded and it leads to bigger deviation in weight of the final printed product. Regression model fitted to experimental results of weight of the printed product and it is given in Appendix A4. Following regression model was obtained to predict the weight of the 3D printed coconut based chocolate.

$$Weight=8.19+0.24A+0.18B+0.99C+0.28D-0.29AB+0.14AC-0.13AD-0.13BC-0.21BD+0.15CD-0.10A^2-0.19B^2+0.15C^2-0.11D^2 \quad \ldots\ldots\ldots\ldots (4.3)$$

where, A is the extruder motor speed, B is the conveying air pressure, C is the nozzle diameter and D is the printing speed. The p-value of the model was <0.05, which indicated that the model fitness was significant. By analysis of variance, the R^2 value of this model was determined to be 0.850, which showed that the regression model defined well the true behavior of the system.

From table 4.5 it was concluded that diameter of each 3D printed sample was within the range between 40.5 mm and 41.8 mm. These results point out that the diameter of the printed products was found to be similar to the pre-determined diameter (design geometry). The results showed a slight variation in the diameter of printed product and statistically it was not significant ($p>0.05$) as shown in the ANOVA table given in Appendix A5. Figure 4.7 shows that, as the height of the product increases, a slight compression happens to the bottom layer under the influence of weight, which leads to a slight increase in diameter of the product which is negligible. Similar results were reported by Mantihal *et al.* (2018) during the study on textural modification of 3D printed dark chocolate.

Based on the Table 4.5, it is concluded that the thickness of each sample was within the range between 8.44 mm and 10.785 mm. Thickness of 3D printed chocolate product was significant as it can influence the structural stability of printed items. From the figure 4.8, it was clear that as the nozzle diameter increases, gradually the thickness of final product also increases. Printing parameters such as printing speed and conveying air pressure have positive effect on the thickness of 3D printed products. It was observed that the variation in the printing parameters had significant effect ($p<0.05$) on the thickness of the 3D printed final product (Appendix A6). The printer extruder movement causes some irregular deposition of chocolate as the layer height is increasing (Severini *et al.,* 2016), which affects the thickness of each printed sample. The layer height setting in the slicing software produces almost precise 3D printed product based on the data collected. A slight increase or decrease in thickness of the product may be assigned due to the uneven deposition of chocolate during printing. Regression model fitted to experimental results of thickness of the printed product and it is given in Appendix A6. Following regression model was obtained to predict the thickness of the 3D printed coconut based chocolate.

$$\text{Thickness}=8.89-0.17A+0.033B+0.84C+0.12D+5.000E\text{-}003AB-0.10AC-0.19AD+0.036BC-0.20BD+0.096CD+0.37A^2+0.44B^2+0.19C^2+0.51D^2 \qquad \text{……………… (4.4)}$$

where, A is the extruder motor speed, B is the conveying air pressure, C is the nozzle diameter and D is the printing speed. The p-value of the model was <0.05, which indicated

that the model fitness was significant. By analysis of variance, the R^2 value of this model was determined to be 0.9065, which showed that the regression model defined well the true behavior of the system.

Based on the visual aspect, the dimensional properties of 3D printed products was not much affected although there was some unevenness on the surfaces. Overall, the 3D printed structure remains as alike to the pre-designed 3D model. This indicates that 3D printer could print a precise dimension of the 3D structure with a personalized design.

Table 4.5 Effect of Printing Parameters on Dimensional evaluation of 3D printed chocolate

Trials	Weight (g)	Diameter (mm)	Thickness (mm)
T1	6.695	41.0	8.515
T2	6.59	41.0	8.48
T3	6.075	41.2	8.51
T4	7.815	41.1	8.495
T5	8.02	41.5	8.95
T6	6.005	41.5	8.935
T7	9.225	40.8	8.725
T8	6.655	41.0	8.95
T9	6.545	41.2	8.82
T10	7.325	41.2	9.45
T11	7.35	41.0	10.35
T12	7.74	41.0	9.705
T13	7.015	41.4	8.59
T14	7.255	41.6	8.895
T15	9.13	41.3	9.685
T16	9.36	41.5	9.105

T17	6.245	41.8	8.48
T18	6.335	41.0	8.91
T19	9.365	41.0	9.745
T20	9.751	40.5	9.27
T21	6.87	41.1	9.44
T22	6.05	41.2	9.065
T23	8.105	41.0	10.585
T24	7.095	41.0	9.43
T25	7.285	41.0	9.72
T26	7.29	40.8	8.495
T27	7.1	40.5	10.785
T28	7.37	40.6	9.61
T29	7.43	41.4	9.44
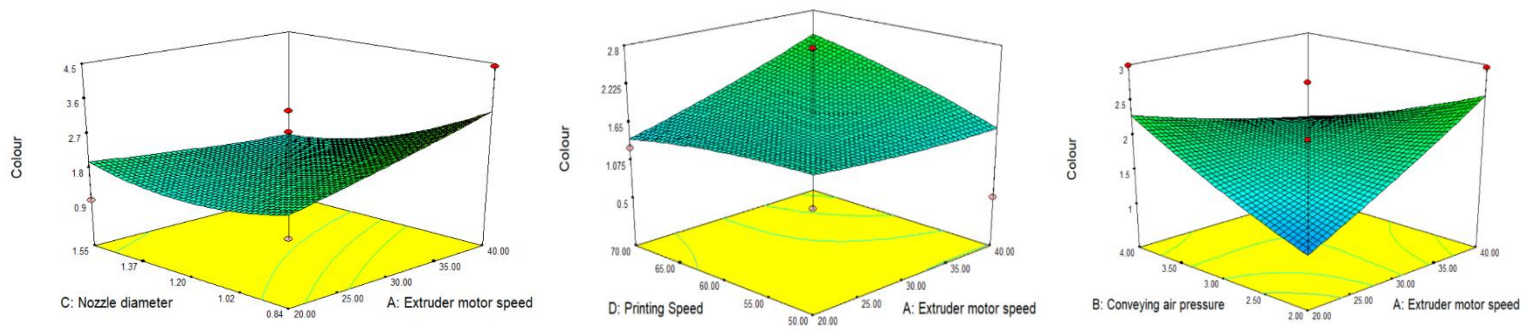
Fig. 4.6 Effect of Printing Parameters on Colour
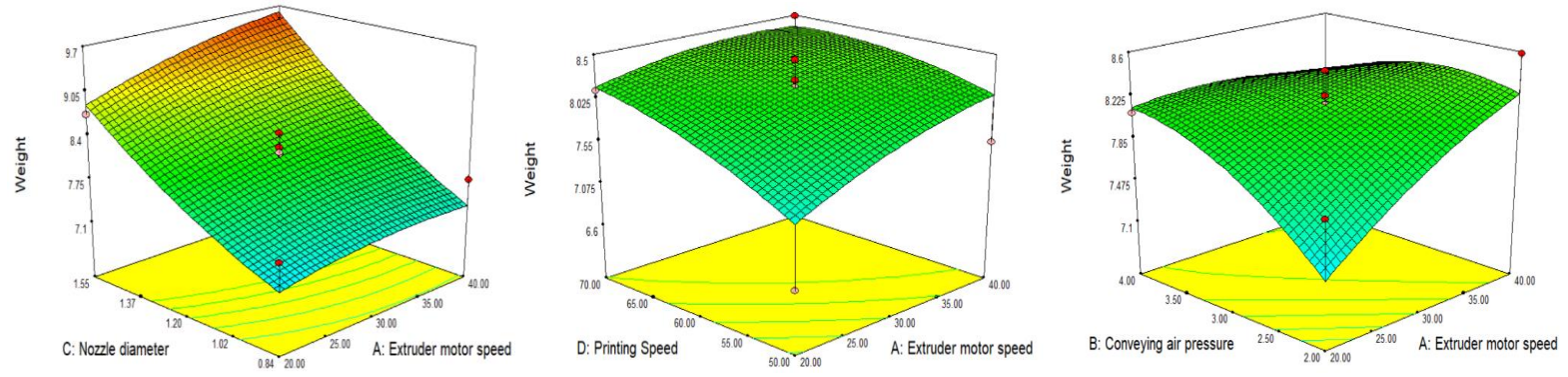
Fig. 4.7 Effect of Printing Parameters on Weight

71
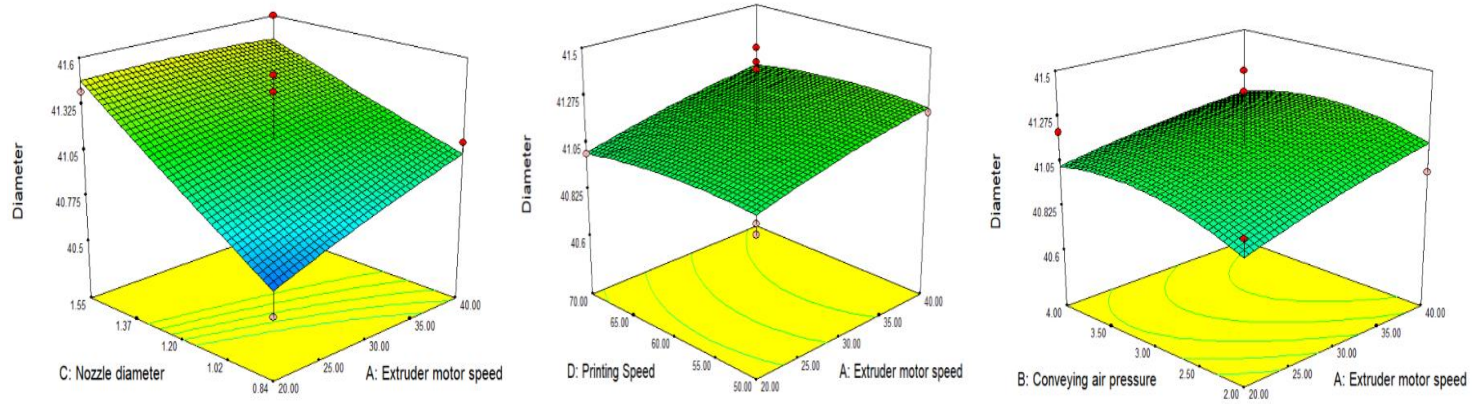
Fig. 4.8 Effect of Printing Parameters on Diameter
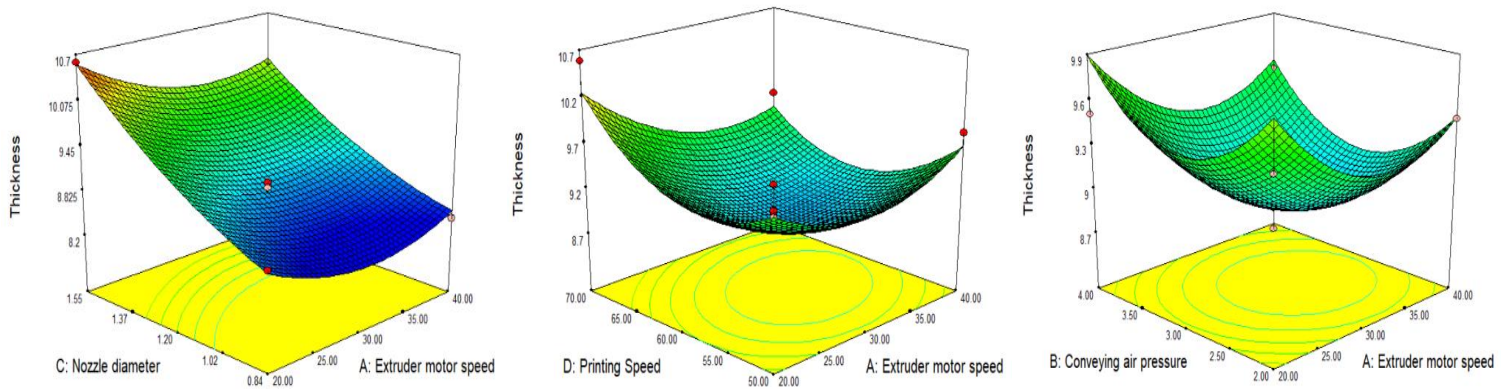
Fig. 4.9 Effect of Printing Parameters on Thickness

72

4.2.6 Effect of 3D printing process parameters on Moisture content

Moisture content of the printed samples was ranged from 0.16-0.37% (Table 4.6). Lowest moisture content was found for the printed sample with 1.2 mm nozzle diameter, 60 mm/s printing speed, 20 rpm motor speed, 4 bar air pressure and highest moisture was found for the product with 1.55 mm nozzle diameter, 60 mm/s printing speed, 20 rpm motor speed and 3 bar air pressure. From the figure 4.9, moisture content had some slight variations with the printing parameters but the statistical analysis in ANOVA table (Appendix A7) showed that the printing process parameters didn't have any significant effect ($p > 0.05$) on the moisture content of the printed products. Since extruder temperature was a fixed variable in this study, moisture content of the product didn't get much affected by the temperature. All samples were printed at ambient temperature (30°C). The results showed that only a negligible change of moisture content was occurred during the printing process.

4.2.7 Effect of 3D printing process parameters on Texture

Texture profile analysis (TPA) was conducted to assess the textural characteristics of the 3D printed product. TPA can explain the rheological property and mechanical stability of a printed material (Kim *et al.,* 2018). Different textural characteristics like hardness, cohesiveness and adhesiveness of the printed product with different combination of printing parameters were determined as given in Table 4.6.

The hardness of the supply material gives the amount of force required to push the chocolate from the feeder tank out to the print head through a small printing nozzle diameter (Wilson *et al.,* 2020). From the table 4.5 the hardness values vary from 11.4125 to 59.7228 N for the 3D printed chocolate products. A higher hardness value of 59.7228 N was found for the sample printed with 1.55 mm nozzle diameter, 60 mm/s printing speed, 30 rpm motor speed and 4 bar air pressure. On the other hand, the sample printed with 0.84 mm nozzle diameter, 60 mm/s printing speed, 30 rpm motor speed and 4 bar air pressure gave very less hardness value of 11.4125 N. Figure 4.10 shows that hardness of printed

samples increased with increasing variation in the printing parameters. With the increase of nozzle diameter, printing speed, motor speed and air pressure, more amount of supply material get extruded and thus the hardness of printed product get enhanced due to the higher thickness of product. ANOVA table (Appendix A8) also showed that the 3D printing parameters had significant effect ($p<0.05$) on the hardness of the final product. Regression model fitted to experimental results of hardness of the printed product and it is given in Appendix A8. Following regression model was obtained to predict the hardness of the 3D printed coconut based chocolate.

$$\text{Hardness} = 38.56 - 0.78A + 3.17B + 9.84C - 4.28D + 6.04AB - 2.11AC + 3.96AD + 7.32BC - 2.02BD - 3.53CD - 5.21A^2 - 0.75B^2 - 6.37C^2 - 10.15D^2 \qquad \text{.................. (4.5)}$$

where, A is the extruder motor speed, B is the conveying air pressure, C is the nozzle diameter and D is the printing speed. The p-value of the model was <0.05, which indicated that the model fitness was significant. By analysis of variance, the R^2 value of this model was determined to be 0.8275, which showed that the regression model defined well the true behavior of the system.

Table 4.6 Effect of Printing Parameters on Moisture content and Texture

Trials	Moisture content (%)	Hardness (N)	Cohesiveness	Adhesiveness
T1	0.25	45.8338	0.0000	-0.0012
T2	0.20	25.2838	0.06944	-0.0004
T3	0.16	34.6851	-0.0004	-0.0007
T4	0.33	38.3081	0.00003	-0.0000
T5	0.18	38.8711	0.04430	-0.0004
T6	0.17	17.4336	0.19041	-0.0004
T7	0.32	38.6414	0.08513	-0.0003
T8	0.28	28.8955	0.17818	-0.0006

T9	0.31	23.7770	0.10033	-0.0008
T10	0.29	25.8679	-0.0003	-0.0004
T11	0.33	36.9437	0.0000	-0.0003
T12	0.35	34.0327	0.10068	-0.0004
T13	0.37	34.6197	0.00004	-0.0008
T14	0.25	31.3567	0.0000	-0.0011
T15	0.29	59.7228	0.00013	-0.0003
T16	0.19	36.1697	0.11703	-0.0005
T17	0.24	24.0826	0.0000	-0.0008
T18	0.29	15.0213	0.0000	-0.0007
T19	0.24	11.4125	0.33578	-0.0004
T20	0.22	14.3330	0.25126	-0.0005
T21	0.35	19.5198	0.20058	-0.0008
T22	0.26	22.6149	0.27785	-0.0004
T23	0.20	11.9081	0.17767	-0.0005
T24	0.17	18.3549	0.19282	-0.0004
T25	0.19	21.3679	0.14714	-0.0006
T26	0.19	19.7934	0.14857	-0.0005
T27	0.32	21.8085	0.0000	-0.0005
T28	0.26	21.6375	0.13842	-0.0005
T29	0.31	19.5862	0.14697	-0.0004

Cohesiveness explains the quality of the supply material to form dough. Comparing all the samples, higher values of cohesiveness indicates the better strength of the supply material, making it more suitable for extrusion-based 3D printing (Zhu *et al.,* 2020). Results showed that the higher cohesive value of 0.33578 and lower cohesive value -0.0004 for 3D printed chocolate sample (Table 4.6). Statistical studies ANOVA table (Appendix

A9) revealed that the printing parameters didn't have any significant effect (p>0.05) on the cohesiveness of the final product.

Adhesiveness represents the stickiness of the supply material and was a main feature that binds the printed layers together. The least adhesive supply material can be related with higher hardness that making it unsuitable for 3D printing with poor flowability (Wilson *et al.,* 2020). Table 4.6 showed that the adhesiveness values ranges from -0.0003 to -0.0012. The printing parameters didn't have any significant effect (p>0.05) on the adhesiveness values of the printed product, ANOVA table (Appendix A10). From the figure 4.12 it was clear that printing parameters could make only a slight negligible change in the adhesiveness of the final printed product.

4.2.8 Verification of the Predicted Variables

The optimum response values were tested using the recommended optimum conditions of the variables and was also used to validate the experimental and predicted values of the responses. The predicted, actual values of the responses and the percentage variation at the optimized condition of 3D printing are presented in Table 4.7. The predicted values of optimized treatment are comparable with the actual value.

Table 4.7 Predicted and actual values of responses of the optimized condition

Sl. No.	Responses	Predicted value	Actual value	Variation (%)
1	Extrusion rate (mm^3/s)	33.250	28.305	0.61
2	Printing rate (g/min)	1.159	1.158	0.07
3	Colour (ΔE)	3.095	2.801	3.74
4	Weight (g)	7.389	6.335	2.62
5	Diameter (mm)	41.1	40.6	3.03
6	Thickness (mm)	9.596	8.851	0.95
7	Moisture content (%)	0.29	0.279	3.94
8	Hardness (N)	15.512	14.333	0.57

| 9 | Cohesiveness | 0.25126 | 0.20058 | 0.25 |
| 10 | Adhesiveness | -0.0004 | -0.0007 | -0.42 |

4.2.9 Optimization of 3D printing process parameters

All the trials for the optimization of 3D printing process parameters was done using the above mentioned optimized supply material composition. Nozzle diameter, printing speed, extruder motor speed and conveying air pressure were considered as the independent variables which have to be optimized.

From the analysis it was clear that, when large nozzle diameter (1.55 mm) was used, the supply material get over extruded with respect to other parameters and it will badly affects the precision and accuracy of the final 3D printed product. Good finishing and external appearance of the finished product was achieved when using small nozzle diameter (0.84 mm) for 3D printing of coconut based chocolate. When the nozzle diameter was increasing, the printing accuracy of the final product varies from the actual design. High printing speed (70 mm/s) significantly influences the entire printing process, which may leads to the improper printing of the product. Discontinuous printing was happened during the chocolate printing with 50 mm/s printing speed. Thus an optimum printing speed of 60 mm/s gave better results.

Three variation of extruded motor speed (20, 30, 40 rpm) was considered for the study. Low motor speed (20 rpm) will slow down the printing process as the extruder motor speed was guiding the total printing procedure. High motor speed of 40 rpm somewhat speed up the extrusion printing process resulted in the over extrusion of supply material. During the entire study we are using air pressure driven extrusion mechanism. Conveying air pressure had a vital role in the complete 3D printing process. Air pressure above 2 bar push the supply material through the nozzle for printing without any control and make the final product with some dissimilarity with the design geometry.
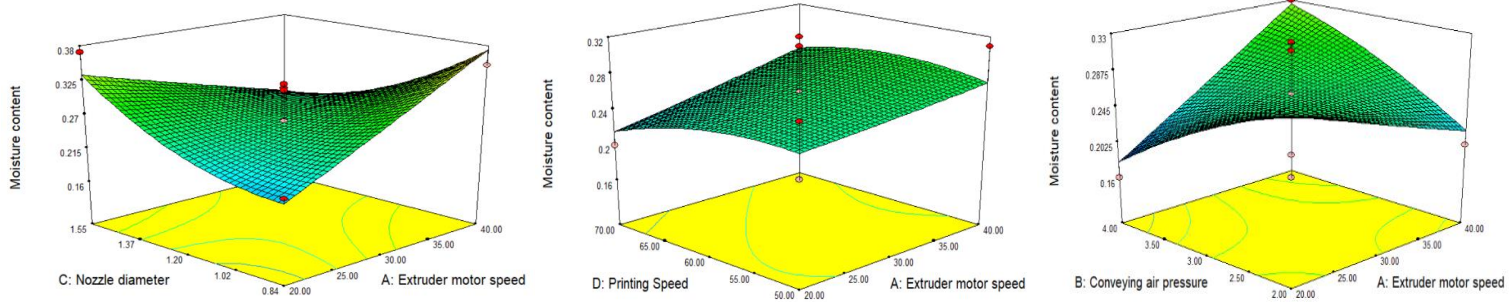
Fig. 4.10 Effect of Printing Parameters on Moisture content
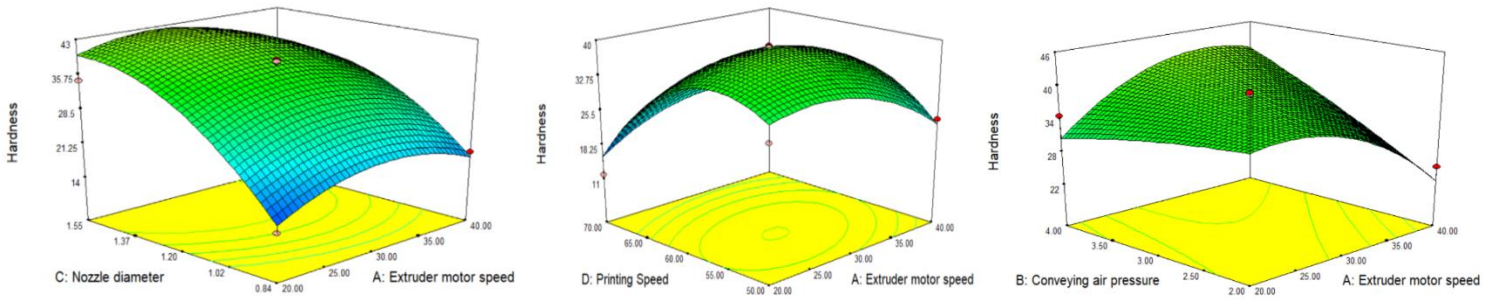
Fig. 4.11 Effect of Printing Parameters on Hardness
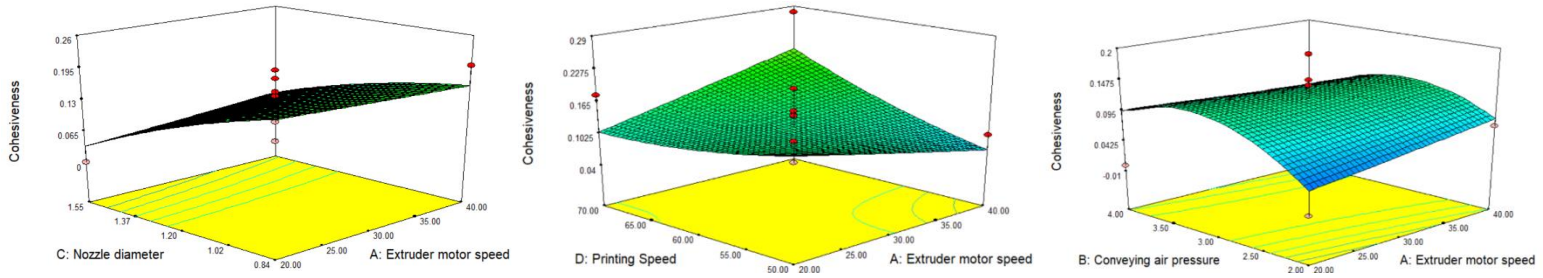
Fig. 4.12 Effect of Printing Parameters on Cohesiveness
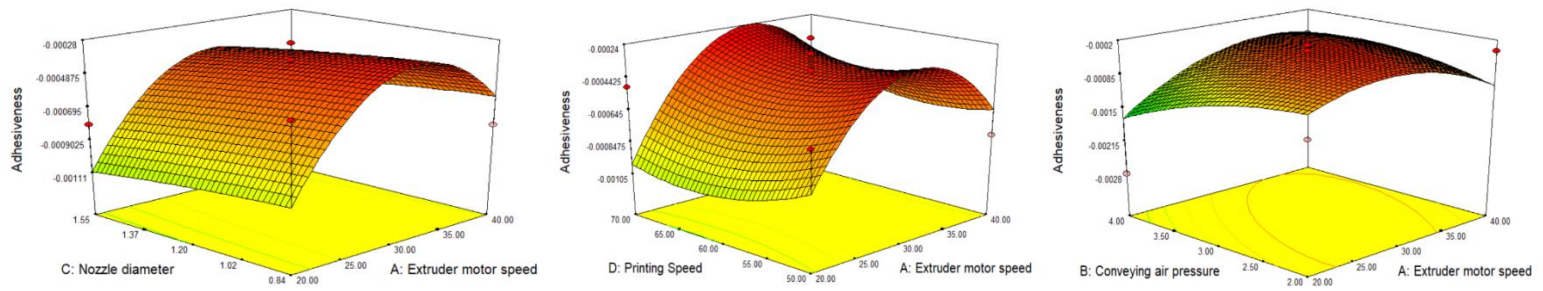
Fig. 4.13 Effect of Printing Parameters on Adhesivenes

Thus the optimized 3D printing process parameters for printing of coconut based chocolate was 0.84 mm nozzle diameter, 60 mm/s printing speed, 30 rpm extruder motor speed and 2 bar air pressure.

4.3. QUALITY ANALYSIS OF 3D PRINTED COCONUT BASED CHOCOLATE DEVELOPED FROM OPTIMIZED 3D PRINTING PROCESS

The final 3D printed coconut based chocolate products developed from optimized printing process were subjected to quality analysis to access the nutritional composition of the chocolate products. The amount of carbohydrate, fat, protein, dietary fiber and total energy value of the 3D printed chocolate products were determined.

4.3.1 Nutritional analysis

The nutritional analysis of the 3D printed coconut based chocolate is given in Table 4.8. The developed 3D printed product was found to have 8% of dietary fiber which contributed to more than 10% of the RDA of dietary fiber intake. The final 3D printed chocolate was also rich in carbohydrates with 54.35%, fat content about 32.26%, 4.54% protein and 0.054% ash content providing an energy value of 549 k Cal/ 100 g. The product being rich in dietary fiber and carbohydrates content serves a highly nutritious product. This study provides insight into the development of dietary fiber enriched chocolate products with enhanced health benefits.

Table 4.8 Nutritional analysis of the 3D printed chocolate from optimized process

Carbohydrate (%)	Protein (%)	Fat (%)	Dietary fiber (%)	Ash (%)	Energy (k Cal/100g)
54.35±0.02	4.54±0.04	32.26±0.06	8±0.10	0.054±0.007	549±0.25

The addition of powdered coconut meal enhances the total dietary fiber content in the chocolate products. Using the coconut meal (byproduct) obtained during the removal of

coconut milk, a highly nutritious food product was developed using 3D food printing technology with an amount of 8% total dietary fiber content.

4.3.2 Sensory Evaluation

The visual appearance of 3D printed coconut based chocolate was assessed by sensory analysis. Based on the 9-point hedonic scale, observations were made by grading the printed products (Fig.4.14). The grading criteria were preferred by considering the appearance of the prints and exterior design. Product printed with nozzle diameter of 1.55 mm showed poor overall acceptability due to over extrusion of the supply material and also the 3D printed product had poor printing precision. Chocolate printed with the 0.8 mm nozzle diameter with printing speeds ranging from 50 to 60 mm/s and motor speeds between 20 and 30 rpm were better rated along with good overall acceptability of the developed product.

Fig. 4.14 Sensory analysis of 3D printed products
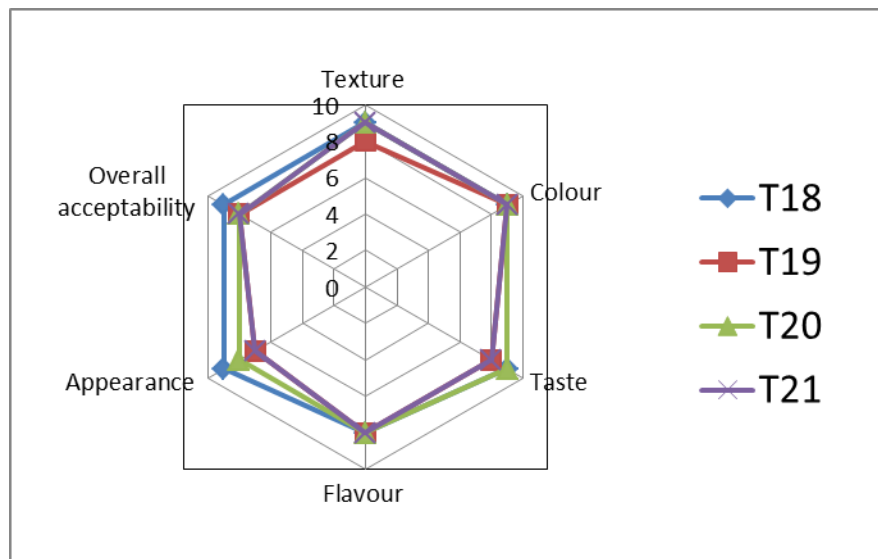
CHAPTER V

SUMMARY AND CONCLUSIONS

The research work was based on the novel 3D food printing technology for process optimization of coconut fortified chocolate. The development of coconut fortified chocolate was done to provide a fixed amount of dietary fiber in the nutrition and also as byproduct utilization from the coconut.

Chocolates are extremely rich sources of many essential nutrients and phyto-chemicals that can contribute to a healthy diet. It is a highly nutritious energy source, with a good digestibility and fast metabolism. Chocolate and cocoa (*Theobroma cacao*) have beneficial health effects related to cardiovascular disease, metabolic syndrome, neurodegenerative diseases and other chronic health conditions. Coconut (*Cocos nucifera*) is a very versatile and indispensable food item for most of the people in the tropical belt. It is a complete food source, rich in calories, vitamins and minerals. Coconut kernel contains 7-11% dietary fiber and 5% proteins, in addition to 34-60% oil content. Coconut kernel protein possesses cardio-protective and anti-diabetic properties and dietary fiber constitutes significant hypo-cholesterolemic effect.

Deficiency of complex carbohydrates like dietary fiber is a matter of concern which poses major health issues causing chronic diseases such as cardiovascular diseases, obesity, colon cancer, hypertension and diabetes mellitus. The recommended acceptable intake of dietary fiber ranges from 28.8 g/day for adults, but actual intake was found to be lower than this limit. With this aim, the study focused on the applicability of 3D food printing for fiber enrichment of chocolate.

3D printing is a novel concept based on the additive manufacturing (AM) technology, in which layer by layer fabrication of supply materials occurs according to the design and develop a complete 3D object. Customization is the main factor behind the 3D food printing while complex geometry and on-demand production being other factors.

Using this technology, it is possible to accurately control the nutritional contents on the food based on individuals' preference and health condition. 3D food printing is a promissory innovative technology with the features of sustainability, flexibility, creativity and efficient utilization of raw materials with new dimensions of food culture by covering the aspects of convenience, novelty, entertainment, nutrition and global food. All these aspects have increased the market potential for 3D printed food products owing to its unique ability to fabricate foods based on an individual's age, diet and health conditions. Hence, in the present study, 3D printed coconut based chocolate was developed and the quality analysis of the final product evaluated.

FABFORGE 3D food printer was used to print chocolate sample. This 3D food printer was based on hot-melt extrusion technology. The 3D design was in STL format and was uploaded into the slicing software, Simplify 3D (ver. 4.1.0) there it converts the information into machine readable G and M codes. A 3D design of 'gear' with dimensions 41.50 mm $\times$ 41.50 mm $\times$ 10.00 mm was used for the studies.

Mello dark compound chocolate, sugar (3%), coconut meal (6%, 9% and 12%) and soya lecithin (0.1%, 0.3% and 0.5%) are used for making the printing ink. The supply material was thoroughly mixed to make a semi-solid form without any lumps. For the optimization of supply material, 3D printing process parameters such as printing speed (50 mm/s), motor speed (30 rpm), nozzle diameter (1.2 mm) and air pressure (2 bar) were set based on the preliminary study. Supply material optimization was done based on Response Surface Methodology (No. of runs: 13) with two variables such as coconut-chocolate ratio and soya lecithin.

For the optimization of 3D printing process parameters, the optimized supply material was manually fed into the barrel tank and subjected to 29 different combination of printing speeds (50, 60 and 70 mm/s), nozzle diameter (0.82, 1.22 and 1.55 mm), extrusion motor speed (20, 30 and 40 rpm) and conveying air pressure (2, 3 and 4 bar). The process

parameters optimization was done based on Response Surface Methodology (No. of runs: 29) with four variables.

The viscosity of supply material decreases with increase in shear rate. The viscosity values were ranged between 24.2-6.15 Pa s. Soya lecithin content had considerable effect on the viscosity of the supply material compositions. The yield stress of supply material decreased with decrease in shear rate. The yield stress values ranged between 85.5-372 Pa. The low concentration of flow enhancer (0.1%) reduced the water activity. The moisture content of the supply material compositions ranged between 0.18-0.52%. Sample with very low amount of soya lecithin showed minimum value for moisture content. Based on the results of all these analysis one supply material was optimized for evaluating the remaining objectives. The optimized supply material composition contains 9% coconut meal, 3% sugar, 0.3% soya lecithin and 87.7% dark compound chocolate.

The optimized supply material was used for printing with different printing parameter combinations. 3D printed products were subjected to different analysis for the optimization of printing parameters. Extrusion rate increases with increase in nozzle diameter and printing speed. The extrusion rate ranged from 94.34 to 132.08 mm^3/s and 27.70 to 38.79 mm^3/s for 1.55 mm and 0.82 mm nozzle, respectively. The values of printing rate ranges from 1.076-1.958 g/min. Sample printed with 1.55 mm nozzle diameter, offered higher printing rate than sample printed with 0.84 mm diameter. Addition of coconut meal and soya lecithin results in the increase of redness (a*) value of dark chocolate. ΔE values vary from 0.7081 to 2.9905 for the all the printed products. . The average weight of final product with small nozzle diameter was between 6.335 g to 7.743 g while weight of product with large nozzle diameter varied between 8.74 g to 9.77 g. The nozzle diameter of the extruder influences the total weight of chocolate product. The diameter of each 3D printed sample was within the range between 40.5 mm and 41.8 mm. Diameter of the printed products was found to be similar to the pre-determined diameter (design geometry). The thickness of each sample was within the range between 8.44 mm and 10.785 mm. Printing parameters such as nozzle diameter, printing speed and conveying air pressure

have positive effect on the thickness of 3D printed products. Moisture content of the printed samples was ranged from 0.16-0.37%. The hardness values vary from 11.4125 to 59.7228 N for the printed chocolate products. With the increase of nozzle diameter, printing speed, motor speed and air pressure, more amount of supply material get extruded and thus the hardness of printed product get enhanced due to the higher thickness of product. The cohesive values vary from 0.33578 to -0.0004 and the adhesiveness values ranges from -0.0003 to -0.0012. Results showed printing parameters didn't have any significant effect on the cohesiveness and adhesiveness values of the printed product. Based on all these analysis and results, it was concluded that chocolate product printed with 0.8 mm nozzle diameter, 60 mm/s printing speed, 30 rpm motor speed and 2 bar air pressure were better rated along with good overall acceptability. The final 3D printed chocolate contributes 8% dietary fibre, carbohydrates with 54.35%, fat content about 32.26% and 4.54% protein content providing an energy value of 549 k Cal/ 100 g.

In the present study, customized coconut based chocolate was developed using 3D printing technology with an enrichment of 8% coconut dietary fibre. Further studies may be undertaken to improve the production by using multi- print head extruder for printing more number of printed products at a time. Moreover the shelf life studies of the 3D printed chocolate products have to be done.

Scope for future work

- Explore the possibility of multi-print head 3D food printer.

- Study on the shelf life of chocolate product enriched with dietary fiber.

CHAPTER VI

REFERENCES

Acan, B. G., Kilicli, M., Bursa, K., Toker, O. S., Palabiyik, I., Gulcu, M., Yaman, M., Gunes, R and Konar, N. 2020. Effect of grape pomace usage in chocolate spread formulation on textural, rheological and digestibility properties. *Food Sci. and Tech.*138: 110451.

Afoakwa, E, O., Paterson, A and Fowler, M. 2007. Factors influencing rheological and textural qualities in chocolate. *Trends in Food Sci. and Technol.*18: 290-298.

Afoakwa, E, O., Paterson, A., Fowler, M and Vieira, J. 2008. Relationship between rheological, textural and melting properties of dark chocolate as influenced by particle size distribution and composition. *Food Res. Technol.* 227:1215-1223.

Afoakwa, E. O., Paterson, A., Fowler, M and Vieira, J. 2008. Particle size distribution and compositional effects on textural properties and appearance of dark chocolates. *J. of Food Eng.* 87,181-190.

Afoakwa, E, O., Paterson, A., Fowler, M and Vieira, J. 2009. Comparison of rheological models for determining dark chocolate viscosity. *Inter. J. Food Sci. and Technol.* 44: 162-167.

Afoakwa, E., Quao, O., Takrama, J., Budu, A. S and Saalia, F. K. 2013. Chemical composition and physical quality characteristics of Ghanaian cocoa beans as affected by pulp pre-conditioning and fermentation. *J. Food Sci. Technol*. 50(6): 1097-1105.

Alcalde, L. R. 2016. Walkthrough Pinya3, 3D food printing platform. 3Digital Cooks. http://3digitalcooks.com/2016/03/walkthrough-pinya3/. Accessed July 2017.

Angioloni, A and Collar, C. 2009. Small and large deformation viscoelastic behaviour of selected fibre blends with gelling properties. *Food Hydrocolloids.* 23: 742-748.

Anukiruthika, T., Moses, J and Anandharamakrishnan, C. 2020. 3D printing of egg yolk and white with rice flour blends. *J. Food Eng.*265:109691.

AOAC, 21st edition, 2019. doi: https://www.aoac.org/official-methods-of-analysis-21st-edition-2019/. Accessed March 2022.

Appaiah, P., Sunil, L., Kumar, P. P. K and Krishna, G. A. G. 2014. Composition of Coconut Testa, Coconut Kernel and its Oil. *J. Am. Oil Chem. Soc. DOI 10.1007/s11746-014-244-9.*

Aremu, C.Y., Agiang, M. A and Ayatse, J. O. 1995. Nutrientand antinutrient profiles of raw and fermented cocoabeans. *Plant Foods for Human Nutrition.* 48**,** 217–223.

Barisic,V., Jozinovic, A., Flanjak, I., Subaric, D., Babic, J., Milicevic, B., Jokic, S., Grgi, I and Ackar D. 2019. Effect of Addition of Fibres and Polyphenols on Properties of Chocolate. *Food Reviews Int.* 8755-9129.

BeeHex. 2016. BeeHex robots 3D-print pizza. http://beehex.com/. Accessed August 2016.

Bernhoft, A**.** 2010*. A Brief Review on Bioactive Compounds in Plants*. Novus Forlag, Oslo, Norway, 543p.

Biehl, B and Voigt. 1995. Postharvest handling, fermentation, proteolysis and formation of aroma precursors in cocoa. *Angewandte Botanik Berichte.* 5:124-137.

Belscak-Cvitanovic, A., Komes, D., Benkovic, M., Karlovic, S., Hecimovic, I., Jezek, D and Ingrid Bauman. 2012. Innovative formulations of chocolates enriched with plant polyphenols from *Rubusidaeus* L. leaves and characterization of their physical, bioactiveand sensory properties. *Food Research Int.* 48: 820-830.

Bertazzo, A., Comai, S., Brunato, I., Zancato, M and Costa, C. V. L. 2011. The content of protein and non-protein (free and protein-bound) tryptophan in *Theobroma cacao* L. beans. *Food Chem*. 124: 93-96.

Bhandari, B. R and Howes, T. 1999. Implication of glass transition for the drying and stability of dried foods. *J. Food Eng.* 40: 71-79.

Bouaziz1, M. A., Abbes, F., Mokni, A.,Blecker, C., Attia, H and Besbes, S. 2017.The addition effect of Tunisian date seed fibers on the quality of chocolate spreads. *J. Texture Studies*. 48(2): 143-150.

Brown, A. C., De Beer, D and Conradie, P. 2014. Development of a stereolithography (STL) input and computer numerical control (CNC) output algorithm for an entry-level 3-D printer. *South African J. Ind. Eng*. 25: 39-47.

Campos, C. M and Benedet, T. H. D. 1994. Aceitabilidade de bombons (saborpassasao rum)-recheioadicionado de proteínas de soja. *Boletim da Sociedade Brasileira Ciência e Tecnologia de Alimentos* 28:113-117.

Chen, H., Xie, F., Chen, L and Zheng, B. 2019. Effect of rheological properties of potato, rice and corn starches on their hot-extrusion 3D printing behaviors. *J. Food Eng*. 244:150-158.

Choc Edge (2014). Choc Creator. http://chocedge.com/. Accessed December 2014.

Cohen, D. L., Jeffrey, I. L and Cutler, M. 2009. Hydrocolloid printing: A novel platform for customizedfood production. In: Proceedings of Solid Freeform Fabrication Symposium (SFF'09), Austin, TX, 3-5.

Chuanxing, F., Qi, W., Hui, L., Quancheng, Z and Wang, M. 2018. Effects of pea protein on the properties of potato starch-based 3D printing materials. *Int J. Food Eng*. 14.

Crump, S.S. 1991. Fast, precise, safe prototypes with FDM. In: Proceedings of ASME Annual Winter Conference, Atlanta, Dec. 1991.

Creative Machines Lab. 2016. Sanna: the food printer of 2020. Columbia University, School of Engineering. https://www.youtube.com/watch?v=yPS6FbNuY_I. Accessed July 2017.

Dankar, I., Haddarah, A., El Omar, F., Sepulcre, F and Pujolà, M. 2018. Assessing the microstructural and rheological changes induced by food additives on potato puree. *Food Chemistry*. 240: 304-313.

Dankar, I., Pujola, M., Omar, F.E., Sepulcre, F and Haddarah, A. 2018. Impact of Mechanical and Micro structural Properties of Potato Puree-Food Additive Complexes on Extrusion-Based 3D Printing Food and Bioprocess Technology.

Dei, H. K., Rose, S. P and Mackenzie, A. M. 2006. Apparent metabolisable energy and digestibility of shea (*Vitellaria paradoxa*) fat, cocoa (*Theobroma cacao* L.) fat and soybean oil in broiler chicks. *Br. Poult. Sci*. 47: 607-612.

Derossi, A.,Caporizzi, R., Azzollini, D and Severini, C. 2018. Application of 3D printing for customized food. A case on the development of a fruit-based snack for children. *J. Food Eng*. 220: 65-75.

Dick, A., Bhandari, B and Prakash, B. 2019. 3D printing of meat. *Meat science*.

Dianez, I., Gallegos, C., la Fuente, E. 2019. 3D printing in situgelification of κ-carrageenan solutions: effect of printing variableson the rheological response. *Food Hydrocoll*. 87: 321-330.

Dodo, H. W and Furtek, D. B. 1994. Cloning and sequencing of a gene encoding a 21 kDa trypsin inhibitor from *Theobroma cacao* L. *Cafe Cocoa* 38: 113-117.

Erdema, O., Gultekin-Ozguven, M., Berktas¸ I., Ers¸S., Tuna, H. E., Karadag, A., Ozcelik, B., Gunes¸ G and Cutting, S. M. 2014. Development of a novel synbiotic dark chocolate enriched withBacillus indicus HU36, maltodextrin and lemon fiber: Optimization byresponse surface methodology. *Food Sci. and Tech*. 56: 187-193.

Feichtinger, A., Scholten, E and Sala, G. 2020. Effect of particle size distribution on rheological properties of chocolate. *Food Funct.* doi: 10.1039/d0fo01655a.

Feng, C., Zhang, M and Bhandari, B. 2019. Materials properties of printable edible inks and printing parameters optimization during 3D printing: A review. *Critical Reviews in Food Sci. and Nutrition.* 59(19):3074-3081.

Ferrazzano, G. F., Amato, I., Ingenito, A., De Natale, A and Pollio, A. 2009. Anti-cariogenic effects of polyphenols from plant stimulant beverages (cocoa, coffee, tea). *Fitoterapia* 80: 255-262.

Garfield, L. 2016. This robot can 3D-print a pizza in under five minutes. Teck insider. http://www.techinsider.io/how-the-beehex-pizza-3d-printer-works-2016-6. Accessed September 2016.

Glicerina, V., Balestra, F., Rosa, M, D and Romani, S. 2013. Rheological, textural and calorimetric modifications of dark chocolate during process. *J. Food Eng.*119: 173–179.

Godoi, F.C., Prakash, S and Bhandari, B.R. 2016. 3D printing technologies applied for food design: Status and prospects. *J. Food Engg.*179: 44-54.

Gross, B. C., Erkal, J. L and Lockwood, S. Y. 2014. Evaluation of 3D printing and its potential impact on biotechnology and the chemical sciences.

Grunewald, S. J. 2015. Multi-material, swappable extruder, portable 3d printer: The Focus launches on Kick starter.

Guerrero, P., Beatty, E., Kerry, J. P and Caba, K. D. L. 2012. Extrusion of soy protein with gelatin and sugars at low moisture content. *J. Food Eng*. 110(1): 53-59.

Hamilton, C.A., Alici, G and Panhuis, M. 2018. 3D printing Vegemite and Marmite: Redefining "breadboards". *J. Food Eng.* 220:83-88.

Hao, L., Mellor, S and Seaman, O. 2010. Material characterisation and process development for chocolate additive layer manufacturing. *Virtual Physical Prototyping.* 5:57–64.

Hao, L., Mellor, S., Seaman, O., Henderson, J., Sewell, N and Sloan, M. 2010. Material characterisation and process development for chocolate additive layer manufacturing. *Virtual and Physical Prototyping.* 5(2): 57-64.

Hii, C. L., Law, C. L and Cloke, M. 2009. Modeling using a new thin layer drying model and product quality of cocoa. *J. Food Eng*. 90: 191-198.

Huang, M., Zhang, M and Bhandari, B. 2019. Assessing the 3D printing precision and texture properties of brown rice induced by infill levels and printing variables. *Food and Bioprocess Technol.*12 (7): 1185-1196.

Ibrahim, S. F., Dalek, N. S. E. M., Raffie, Q. A. F. M and Ain, M. R. F. 2020. Quantification of physicochemical and microstructure properties of dark chocolate incorporated with palm sugar and dates as alternative sweetener. *J. Materials Today: Proceedings.* https://doi.org/10.1016/j.matpr.2020.06.235.

Johansson, D and Bergensthal, B. 1992. The influence of food emulsifiers on fat and sugar dispersions in oils. I. Adsorption, sedimentation. *J. American Oil Chemists' Society.* 69, 705-717.

Karavasilia, C., Gkaragkounisa, A., Moschakisb, T., Ritzoulisc, C and Fatourosa, D, G. 2020. Pediatric-friendly chocolate-based dosage forms for the oral administration of both hydrophilic and lipophilic drugs fabricated with extrusion-based 3D printing. *European J. Pharmaceutical Sci.* 147: 105291.

Kha, T. C., Nguyen, M. H and Roach, P. D. 2010. Effects of spray drying conditions on the physico-chemical and antioxidant properties of the Gac (*Momordica cochinchinensis*) fruit aril powder. *J. Food Eng.* 98(3): 385-392.

Kim, H.W., Lee, J. H., Park, S. M., Lee, M. H., Lee, I.W., Doh, H. S and Park, H. J. 2018. Effect of hydrocolloids on rheological properties and printability of vegetable inks for 3D food printing. *J Food Sci.* 83(12), 2923-2932.

Kim, J., Kim, J., Shim, J., Lee, C. Y., Lee, C. W and Lee, H. J. 2014. Cocoa Phytochemicals: Recent Advances in Molecular Mechanisms on Health. *Critical Reviews in Food Science and Nutrition.* 54:11, 1458-1472. doi: 10.1080/10408398.2011.641041.

Kobus-Cisowska, J., Szymanowska, D., Maciejewska, P., Szczepaniak, O., Kmiecik, D.,Gramza-Michałowska, A., Kulczyński, B and Cielecka-Piontek, J. 2019. Enriching novel dark chocolate with Bacilluscoagulans as a way to provide beneficial nutrients. *The Royal Society of Chem.* 10 (2): 997-1006.

Krassenstein, B. 2014.Tytan 3D to launch a multi-material 3d printer which prints in salt, paper,food, adhesives & more. 3DPrint.com. https://3dprint.com/6893/tytan-3d-printer/. Accessed July 2017.

Krishnaraj, P., Anukiruthika, T., Choudhary, P., Moses, J and Anandharamakrishnan, C. 2019. 3D Extrusion Printing and Post-Processing of Fibre-Rich Snack from Indigenous Composite Flour. *Food and Bioprocess Technol.* 12 (10): 1776-1786.

Kumar, S., Anukiruthika, T., Dutta, S., Kashyap, A., Moses, J. A and Anandharamakrishnan, C. 2020. "Iron deficiency anemia: A comprehensive review on iron absorption, bioavailability and emerging food fortification approaches." *Trends in Food Sci. and Technol*.

Lanaro, M., Forrestal, D. P.,Scheurer, S., Slinger, D. J., Liao, S., Powell, S. K and Woodruff, M. A. 2017. 3D printing complex chocolate objects: Platform design, optimization and evaluation. *J. Food Eng.* 215: 13-22.

Lee, K. W., Kim, Y. J., Lee, H. J and Lee, C. Y. 2003. Cocoa has more phenolic phytochemicals and a higher antioxidant capacity than teas and red wine. *J. Agric. Food Chem.* 51(25): 7292-7295.

Lees, R and Jackson, E. B. 1973. *Sugar Confectionery and Chocolate Manufacture.* (Leonard Hill Books, Aylesbury,Bucks).

Lefeber, T., Janssens, M., Kamu, N and Vuyst, D. L. 2010. Kinetic analysis of strains of Lactic acid bacteria and acetic acid bacteria in cocoa pulp simulation media toward development of a starter culture for cocoa bean fermentation. *Appl. Environ. Microbiol.* 76: 7708-7716.

Lille, M., Nurmela, A., Nordlund, E., Metsa-Kortelainen, S and Sozer, N. 2018. Applicability of protein and fiber rich food materials in extrusion based 3D printing. *J. Food Eng.* 220: 20-27.

Liu, Z., Zhang, M., Bhandari, B and Wang, Y. 2017. 3D printing: printing precision and application in food sector. *Trends in Food Sci. Technol.* 69: 83-94.

Liu, Y., Liang, X., Saeed, A., Lan, W and Qin, W. 2019. Properties of 3D printed dough and optimization of printing parameters. *Innovative Food Sci. and Emerging Technol.* 54: 9-18.

Lipton, J. I. 2017. Printable food: the technology and its application in human health. *Curr.Opin. Biotechnol.* 44:198-201.

Lipton, J., Arnold, D andNigl, F. 2010.Multi-material food printing with complex internal structure suitable for conventional post-processing. In: Proceedings of Solid Freeform Fabrication Symposium, Austin TX, Aug 2010, p, 809-815.

Lupton, D. 2017. 'Download to delicious': Promissory themes and sociotechnical imaginaries in coverage of 3D printed food in online news sources. *Futures.* 93: 44-53.

Lupton, D and Turner, B. 2018. "I can't get past the fact that it is printed": consumer attitudes to 3D printed food." *Food Culture and Society*. 21 (3): 402-418.

Manach, C., Scalbert, A., Morand, C., Remce, C and Jimenezl. 2004. Polyphenols: food sources and bio availability. *Am. J. Clinic. Nutri*. 79(5): 727-747.

Mantihal, S., Prakash, S., Godoi, F. C and Bhandari, B. 2017. Optimization of chocolate 3D printing by correlating thermal and flow properties with 3D structure modeling. *Innov. Food Sci. Emerg. Technol*. 44: 21–29.

Mantihal, S., Prakash, S and Bhandari, B. 2018. Textural modification of 3D printed dark chocolate by varying internal infill structure. *Food Res. Int.* 121: 648-657.

Mantihal, S., Prakash, S., Godoi, F. C and Bhandari, B. 2019. Effect of additives on thermal, rheological and tribological properties of 3D printed dark chocolate. *Food Res. Int.* 119: 161-169.

Manstan, T and McSweeney, M. B. 2020. "Consumers' attitudes towards and acceptance of 3D printed foods in comparison with conventional food products." *Inter. J. Food Sci. and Technol.* 55 (1): 323-331.

Michiel CornelissenOntwerp (n.d.) XOCO chocolate printer. http://www.michielcornelissen.com/portfolio_page/xoco-chocolate-printer/. Accessed July 2017.

Millen, C. I. 2012. The development of colour 3D food printing system. Master thesis. Massey University, New Zealand.

Miller, K. B., Hurst, W. J., Flannigan, N., Ou, B., Lee, C. Y and Smith, N. 2009. Survey of commercially available chocolate- and cocoa-containing products in the United States. 2. Comparison of flavan-3-ol content with non-fat cocoa solids, total polyphenols and percent cacao. *J. Agric. Food Chem*. 57(19): 9169-9180.

Minifie, B. W. 1989. *Chocolate, Cocoa and Confectionery: Sci. and Technol.* doi:10.1007/978-94-011-7924-9.

Murphy, S. Vand Atala, A. 2014. 3D bioprinting of tissues and organs. *Nat. Bio. Technol*. 32:773-785.

Nachal, N., Moses,J., Karthik, P and Anandharamakrishnan, C. 2019. Applications of 3D Printing in Food Processing. *Food Eng. Reviews* 11 (3): 123-141.

Natural Machines. 2014. Foodini. http://www.naturalmachines.com/press-kit/. Accessed December 2014.

Nebesny, E and Zyzelewicz, D. 2005. Effect of lecithin concentration on properties of sucrose-free chocolate masses sweetened with isomalt. *Eur Food Res. Technol.* 220:131–135.

Nowak, J. 2015. Robotics in the food and beverage industry. Bastian Solutions. doi: https://www.bastiansolutions.com/blog/index.php/2015/05/28/robotics-in-the-food-and-beverage-industry/#.WYaZV4SGNFE. Accessed July 2017.

Ozguven, M. G., Karadag, A., Dumanc, M., Ozkal, B and Ozcelik, B. 2016. Fortification of dark chocolate with spray dried black mulberry (*Morus nigra*) waste extract encapsulated in chitosan-coated liposomes and bioaccessability studies. *Food Chem.* 201: 205-212.

Periard, D., Schaal, N and Schaal, M. 2007. Printing food. In: Proceedings of the 18th Solid Freeform Fabrication Symposium, Austin TX, 564-574.

Periard, D., Schaal, N., Schaal, M and Malone, E. L.H. 2007. Printing food. In: proceedings of the 18th solid freeform fabrication symposium, 564-574.

Peressini, D., Bravin B., Lapasin R., Sensidoni, A. 2006. Rheological Characterization of cocoa creams. In: Presented at 4th International Symposium on Food Rheology and Structure. Zurich, CH, September 12-14.

Peng, Z. 2015. 3D Food Printer: Development of Desk-top 3D Printing System for Food Processing (Master Thesis). National University of Singapore, Mechanic Engineering, Singapore.

Porsgaard, T and Hoy, C. E. 2000. Lymphatic transport in rats of several dietary fats differing in fatty acid profile and triacylglycerol structure. *J. Nutr.* 130: 1619-1624.

Rando, P and Ramaioli, M. 2020. Food 3D Printing: Effect of Heat Transfer on Print Stability of Chocolate. *J. Food Eng.* 294: 110415.

Saldana, E., Saldarriaga, L., Cabrera, J., Behrens, J. H., Selani, M. M., Rios-Mera, J and Contreras-Castillo, C. J. 2019. Descriptive and hedonic sensory perception of Brazilian consumers for smoked bacon. *J. Meat Science.* 147: 60-69.

Saputro, A. D., Walle, D. V., Caiquo, B. A., Hinneh, M., Kluczykoff, M and Dewettinck, K. 2019. Rheological behaviour and microstructural properties of dark chocolate produced by combination of a ball mill and a liquefier device as small scale chocolate production system. *J. Food Sci. and Technol.* 100: 10-19.

Schantz, B., Rohm, H. 2005. Influence of lecithin–PGPR blends on the rheological properties of chocolate. *Society of Food Sci. and Technol.*38:41-45.

Schwan, R. F and Wheals, A. E. 2004. The microbiology of cocoa fermentation and its role in chocolate quality. *Critical Reviews in Food Sci. Nutr*. 44: 205-221.

Severini, C., Azzollini,D., Albenzio, M and Derossi. A. 2018. On printability, quality and nutritional properties of 3D printed cereal based snacks enriched with edible insects. *Food Research Inter.*106: 666-676.

Severini.C., Derossi, A and Azzollini, D. 2016. Variables affecting the printability of foods: Preliminary tests on cereal-based products. *Innovative Food Sci. and Emerging Technol*. 38: 281-291.

Severini, C., Derossi, A., Ricci, I., Caporizzi, R and Fiore, A. 2018. Printing a blend of fruit andvegetables.New advances on critical variables and shelf life of 3D edible objects. *J. Food Eng*. 220: 89-100.

Serizawa, R., Shitara, M and Gong, J. 2014. 3D jet printer of edible gels for food creation. In: Proceedings of SPIE Smart Structures and Materials+ Nondestructive Evaluation and Health Monitoring, San Diego, 9-13.

Shourideh, M., Taslimi, A., Azizi,M. H and Mohammadifar, M. A. 2012. Physicochemical, Rheological and Sensory Properties of Dark Chocolate. *Inter. J. of Bioscience, Biochem. and Bioinformatics.* 2: 5.

Silva, E. S., Cavallazzi, J. R and Souza, J. V. 2007. Biotechnological applications of Lentinusedodes.

Slade, L and Levine, H. 1994. Water and the glass transition-Dependence of the glass transition on composition and chemical structure: Special implications for flour functionality in cookie baking. *J. Food Eng*. 22(1-4): 143-188.

Southerland, D., Walters, P and Huson, D. 2011. Edible 3D printing. In: Proceeding of NIP & Digital Fabrication Conference, Society for Imaging Science and Technology, p 819-822.

Statista, 2020. Coconut production. doi: https://www.statista.com/statistics/577497/world-coconut-production/. Accessed October 2022.

Statista, 2021. 3D printing. doi: https://www.statista.com/statistics/315386/global-market-for-3d-printers/. Accessed September 2022.

Statista, 2022. Cocoa industry. doi: https://www.statista.com/topics/3211/cocoa-industry/#dossierKeyfigures. Accessed October 2022.

Sun, J., Peng, Z., Yan, L., Fuh, J. Y. H., Hong, G. S., Fuh, J. Y. H and Hong, G. S. 2015. 3D food printing-An innovative way of mass customization in food fabrication. *J. Bioprinting.* 1(1): 27-38.

Sun, J., Zhou,W., Huang, D., Fuh,J. Y and Hong, G.S. 2015. An overview of 3D printing technologies for food fabrication. *Food and Bioprocess Technol.* 8 (8): 1605-1615.

Sun, J., Zhou, W., Yan, L., Huang, D and Lin, L. 2018. Extrusion based food printing for digitalized food design and nutrition control. *J. Food Eng.* 220: 1-11.

Sun, J., Zhou, W., Yan, L., Huang, D and Yan, L. 2018. 3D Food Printing: Perspectives *Polymers for Food Applications.*

Svanberg, L., Ahrne, L., Loren, N and Windhab, E. 2012. Impact of pre-crystallization process on structure and product properties in dark chocolate. *J. Food Eng.*114: 90-98.

Theagarajan, R., Moses, J and Anandharamakrishnan, C. 2020. 3D Extrusion Printability of Rice Starch and Optimization of Process Variables. *Food and Bioprocess Technol.*

Theagarajan, R., Narayanaswamy, M. L., Dutta, S., Moses, J. A. and Chinnaswamy, A. 2019. Valorisation of grape pomace (cv.Muscat) for development of functional cookies. *Inter J. Food Sci. and Technol.*

Tohic, C. L., O'Sullivan, J. J., Drapala, K. P., Chartrin, V., Chan, T., Morrison, A. P and Kelly, A. L. 2017. Effect of 3D printing on the structure and textural properties of processed cheese. *J. Food Eng.* 1-9.

Tolve, R., Condelli, N., Caruso, M. C., Barletta, D., Favati, F and Galgano, F. 2018. Fortification of dark chocolate with microencapsulated phytosterols: chemicaland sensory evaluation. *The Royal Society of Chem.* 9 (2): 1265-1273.

van der Linden, D. 2015. 3D food printing. TNO. doi: https://www.tno.nl/media/5517/3d_food_printing_march_2015.pdf. Accessed September 2016.

Wang, L., Zhang, M and Yang, C. 2017. Investigation on fish surimi gel as promising food material for 3D printing. *J. Food Eng.* 220: 101-108.

Wieland, H. 1972. *Cocoa and Chocolate Processing*. (Noyes Data Corporation, Park Ridge, NJ).

Wilson, A., Anukiruthika, T., Moses, J. A and Anandharamakrishnan, C. 2020. Customized Shapes for Chicken Meat Based Products: Feasibility Study on 3D Printed Nuggets. *Food and Bioprocess Technol.*13: 1968-1983.

Wegrzyn, T. F., Golding, M and Archer, R. H. 2012. Food layered manufacture: a new process for constructing solid foods. *Trends Food Sci. Technol.* 27: 66-72.

Wollgast, J and Anklam, E. 2000. Polyphenols in chocolate: Is there a contribution to human health. *Food Res. Int.* 33: 449-459.

Wood, J. D., Richardson, R. I., Nute, G. R., Fisher, A.V., Campo, M. M., Kasapidou, E., Sheard, P. R and Enser, M. 2004. Effects of fatty acids on meat quality: a review. *Meat Science*. 66(1): 21-32.

Yang, F., Zhang, M., Bhandari, B and Liu, Y. 2017. Investigation on lemon juice gel as food material for 3D printing and optimization of printing parameters. *Food Sci. and Technol.* 87: 67-76.

Yang, F., Zhang, M and Bhandari, B. 2017. Recent development in 3D food printing. *Critical Reviews in Food Sci. and Nutrition.* 57 (14): 3145-3153.

Yang, F., Zhang, M., Prakash, S and Liu, Y. 2018. Physical properties of 3D printed baking dough as affected by different compositions. *Innovative Food Sci. and Emerging Technol*. 49: 202-210.

Young, V. R and Pellett, P. L. 1991. Protein evaluation, amino acid scoring and the food and drug administration's proposed food labelling regulations. *J. Nutr.* 121(1): 145-150.

Zak, D. L and Keeney, P. G. 1996. Extraction and fractionation of cocoa proteins as applied to several varieties of cocoa beans. *J. Agric. Food Chem*. 24: 479-483.

Zhu, Y., Li, C., Cui, H. and Lin, L. 2020. Plasma enhanced-nutmeg essential oil solid liposome treatment on the gelling and storage properties of pork meat batters. *J. Food Eng.* 266, 109696.

3D Systems, 2015. CocoJet 3D Printer. Retrieved September, 2016, from 3D System.

Table A1. Analysis of variance (ANOVA) for Extrusion rate

Source	Sum of Squares	Df	Mean Square	F Value	p-value Prob> F	Coeff. Est.	Df	SE	95% CI Low	95% CI High
Model	21181.04	14	1512.93	9899.31	<0.0001	67.86	1	0.17	67.48	68.23
A- Motor speed	0.000	1	0.000	0.000	1.0000	0	1	0.11	-0.24	0.24
B- Air pressure	0.000	1	0.000	0.000	1.0000	0	1	0.11	-0.24	0.24
C-Nozzle diameter	19183.12	1	19183.12	1.26E+05	< 0.0001	39.98	1	0.11	39.74	40.22
D-Printing Speed	1617.11	1	1617.11	10580.97	< 0.0001	11.61	1	0.11	11.37	11.85
AB	0.000	1	0.000	0.000	1.0000	0	1	0.2	-0.42	0.42
AC	0.000	1	0.000	0.000	1.0000	0	1	0.2	-0.42	0.42
AD	0.000	1	0.000	0.000	1.0000	0	1	0.2	-0.42	0.42
BC	0.000	1	0.000	0.000	1.0000	0	1	0.2	-0.42	0.42
BD	0.000	1	0.000	0.000	1.0000	0	1	0.2	-0.42	0.42
CD	177.62	1	177.62	1162.21	< 0.0001	6.66	1	0.2	6.24	7.08
A^2	0.000	1	0.000	0.000	1.0000	4.167E-005	1	0.15	-0.33	0.33
B^2	0.000	1	0.000	0.000	1.0000	4.167E-005	1	0.15	-0.33	0.33
C^2	187.36	1	187.36	1225.91	< 0.0001	5.37	1	0.15	5.05	5.7
D^2	0.000	1	0.000	0.000	1.0000	-8.333E-005	1	0.15	-0.33	0.33
Residual	2.14	14	0.15							
Lack of Fit	2.14	10	0.21							
Pure Error	0.000	4	0.000							
Cor Total	21183.18	28								

Std. Dev.	0.39	R-Squared	0.999	df= degrees of freedom; SE= Standard Error	
Mean	70.08	Adj R-Squared	0.9998	Coeff. Est = Coefficient of estimate	
C.V. %	0.56	Pred R-Squared	0.9994	CI = Confidence of Interval	
PRESS	12.32	Adeq Precision	366.987	ns= non significance	

Table A2. Analysis of variance (ANOVA) for Printing Rate

Source	Sum of Squares	Df	Mean Square	F Value	p-value Prob> F	Coeff. Est.	Df	SE	95% CI Low	95% CI High
Model	1.48	14	0.11	5.45	0.0016	1.35	1	0.062	1.21	1.48
A-Motor speed	0.018	1	0.018	0.94	0.3498	0.039	1	0.04	-0.047	0.12
B-Air pressure	1.564E-003	1	1.546E-003	0.081	0.7803	0.011	1	0.04	-0.075	0.098
C-Nozzle diameter	0.76	1	0.76	39.32	<0.0001	0.25	1	0.04	0.17	0.34
D-Printing Speed	0.033	1	0.033	1.69	0.2148	0.052	1	0.04	-0.034	0.14
AB	0.076	1	0.076	3.91	0.068	0.14	1	0.07	-0.012	0.29
AC	0.045	1	0.045	2.32	0.1497	0.11	1	0.07	-0.043	0.26
AD	4.000E-004	1	4.000E-004	0.021	0.8877	-0.01	1	0.07	-0.16	0.14
BC	0.015	1	0.015	0.78	0.3933	-0.061	1	0.07	-0.21	0.088
BD	8.836E-003	1	8.836E-003	0.46	0.5101	-0.047	1	0.07	-0.20	0.10
CD	0.01	1	0.01	0.53	0.4797	-0.051	1	0.07	-0.20	0.099
A^2	9.198E-004	1	9.198E-004	0.048	0.8305	-0.012	1	0.055	-0.13	0.11
B^2	1.912E-005	1	1.912E-005	9.883E-004	0.9754	1.717E-03	1	0.055	-0.12	0.12
C^2	0.37	1	0.37	18.91	0.0007	0.24	1	0.055	0.12	0.35
D^2	0.059	1	0.059	3.04	0.1033	-0.095	1	0.055	-0.21	0.022
Residual	0.27	14	0.019							
Lack of Fit	0.27	10	0.027	98.5	0.0002					
Pure Error	1.095E-003	4	2.74E-04							
Cor Total	1.75	28								

Std. Dev.	0.14	R-Squared	0.8450	df= degrees of freedom; SE= Standard Error
Mean	1.40	Adj R-Squared	0.6899	Coeff. Est = Coefficient of estimate
C.V. %	9.93	Pred R-Squared	0.1096	CI = Confidence of Interval
PRESS	1.56	Adeq Precision	8.341	ns= non significance

Table A3. Analysis of variance (ANOVA) for Colour

Source	Sum of Squares	Df	Mean Square	F Value	p-value Prob> F	Coeff. Est.	Df	SE	95% CI Low	95% CI High
Model	7.47	14	0.53	0.58	0.8390	1.8	1	0.43	0.88	2.72
A- Motor speed	0.56	1	0.56	0.61	0.4464	0.22	1	0.28	-0.38	0.81
B-Air pressure	0.072	1	0.072	0.078	0.7841	0.077	1	0.28	-0.52	0.67
C-Nozzle diameter	2.3	1	2.3	2.51	0.1355	-0.44	1	0.28	-1.03	0.16
D-Printing Speed	0.22	1	0.22	0.24	0.6341	0.13	1	0.28	-0.46	0.73
AB	1.09	1	1.09	1.19	0.2946	-0.52	1	0.48	-1.55	0.51
AC	0.75	1	0.75	0.82	0.3803	-0.43	1	0.48	-1.46	0.59
AD	0.32	1	0.32	0.35	0.5658	0.28	1	0.48	-0.75	1.31
BC	0.11	1	0.11	0.12	0.7331	0.17	1	0.48	-0.86	1.19
BD	1.08	1	1.08	1.18	0.2957	-0.52	1	0.48	-1.55	0.51
CD	1.28E-03	1	1.28E-03	1.40E-03	0.9707	0.018	1	0.48	-1.01	1.05
A^2	0.012	1	0.012	0.013	0.9117	0.042	1	0.38	-0.76	0.85
B^2	0.028	1	0.028	0.031	0.8633	0.066	1	0.38	-0.74	0.87
C^2	0.84	1	0.84	0.91	0.3563	0.36	1	0.38	-0.45	1.17
D^2	0.03	1	0.03	0.033	0.8589	-0.068	1	0.38	-0.88	0.74
Residual	12.85	14	0.92							
Lack of Fit	11.71	10	1.17	4.08	0.0939					
Pure Error	1.15	4	0.29							
Cor Total	20.33	28								

Std. Dev.	0.96	R-Squared	0.3677	df= degrees of freedom; SE= Standard Error	
Mean	1.97	Adj R-Squared	-0.2646	Coeff. Est = Coefficient of estimate	
C.V. %	48.71	Pred R-Squared	-2.4049	CI = Confidence of Interval	
PRESS	69.22	Adeq Precision	3.228	ns= non significance	

Table A4. Analysis of variance (ANOVA) for Weight

Source	Sum of Squares	df	Mean Square	F value	p-value Prob> F	Coeff. Est.	Df	SE	95% CI Low	95% CI High
Model	16.73	14	1.2	0.64	0.792	7.85	1	0.61	6.54	9.16
A-Motor speed	0.074	1	0.074	0.04	0.845	0.078	1	0.39	-0.77	0.92
B- Air pressure	1.41	1	1.41	0.76	0.3984	0.34	1	0.39	-0.5	1.19
C-Nozzle diameter	2.09	1	2.09	1.12	0.3078	0.42	1	0.39	-0.43	1.26
D-Printing Speed	0.92	1	0.92	0.49	0.4942	0.28	1	0.39	-0.57	1.12
AB	2.02	1	2.02	1.09	0.3151	0.71	1	0.68	-0.75	2.18
AC	0.05	1	0.05	0.027	0.872	0.11	1	0.68	-1.35	1.58
AD	0.061	1	0.061	0.033	0.8587	0.12	1	0.68	-1.34	1.59
BC	0.058	1	0.058	0.031	0.863	0.12	1	0.68	-1.34	1.58
BD	6.81E-03	1	6.81E-03	3.65E-03	0.9527	0.041	1	0.68	-1.42	1.51
CD	0.09	1	0.09	0.048	0.8292	0.15	1	0.68	-1.31	1.61
A^2	0.42	1	0.42	0.23	0.6409	-0.26	1	0.54	-1.41	0.89
B^2	6.32	1	6.32	3.39	0.0868	-0.99	1	0.54	-2.14	0.16
C^2	1.59	1	1.59	0.85	0.3719	0.49	1	0.54	-0.66	1.64
D^2	0.064	1	0.064	0.034	0.8562	0.099	1	0.54	-1.05	1.25
Residual	26.1	14	1.86							
Lack of Fit	20.68	10	2.07	1.53	0.3629					
Pure Error	5.41	4	1.35							
Cor Total	42.83	28								

Std. Dev.	1.37	R-Squared	0.850	df= degrees of freedom; SE= Standard Error
Mean	7.58	Adj R-Squared	-0.2186	Coeff. Est = Coefficient of estimate
C.V. %	18.01	Pred R-Squared	-1.9791	CI = Confidence of Interval
PRESS	127.59	Adeq Precision	3.724	ns= non significance

Table A5. Analysis of variance (ANOVA) for Diameter

Source	Sum of Squares	Df	Mean Square	F Value	p-value Prob> F	Coeff. Est.	Df	SE	95% CI Low	95% CI High
Model	0.24	14	0.017	1.64	0.1835	4.23	1	0.046	4.13	4.33
A- Motor speed	0.092	1	0.092	8.83	0.0101	0.087	1	0.029	0.024	0.15
B- Air pressure	0.017	1	0.017	1.62	0.2235	0.037	1	0.029	-0.026	0.1
C-Nozzle diameter	5.21E-03	1	5.21E-03	0.5	0.4908	0.021	1	0.029	-0.042	0.084
D-Printing Speed	1.88E-03	1	1.88E-03	0.18	0.6776	-0.013	1	0.029	-0.076	0.051
AB	5.63E-03	1	5.63E-03	0.54	0.4742	0.038	1	0.051	-0.072	0.15
AC	5.63E-03	1	5.63E-03	0.54	0.4742	-0.038	1	0.051	-0.15	0.072
AD	5.63E-03	1	5.63E-03	0.54	0.4742	0.038	1	0.051	-0.072	0.15
BC	0.023	1	0.023	2.16	0.1635	0.075	1	0.051	-0.034	0.18
BD	2.50E-03	1	2.50E-03	0.24	0.6315	0.025	1	0.051	-0.084	0.13
CD	2.50E-03	1	2.50E-03	0.24	0.6315	-0.025	1	0.051	-0.13	0.084
A^2	1.46E-03	1	1.46E-03	0.14	0.7136	-0.015	1	0.04	-0.1	0.071
B^2	0.053	1	0.053	5.05	0.0412	-0.09	1	0.04	-0.18	-4.11E-03
C^2	7.95E-03	1	7.95E-03	0.76	0.3968	0.035	1	0.04	-0.051	0.12
D^2	3.28E-03	1	3.28E-03	0.32	0.5831	0.022	1	0.04	-0.063	0.11
Residual	0.15	14	0.01							
Lack of Fit	0.12	10	0.012	1.53	0.3628					
Pure Error	0.03	4	7.55E-03							
Cor Total	0.38	28								

Std. Dev.	0.10	R-Squared	0.539	df= degrees of freedom; SE= Standard Error
Mean	4.21	Adj R-Squared	0.2418	Coeff. Est = Coefficient of estimate
C.V. %	2.42	Pred R-Squared	-0.8537	CI = Confidence of Interval
PRESS	0.71	Adeq Precision	4.317	ns= non significance

Table A6. Analysis of variance (ANOVA) for Thickness

Source	Sum of Squares	Df	Mean Square	F Value	p-value Prob> F	Coeff. Est.	Df	SE	95% CI Low	95% CI High
Model	8.9	14	0.64	1.71	0.1631	8.75	1	0.27	8.16	9.33
A-Motor speed	0.03	1	0.03	0.081	0.7804	-0.05	1	0.18	-0.43	0.33
B-Air pressure	0.34	1	0.34	0.91	0.3561	0.17	1	0.18	-0.21	0.55
C-Nozzle diameter	0.85	1	0.85	2.28	0.1537	-0.27	1	0.18	-0.64	0.11
D-Printing Speed	0.53	1	0.53	1.42	0.2525	0.21	1	0.18	-0.17	0.59
AB	1.00E-04	1	1.00E-04	2.69E-04	0.9871	5.00E-03	1	0.3	-0.65	0.66
AC	0.32	1	0.32	0.87	0.3676	0.28	1	0.3	-0.37	0.94
AD	0.78	1	0.78	2.1	0.1697	-0.44	1	0.3	-1.09	0.21
BC	0.18	1	0.18	0.49	0.4946	-0.21	1	0.3	-0.87	0.44
BD	0.093	1	0.093	0.25	0.6246	-0.15	1	0.3	-0.81	0.5
CD	2.12	1	2.12	5.72	0.0314	-0.73	1	0.3	-1.38	-0.075
A^2	0.45	1	0.45	1.22	0.288	-0.26	1	0.24	-0.78	0.25
B^2	0.71	1	0.71	1.9	0.1895	0.33	1	0.24	-0.18	0.84
C^2	0.31	1	0.31	0.84	0.3761	0.22	1	0.24	-0.29	0.73
D^2	2.06	1	2.06	5.54	0.0338	0.56	1	0.24	0.05	1.08
Residual	5.2	14	0.37							
Lack of Fit	5.03	10	0.5	11.9	0.0145					
Pure Error	0.17	4	0.042							
Cor Total	14.1	28								

Std. Dev.	0.61	R-Squared	0.9065	df= degrees of freedom; SE= Standard Error
Mean	9.10	Adj R-Squared	0.2624	Coeff. Est = Coefficient of estimate
C.V. %	6.70	Pred R-Squared	-1.0741	CI = Confidence of Interval
PRESS	29.25	Adeq Precision	5.773	ns= non significance

Table A7. Analysis of variance (ANOVA) for Moisture content

Source	Sum of Squares	Df	Mean Square	F Value	p-value Prob> F	Coeff. Est.	Df	SE	95% CI Low	95% CI High
Model	0.089	14	6.35E-03	0.71	0.7348	0.32	1	0.042	0.23	0.41
A- Motor speed	0.023	1	0.023	2.62	0.1279	0.044	1	0.027	-0.014	0.1
B- Air pressure	6.75E-04	1	6.75E-04	0.076	0.7875	7.50E-03	1	0.027	-0.051	0.066
C-Nozzle diameter	3.33E-05	1	3.33E-05	3.73E-03	0.9522	-1.67E-03	1	0.027	-0.06	0.057
D-Printing Speed	4.03E-03	1	4.03E-03	0.45	0.5127	-0.018	1	0.027	-0.077	0.04
AB	2.50E-05	1	2.50E-05	2.80E-03	0.9586	-2.50E-03	1	0.047	-0.1	0.099
AC	0.016	1	0.016	1.75	0.2073	-0.062	1	0.047	-0.16	0.039
AD	5.63E-03	1	5.63E-03	0.63	0.4408	-0.038	1	0.047	-0.14	0.064
BC	2.50E-05	1	2.50E-05	2.80E-03	0.9586	-2.50E-03	1	0.047	-0.1	0.099
BD	0.018	1	0.018	2.04	0.1752	-0.068	1	0.047	-0.17	0.034
CD	8.10E-03	1	8.10E-03	0.91	0.3573	-0.045	1	0.047	-0.15	0.056
A^2	6.27E-04	1	6.27E-04	0.07	0.795	-9.83E-03	1	0.037	-0.089	0.07
B^2	3.53E-05	1	3.53E-05	3.95E-03	0.9508	-2.33E-03	1	0.037	-0.082	0.077
C^2	1.68E-03	1	1.68E-03	0.19	0.6714	-0.016	1	0.037	-0.096	0.064
D^2	0.012	1	0.012	1.38	0.26	-0.044	1	0.037	-0.12	0.036
Residual	0.13	14	8.94E-03							
Lack of Fit	0.11	10	0.011	2.67	0.1778					
Pure Error	0.016	4	4.07E-03							
Cor Total	0.21	28								

Std. Dev.	0.095	R-Squared	0.3917	df= degrees of freedom; SE= Standard Error
Mean	0.29	Adj R-Squared	-0.1694	Coeff. Est = Coefficient of estimate
C.V. %	32.80	Pred R-Squared	-2.0487	CI = Confidence of Interval
PRESS	0.65	Adeq Precision	3.137	ns= non significance

Table A8. Analysis of variance (ANOVA) for Hardness

Source	Sum of Squares	Df	Mean Square	F Value	p-value Prob> F	Coeff. Est.	Df	SE	95% CI Low	95% CI High
Model	2899.73	14	207.12	4.8	0.0029	38.56	1	2.94	32.26	44.86
A-Motor speed	*7.39*	*1*	*7.39*	*0.17*	*0.6854*	-0.78	1	1.9	-4.85	3.28
B- Air pressure	*120.62*	*1*	*120.62*	2.79	0.1169	3.17	1	1.9	-0.9	7.24
C-Nozzle diameter	*1162.22*	*1*	*1162.22*	26.91	0.0001	9.84	1	1.9	5.77	13.91
D-Printing Speed	*219.4*	*1*	*219.4*	5.08	0.0407	-4.28	1	1.9	-8.34	-0.21
AB	*146.08*	*1*	*146.08*	*3.38*	*0.0872*	6.04	1	3.29	-1	13.09
AC	17.85	*1*	17.85	*0.41*	*0.5307*	-2.11	1	3.29	-9.16	4.93
AD	62.61	*1*	62.61	*1.45*	*0.2485*	3.96	1	3.29	-3.09	11
BC	214.61	*1*	214.61	*4.97*	*0.0427*	7.32	1	3.29	0.28	14.37
BD	16.25	*1*	16.25	*0.38*	*0.5494*	-2.02	1	3.29	-9.06	5.03
CD	49.72	*1*	49.72	*1.15*	*0.3014*	-3.53	1	3.29	-10.57	3.52
A^2	176.09	*1*	176.09	*4.08*	*0.063*	-5.21	1	2.58	-10.74	0.32
B^2	3.63	*1*	3.63	*0.084*	*0.7762*	-0.75	1	2.58	-6.28	4.79
C^2	263.04	*1*	263.04	*6.09*	*0.0271*	-6.37	1	2.58	-11.9	-0.83
D^2	668.8	*1*	668.8	*15.49*	*0.0015*	-10.15	1	2.58	-15.69	-4.62
Residual	604.56	14	43.18							
Lack of Fit	*604.4*	*10*	*60.44*	*1521.34*	*< 0.0001*					
Pure Error	*0.16*	*4*	*0.04*							
Cor Total	3504.29	28								

Std. Dev.	6.57	R-Squared		0.8275	df= degrees of freedom; SE= Standard Error
Mean	29.26	Adj R-Squared		0.6550	Coeff. Est = Coefficient of estimate
C.V. %	22.46	Pred R-Squared		0.0065	CI = Confidence of Interval
PRESS	3481.59	Adeq Precision		8.534	ns= non significance

Table A9. Analysis of variance (ANOVA) for Cohesiveness

Source	Sum of Squares	Df	Mean Square	F Value	p-value Prob>F	Coeff. Est.	Df	SE	95% CI Low	95% CI High
Model	0.13	14	9.13E-03	0.89	0.5874	0.12	1	0.045	0.024	0.22
A- Motor speed	1.43E-04	1	1.43E-04	0.014	0.9078	3.46E-03	1	0.029	-0.059	0.066
B- Air pressure	1.20E-03	1	1.20E-03	0.12	0.7378	0.01	1	0.029	-0.053	0.073
C-Nozzle diameter	0.043	1	0.043	4.17	0.0603	-0.06	1	0.029	-0.12	2.98E-03
D-Printing Speed	5.28E-03	1	5.28E-03	0.51	0.4858	0.021	1	2.90E-02	-0.042	0.084
AB	1.19E-03	1	1.19E-03	0.12	0.7389	-0.017	1	0.051	-0.13	0.092
AC	6.41E-04	1	6.41E-04	0.062	0.8066	0.013	1	0.051	-0.096	0.12
AD	7.92E-03	1	7.92E-03	0.77	0.3952	0.045	1	0.051	-0.064	0.15
BC	0.048	1	0.048	4.62	0.0495	-0.11	1	0.051	-0.22	-2.47E-04
BD	5.29E-04	1	5.29E-04	0.051	0.8241	-0.011	1	5.10E-02	-0.12	0.097
CD	2.49E-04	1	2.49E-04	0.024	0.8787	7.89E-03	1	0.051	-0.1	0.12
A^2	2.73E-06	1	2.73E-06	2.65E-04	0.9873	6.48E-04	1	0.04	-0.085	0.086
B^2	0.017	1	0.017	1.61	0.2252	-0.051	1	0.04	-0.14	0.035
C^2	9.29E-04	1	9.29E-04	0.09	0.7684	-0.012	1	0.04	-0.097	0.074
D^2	8.12E-04	1	8.12E-04	0.079	0.783	0.011	1	0.04	-0.074	0.097
Residual	0.14	14	0.01							
Lack of Fit	0.13	10	0.013	4.05	0.095					
Pure Error	0.013	4	3.24E-03							
Cor Total	0.27	28								

Std. Dev.	0.10	R-Squared	0.4700	df= degrees of freedom; SE= Standard Error	
Mean	0.10	Adj R-Squared	-0.0600	Coeff. Est = Coefficient of estimate	
C.V. %	101.42	Pred R-Squared	-1.8528	CI = Confidence of Interval	
PRESS	0.78	Adeq Precision	4.629	ns= non significance	

Table A10. Analysis of variance (ANOVA) for Adhesiveness

Source	Sum of Squares	Df	Mean Square	F Value	p-value Prob> F	Coeff. Est.	Df	SE	95% CI Low	95% CI High
Model	2.95E-06	14	2.11E-07	0.86	0.6092	4.00E-04	1	2.21E-04	-8.75E-04	7.47E-05
A-Motor speed	4.03E-07	1	4.03E-07	1.65	0.2203	1.83E-04	1	1.43E-04	-1.23E-04	4.90E-04
B- Air pressure	2.13E-07	1	2.13E-07	0.87	0.3665	-1.33E-04	1	1.43E-04	-4.40E-04	1.73E-04
C-Nozzle diameter	4.08E-08	1	4.08E-08	0.17	0.6892	-5.83E-05	1	1.43E-04	-3.65E-04	2.48E-04
D-Printing Speed	8.33E-10	1	8.33E-10	3.40E-03	0.9543	8.33E-06	1	1.43E-04	-2.98E-04	3.15E-04
AB	4.23E-07	1	4.23E-07	1.72	0.2102	3.25E-04	1	2.48E-04	-2.06E-04	8.56E-04
AC	0	1	0	0	1	0	1	2.48E-04	-5.31E-04	5.31E-04
AD	2.25E-08	1	2.25E-08	0.092	0.7663	7.50E-05	1	2.48E-04	-4.56E-04	6.06E-04
BC	1.00E-08	1	1.00E-08	0.041	0.8428	-5.00E-05	1	2.48E-04	-5.81E-04	4.81E-04
BD	2.25E-08	1	2.25E-08	9.20E-02	0.7663	-7.50E-05	1	2.48E-04	-6.06E-04	4.56E-04
CD	6.25E-08	1	6.25E-08	0.26	0.6213	-1.25E-04	1	2.48E-04	-6.56E-04	4.06E-04
A^2	1.31E-06	1	1.31E-06	5.36	0.0363	-4.50E-04	1	1.94E-04	-8.67E-04	-3.32E-05
B^2	2.60E-07	1	2.60E-07	1.06	0.3208	-2.00E-04	1	1.94E-04	-6.17E-04	2.17E-04
C^2	1.01E-09	1	1.01E-09	4.14E-03	0.9496	-1.25E-05	1	1.94E-04	-4.29E-04	4.04E-04
D^2	8.21E-08	1	8.21E-08	0.34	0.5718	1.13E-04	1	1.94E-04	-3.04E-04	5.29E-04
Residual	3.43E-06	14	2.45E-07							
Lack of Fit	3.41E-06	10	3.41E-07	68.18	0.0005					
Pure Error	2.00E-08	4	5.00E-09							
Cor Total	6.38E-06	28								

Std. Dev.	4.949E-004	R-Squared	0.4623	df= degrees of freedom; SE= Standard Error	
Mean	-6.276E-004	Adj R-Squared	-0.0753	Coeff. Est = Coefficient of estimate	
C.V. %	78.86	Pred R-Squared	-2.0838	CI = Confidence of Interval	
PRESS	1.967E-005	Adeq Precision	4.448	ns= non significance	

ABSTRACT

Chocolate is one of the chief ingredients in the global confectionary market. It contains high concentrations of refined sugar and saturated fat content. Chocolate and cocoa (*Theobroma cacao*) provides health benefits to cure cardiovascular disease, metabolic syndrome, neurodegenerative diseases and other chronic health conditions. Coconut (*Cocos nucifera*) is a very versatile and indispensable food item that is considered a complete food source, rich in calories, vitamins and minerals. Coconut kernel contains 7-10% dietary fiber and 5% proteins, in addition to 34-60% oil content. The dietary fiber constitutes significant hypo-cholesterolemic effect. The deficiency of complex carbohydrates like dietary fiber is a matter of concern that poses major health issues causing chronic diseases such as cardiovascular diseases, obesity, colon cancer, hypertension and diabetes mellitus. The recommended acceptable intake of dietary fiber is 28.8 g/day for adults, but the actual intake was found to be lower than this limit. The present study envisages the development of chocolate enriched with coconut dietary fiber using the advanced technology of 3D food printing.

Three-dimensional (3D) printing is a novel food preparation concept based on the additive manufacturing (AM) technique. The technology offers features like personalized nutrition, taking into consideration of the age, health and diet of the consumer and also customized designing of foods based on individual preferences. The study focused on the applicability of 3D printing for dietary fiber enrichment of chocolate. A 3D model of 'gear' with dimensions 41.50 mm × 41.50 mm × 10.00 mm was considered to study the 3D food printing.

The treatment combinations for the formulation of supply material and experimental design for optimization of process parameters were done using Central Composite Design (CCD) and Box-Behnken Design (BBD) of Response Surface Methodology (RSM) respectively. Based on the analysis, the supply material composition with 9% coconut meal, 3% sugar, 0.3% soya lecithin and 87.7% dark compound chocolate was optimized. 3D food

printing process parameters such as extruder motor speed, nozzle diameter, conveying air pressure and printing speed were considered as independent variables. The printing parameters have significant effect on extrusion rate, printing rate, weight, thickness and hardness of the printed products. The results showed that diameter, colour, moisture content, cohesiveness and adhesiveness of the printed products were not significantly affected by the printing process parameters ($p > 0.05$). Based on these results, the optimized condition for printing of coconut based chocolate was 0.8 mm nozzle diameter, 60 mm/s printing speeds, 2 bar conveying air pressure and 30 rpm motor speed. Nutritional analysis showed that the developed product have 8% of dietary fiber along with 54.35% carbohydrates, 32.26% fat and 4.54% protein content providing an energy value of 549 k Cal/100g.